EVALUATION OF HEPATOPROTECTIVE EFFECTS OF *BOESENBERGIA ROTUNDA* AND *CURCUMA LONGA* RHIZOMES EXTRACTS IN THIOACETAMIDE-INDUCED LIVER DAMAGE IN RATS

SUZY MUNIR SALAMA FANOUS

THESIS SUBMITTED IN FULFILMENT OF THE REQUIREMENTS FOR THE DEGREE OF DOCTOR OF PHILOSOPHY

FACULTY OF MEDICINE

UNIVERSITY OF MALAYA

KUALA LUMPUR

2013

UNIVERSITI MALAYA

ORIGINAL LITERARY WORK DECLARATION

Name of Candidate: Suzy Munir Salama Fanous

Passport No: A00259789

Registration/Matric No: MHA 120007

Name of Degree: Ph.D

Title of Thesis: ("Evaluation of Hepatoprotective effects of *Boesenbergia rotunda* and *Curcuma longa* rhizomes extracts in thioacetamide-induced liver damage in rats"):

Field of Study: Medical Science

I do solemnly and sincerely declare that:

(1) I am the sole author/writer of this Work;
(2) This Work is original;
(3) Any use of any work in which copyright exists was done by way of fair dealing and for permitted purposes and any excerpt or extract from, or reference to or reproduction of any copyright work has been disclosed expressly and sufficiently and the title of the Work and its authorship have been acknowledged in this Work;
(4) I do not have any actual knowledge nor do I ought reasonably to know that the making of this work constitutes an infringement of any copyright work;
(5) I hereby assign all and every rights in the copyright to this Work to the University of Malaya ("UM"), who henceforth shall be owner of the copyright in this Work and that any reproduction or use in any form or by any means whatsoever is prohibited without the written consent of UM having been first had and obtained;
(6) I am fully aware that if in the course of making this Work I have infringed any copyright
whether intentionally or otherwise, I may be subject to legal action or any other action as may be determined by UM.

Candidate's Signature Suzy Munir **Date** 6/6/2013

Subscribed and solemnly declared before,

Witness's Signature **Date** 7/6/2013

Name: Mahmood Ameen Abdulla

Designation: professor

Professor Dr Mahmood Ameen Abdulla
Lecturer
Department of Biomedical Science
Faculty of Medicine
University of Malaya

ABSTRACT

Researchers focused on developing traditional therapies as pharmacological medicines to treat liver cirrhosis that is accompanied by abnormality in liver functions. This study evaluated the mechanisms of hepatoprotective activity of *Boesenbergia rotunda* and *Curcuma longa* rhizome ethanolic extract on liver damage induced by thioacetamide in rats.

The crude extracts of *Boesenbergia rotunda* and *Curcuma longa* were tested for acute toxicity and antioxidant properties evaluated by 2,2-diphenyl-1-picrylhydrazyl (DPPH), the antioxidant power of reducing iron (FRAP) and total phenolic content (TPC) The hepatoprotective effect of the plant extracts was evaluated in a rat model of thioacetamide-induced liver damage over 8 weeks. Male *Sprague Dawley* rats were intraperitonealy injected with 200 mg/kg thioacetamide (TAA) 3 times/week for 8 weeks and daily oral administration of 250 mg/kg and 500 mg/kg for 8 weeks. Silymarin was used as a reference drug that was orally administered to the animals at a daily dose of 50 mg/kg. At the end of the 8 weeks, liver damage was evaluated by weight changes, liver gross and histopathology and biochemical measurements of liver parameters, (AP, ALT, AST, GGT and LDH), prothrombin time ratio, total protein, albumin and bilirubin and lipid profile. The degree of liver fibrosis was measured by Masson's Trichrome staining. Hepatic cytochrome P450 2E1, Matrix metalloproteinase (MMP-2 and MMP 9) and tissue inhibitor of metalloproteinase (TIMP-1) were measured. Serum levels of transforming growth factor TGF-β1, nuclear transcription factor NF-κB, pro-inflammatory cytokine IL-6 and caspase-3 were evaluated. Stress due to oxidation was evaluated by liver malondialdehyde, nitrotyrosine and urinary hydroxyl deoxyguanosine levels. The hepatoprotective activity of *B. rotunda* and *C. longa* extracts was evaluated through the liver level of antioxidant

enzymes superoxide dismutase (SOD), catalase (CAT) and glutathione peroxidase (GPx). Protein expression of pro-apoptotic Bax and anti-apoptotic Bcl-2 proteins in the animal blood sera was determined and confirmed by immunohistochemistry of Bax, Bcl-2 proteins and proliferating cell nuclear antigen (PCNA).

Panduratin A and Germacrone compounds of *B. rotunda* and *C. longa* rhizomes respectively were tested for their cytotoxicity and protective activity against TAA-induced oxidative damage in embryonic normal liver cell line WRL-68. The compounds were isolated from the ethanolic crude extracts by Column chromatography, thin layer chromatography and high performance liquid chromatography and their mass was determined by Liquid Chromatography Mass Spectrometry (LCMS) (m/z = 407.22 for Panduratin A and 219.17 for Germacrone). The hepatoprotective activity of the isolated Panduratin A was evaluated *in vivo* in a similar rat model for a period of 4 weeks using 3 different doses 5, 10 and 50 mg/kg. The effect of Panduratin A on hepatic stellate cells (HSCs) activity was measured by alpha-smooth muscle actin staining.

B. rotunda and *C. longa* treatment improved liver histopathology, immunohistochemistry and biochemistry, triggered apoptosis, inhibited serum cytokines, extracellulat matrix proteins and hepatocytes proliferation, but *C. longa* had no impact on hepatic CYP2E1, MMP-2 or TIMP-1 levels. Moreover, Panduratin A showed significant improvement in the liver biochemistry, histopathology and inhibited HSCs activity.

The development of liver fibrosis can be attenuated by the antioxidant and anti-inflammatory activities of *C. longa* and *B. rotunda* ethanolic extracts and its active compound Panduratin A while the normal status of the liver can be preserved.

ABSTRAK

Kebelakangan ini, para penyelidik memberi tumpuan bagi membangunkan terapi tradisional sebagai ubat farmakologi untuk merawat sirosis hati yang menyebabkan gangguan fungsi hati. Kajian ini bertujuan menilaik mekanisme hepatoprotif oleh ektrak etanol rizom *Boesenbergia rotunda* dan *Curcuma* terhadap thioacetamide yang menyebabkan sirosis hati dalam tikus.

Ekstrak mentah *B. rotunda* dan *C. longa* telah diuji ketoksikannya serta ciri antioksidan telah dinilai oleh DPPH, penurunan kuasa antioxidan ferric (FRAP) dan jumlah kandungan fenolik (TPC). Kesan hepatoprotectif ekstrak tumbuhan telah diukur menggunakan model tikus terhadap kerosakan hati oleh thioacetamide selama lebih 8 minggu. Tikus jantan Sprague Dawley telah diberi suntikan intraperitoneal sebanyak 200 mg / kg TAA 3 kali / minggu selama 8 minggu dan pengambilan secara oral sebanyak 250 mg / kg dan 500 mg / kg selama 8 minggu. Silymarin telah digunakan sebagai dadah rujukan telah diberikan secara oral kepada haiwan tersebut dengan dos harian sebanyak 50 mg / kg. Pada akhir minggu ke-8, kerosakan hati telah dinilai oleh perubahan berat, pembengkakkan hati pengukuran histopatologi dan biokimia parameter hati, (AP, ALT, AST, GGT dan LDH), nisbah masa prothrombin, jumlah protein, albumen dan bilirubin dan profil lipid. Tahap fibrosis hati telah diukur oleh pewarnaan Masson Trichrome. Hepatik Cytochrome 2E1 P450, Matrix metalloproteinase (MMP-2 dan MMP 9) dan perencat tisu metalloproteinase (TIMP-1) telah diukur. Tahap serum pengubah faktor pertumbuhan TGF-β1, faktor transkripsi nuklear NF-κB, sitokin pro-inflamasi IL-6 dan caspase-3 telah dinilai. Tekanan oksidatif telah diukur oleh malondialdehida, urinari 8-hidroksiguanosin dan tahap nitrotirosin. Aktiviti protektif oleh ekstrak *B. rotunda* dan *C. longa* telah dinilai melalui

tahap enzim antioksidan pada hati (SOD, CAT dan Gpx). Ekspresi protein pro-apoptotik Bax dan anti-apoptotik Bcl-2 protin dalam serum darah haiwan telah ditentukan dan disahkan oleh Immunohistokimia Bax, Bcl-2 protin dan sel membiak antigen nuklear (PCNA). Panduratin A yang terdapat pada rizom *B. rotunda* dan sebatian Germacron yang terdapat pada rizom *C. longga* masing-masing telah diuji untuk ujian sitotosik dan aktiviti protektif terhadap TAA peyebabkan kerosakan oksidatif dalam embrio sel hati normal WRL-68. Sebatian yang terdapat dalam ekstrak etanolik mentah telah dipisahkan secara kromatografi turus kromatografi (CC) kromatografi lapisan nipis (TLC), kromatografi cecair berprestasi tinggi (HPLC) dan jisim molekul sebatian telah ditentukan oleh kromatografi cecair-spektrometri jisim (LC-MS). Aktiviti hepatoprotektif oleh Panduratin-A tulen telah dinilai dalam ujian in-vivo dalam model tikus yang sama untuk tempoh 4 minggu menggunakan 3 dos berbeza 5, 10 dan 50 mg / kg. Kesan Panduratin-A ke atas sel hepatik stallete (HSCs) telah diukur oleh pewarnaan actin otot alfa-licin. Rawatan extrak *B.Rotunda* dan *C. longga* memberi kesan memberangsangkan terhadap histopatologi hati, immunohistokimia dan biokimia, mencetuskan apoptosis, menghalang sitokin serum, sel luaran matriks protin dan proliferasi hepatosit, tetapi *C. longa* tidak mempunyai kesan ke atas tahap hepatik CYP2E1, MMP-2 atau TIMP-1. Selain itu, Panduratin A menunjukkan peningkatan yang ketara dalam biokimia hati, histopatologi dan menghalang aktiviti HSCs.

Perkembangan sirosis hati boleh direncat oleh aktiviti antioksidan dan anti-inflamasi oleh ekstrak etanolik *C. longa* dan *B. rotunda* dan dengan sebatian Panduratin A serta memulihara ke status normal.

TABLE OF CONTENT

LIST OF FIGURES

LIST OF TABLES

LIST OF SYMBOLS AND ABBREVIATIONS

Abbreviations	Description
ROS	Reactive Oxygen Species
MDA	Malondialdehyde
PDGF	Platelet-derived growth factor
TGF-β	Transforming growth factor β
TIMP	Tissue inhibitors of metaloproteinase
DPPH	α, α-diphenyl-β-picryl-hydrazyl radical scavenging assay
DNA	Deoxy ribonucleic acid
IL-6	Interlukin 6
TNF-α	Tumor necrosis factor-alpha
SOD	Superoxide dismutase
GPx	Glutathione peroxidase
ECM	Extracellular matrix
CAT	Catalase
FRAP	Ferric reducing antioxidant power
ATP	Adenosine triphosphate
O_2^-	Superoxide
$O_2^=$	Peroxide
OH	Hydroxyl radical

H_2O_2	Hydrogen peroxide
OECD	Organization for Economic Cooperation and Development
LD_{50}	Lethal dose 50
SEM	Standard error of the mean
HPLC	High performance liquid chromatography
LC-MS	Liquid chromatography-mass spectrometry
ANOVA	Analysis of variance
P value	Level of significance
FBS	Fetal bovine serum
TLC	Thin layer chromatography
BHT	Butylated hydroxyltoluene
NF-kB	Nuclear factor kB
MMPs	Matrix metalloproteinases
MMP-2	Matrix metalloproteinase-1
MMP-9	Matrix-metalloproteinase-9
8-OH-dG	8- Hydroxy deoxy guanosine
TPC	Total Phenolic Content
CV	Central vein
TAA	Thioacetamide

ACKNOWLEDGEMENT

First of all, by the name of god, who gave me health, power, knowledge and enable me to success in this academic merit. I would like to express my sincere appreciation to my both supervisors, Professor Dr. Mahmood Ameen Abdulla and Associate Professor Dr. Salmah Bint Ismail for their invaluable guidance, assistance, and encouragement to help me finishing this Research project.

My special thanks go to my family and for their invaluable advices, supports and endless help throughout this study. Without their help, it was impossible to finish.

Further thanks to all staffs, research assistants and postgraduate students at the Biomedical Science and Molecular Medicine Departments, Laboratory of Immunology, Biochemistry Laboratory and Animal Science Centre and Teaching hospital University of Malaya Diagnostic Laboratories. I am taking this opportunity to thank Professor Dr. Umah, the Head of Biomedical Science Departmento let us access and use her Laboratories within the department. In addition, I would like to thank who have supported and shared the happiness or sadness along the way.

Finally, without mentioning their names, I would like to express my gratitude for all those who generously provided support and shared advises throughout and until the thesis was completed.

Dedicating this thesis to my beloved late parents

God might keep them in paradise

CHAPTER I

INTRODUCTION

1.1. Introduction

The liver is the largest organ within human body, it performs a variety of functions such as bile secretion, detoxification, and metabolism of carbohydrate food, necessary protein and fats, transformation of food nutrients into essential blood vessels components, storing vitamins, and minerals and maintaining hormone balances. The liver organ makes factors that help the individual defense mechanisms and eliminates bacteria from the blood (Nemeth *et al*., 2009).

Liver diseases are the circumstances that cause injury or inflammation of the liver and impacts liver functions. Liver diseases can be classified to different groups. Factors like infections or contact with medication like paracetamol or toxins like alcohol, or viruses like hepatitis B and hepatitis C may affect liver functions in obstructions, inflammations, pathological tissue changes, scarring damage and liver failure. Liver fibrosis and its end-stage cirrhosis signify a large worldwide medical care problem, according to the National Institutions of Health; cirrhosis is the twelfth major cause of loss of life. Liver fibrosis is the last stage in many liver injuries and cirrhosis is the last stage in liver fibrosis and all chronic liver diseases major in the development of nodules that change the hepatic function and prevent the blood flow (Pinzani *et al*., 2011). Liver damage due to various toxicants such as certain chemotherapeutic drugs, thioacetamide, CCl4, ethanol, is well-studied. Thioacetamide (TAA) triggered hepatotoxicity in experimental animals for the research of

hepatoprotective outcomes. The induction of liver cirrhosis in experimental animals by prolonged exposure of TAA results in clear changes in the histology and biochemistry appearing like human liver cirrhosis (Zimmermann *et al.*, 1992).

Liver cirrhosis was first presented in 1819 by Laennec (Roguin, 2006). It resulted from the Ancient term scirrhus and is used to explain the yellow-colored of the liver seen at autopsy. Cirrhosis affects an incredible number of sufferers globally. Due to serious liver fibrosis, the overall problem of liver diseases is constantly on the flourish, challenging and increasing in social and economic cost. Cirrhosis has previously been considered as the level at which fibrotic liver became permanent however, these days, strong facts indicate that fibrosis and even cirrhosis is reversible by reducing the cause of the disease in experimental animals, which provide vital facts to the actual procedure (Friedman *et al*., 2006).

In spite of pharmacological drugs advances, they lack efficiency, relatively costly and have unfavorable adverse reactions (Stickel & Schuppan, 2007). Treatment options of liver diseases as chronic hepatitis, cirrhosis and fatty liver are still problematic. Medical professionals and patients are in need of efficient treatment solutions with a low occurrence of side-effects. Therefore, an alternative treatment is required to treat these disorders. For centuries plants have formed the basis of conventional medicinal practices techniques that provide human with new remedies. Folk medicine in various cultures had been comprehensively documented. These plant-based techniques continue to play an essential role in health care of many nations and according to World Health Organization, 80% of the patients of the world consume herbal medicine for their disease (Gurib-Fakim, 2006).

The use of traditional medicine in treating liver diseases has long history starting with the Ayurvedic therapy (the ancient Native Indian system) and increasing to the European, Chinese and other systems of conventional medicinal practices. Large number of plants with nearly 160 phyto-constituents from 101 herbs has been reported for their hepatoprotective activities (Saleem *et al*., 2010). With the development of chromatography and spectroscopy techniques, Malaysian herbal medicines have advanced and became safe for human use. These new techniques have remarkable effect on the analysis of the active ingredients of herbal medicines (Jantan, 2004).

Among the well recorded hepatoprotective plants is *Silybum marianum* (milk thistle) since its seed extract silymarin has been stated to possess hepatoprotective activity that was verified in many *in vivo* and *in vitro* researches (Pradhan & Girish, 2006). Also it has been revealed to prevent the liver injuries caused by various drugs via its anti-inflammatory, anti-lipid peroxidative, antioxidative, antifibrotic, and immuno-modulatory actions (Cragg & Newman, 2005). Many therapeutic herbs were known to improve the activity of the immune function through their strong control of cytokines that are released in response to injury stimulating elements, natural inflammation related reactions, cell growth, angiogenesis, and repair procedures (Spelman *et al.*, 2006). The root extracts of two types of the traditional Chinese herbs *Paeonia lactiflora* and *Astragalus membranaceus* were found to acquire immuno-modulatory hepatoprotective activity via inhibition of pro-inflammatory cytokines (Sun *et al*., 2008).

Due to the serious role played by oxidative stress in the occurrence of liver cirrhosis, therefore, in the past few years the therapeutic herbs have been examined for their

anti-oxidants and toxic scavenging actions as an organic source of anti-oxidants. They were assumed for their health, safety and healing value to substitute the artificial anti-oxidants that have been limited due to their health hazards and unwanted toxicities. Plants produced organic anti-oxidants mainly are in the form of phenolic substances as, flavonoids and tocopherols, vitamin C and carotenoids which were thought to scavenge free radicals (Ali *et al.*, 2008). Many patients have been treated by antioxidants. For example, in a recent clinical trial, 44% of patients having chronic HCV showed normal liver enzymes when treated in combination with antioxidant therapy and 36.1% showed histological improvement (Melhem *et al.*, 2005). Several medicinal plants have been used worldwide. Herbal therapy such as Chinese herbal medicines and curcumin extracted from turmeric, have been used to treat liver diseases (Bruck *et al*., 2007).

In this study, we will assess the hepatoprotective activity of *Boesenbergia rotunda* and *Curcuma longa* ethanolic extracts against liver cirrhosis induced by thioacetamide in *Sprague Dawley* rats by determining the presence of antioxidant in the plant extracts along with morphological, serum biochemical and histopathological changes.

1:2 Objectives

1.2.1. General

To evaluate the hepatoprotective activity of *B. rotunda* and *C. longa* rhizomes crude extracts *in vivo* and Panduratin A an active compound from *B. rotunda* rhizomes *in vivo*

and *in vitro* against TAA-induced liver injury. Also to study the possible mechanism of the *in vivo* hepatoprotective activity of *B. rotunda* and *C. longa* rhizomes crude extracts.

1.2.2. Specific

1. To determine the *in-vitro* antioxidant effects of ethanolic extracts of *B. rotunda* and *C. longa* rhizomes.
2. To determine the acute toxicity study and to investigate the preventive effects of ethanolic extracts in TAA-induced liver cirrhosis in rats by biochemical and histological analysis.
3. To isolate Panduratin A from *B. rotunda* and germacrone from *C. longa* ethanolic extracts and to determine the protective effects against *in-vitro* TAA cytotoxicity in WRL-68 cell line.
4. To evaluate the *in-vivo* hepatoprotective activity of Panduratin A in TAA-induced liver injury in rats.

CHAPTER II

LITERATURE REVIEW

2.1. The Liver

2.1.1 Gross Anatomy of the Liver

Inside the human body, the liver is considered the largest gland in the human body. It is reddish brown in colour constitutes approximately 1400 – 1600 g in adult male (Akshatha, 2011). The normal liver occupies the right upper quadrant extending from the fifth intercostals space in the mid-clavicular line down to the right costal margin (Block, 2011). The visceral peritoneum almost covers the liver, which is completely covered by dense connective tissue layer.

The liver is divided into two lobes right and left that with falciform ligament separates between them from the anterior side and by ligamentum teres from the inferior side **(**Figure **2.1**). The size of the right is bigger 6 times more than the left lobe. The right lobe is divided into two minor subdivisions, the quadrate and caudate lobes (Sherlock & Dooley, 2002).

The liver supplies blood from two sources, the portal vein which receives 75% - 80% and the hepatic artery which receives 20% - 25% of the cardiac output. The portal vein and the hepatic artery are divided into branches that carry the blood to the lobules, and then flows through sinusoids (Cunningham & Van Horn, 2003)

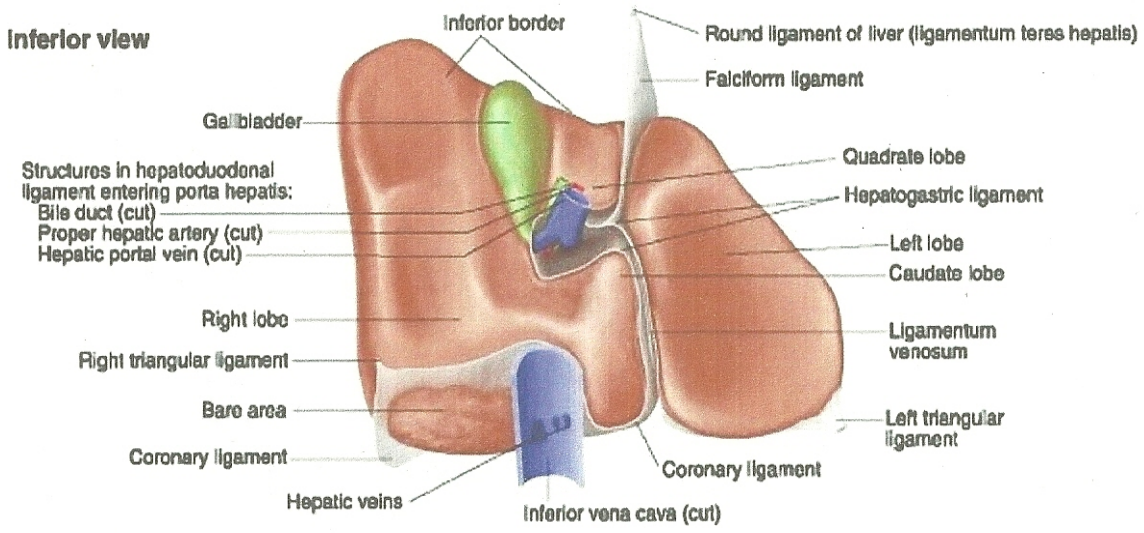

Figure.2.1: Diagram showing anatomy of the liver. (Agur & Dalley, 2008).

2.1.2 Histology of the Liver

The liver is formed of bile canaliculi, parenchyma cells called hepatocytes, and hepatic vessels called sinusoids. Hepatic cells are specialized epithelial cells arranged in plates of one cell thick; they form about 80% of the liver volume and perform many functions endocrine, secretory and metabolic functions. Bile canaliculi are fine ducts spreading between hepatic cells and collect the bile produced by hepatocytes. Hepatic sinusoids are permeable blood capillaries found between the plates of hepatic cells receiving oxygenated blood from the hepatic artery branches and nutrients content of the deoxygenated blood from hepatic portal vein branches, and then pass the blood to a central vein (Tortora & Derrickson, 2009).

The hepatocytes, bile duct system and hepatic sinusoids can be functionally and anatomically organized in two different acceptable models:

2.1.2.1. Hepatic Lobule

The liver lobes composed of many small lobules defined as the classic lobule according to Kiernan (Preedy & Watson, 2007). The lobule is generally hexagonal composed of joined hepatocyte plates with endothelium lined sinusoids separating between them. The centrolobular vein crosses each lobule. This model represents the functional unit of the liver (Tortora & Derrickson, 2009). The portal vein, hepatic artery, the bile canaliculi and the connective tissue which surrounds them, constitute the portal triads and found at the angles of the hexagon (Tortora & Derrickson, 2009).

2.1.2.2. Hepatic Acinus

Recently, scientists accepted this structural and functional unit of the liver that includes portions of two neighboring hepatic lobules. Hepatocytes in the hepatic acinus are grouped into 3 zones based on the blood supply. **Zone 1** is called the peripheral zone **(periportal zone)** as it is situated near the portal tract, zone three surrounds the vena centrolobularis **(centrilobular zone)**, while **zone 2 (midzonal)** represents the liver parenchyma and situated in between zones one and three (Koek *et al*., 2007). The blood enters zone one first, and then flows through the second and the third zones before leaving the liver. Each zone has a specific function. Blood rich in oxygen and nutrients reaches the hepatocytes in zone 1, so many synthetic processes occur in this zone such as albumin production. These

are the first cells which take up glycogen after a meal and store it as glycogen and break down the stored glycogen during fasting. When the bile duct is obstructed or the liver is exposed to toxins, zone 1 cells are the first ones which show morphological changes (Tortora & Derrickson, 2009). Hepatocytes in zone 3 are very sensitive to toxins, while those in zone 2 have intermediated structure and function between those cells of zone 1 and 3 (Tortora & Derrickson, 2009). **(**Figure **2.2)**

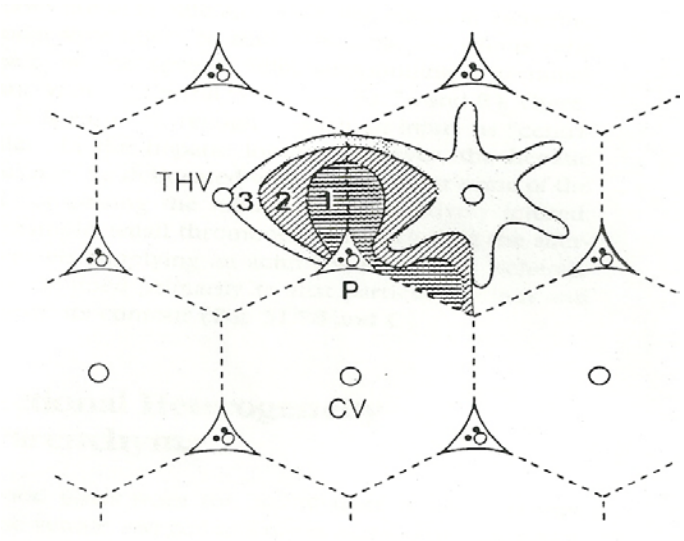

Figure.**2.2**: Diagram showing two Hepatic Acini showing Portal Tract (P), Central Vein (CV), Terminal Hepatic Venule (THV), Periportal zone (1), Intermediate zone (2) and Centrilobular zone (3) (Tortora & Derrickson, 2009).

2.1.3 Hepatic Microstructure

Hepatocytes are polyhedral cells contain well-developed organelles. The rough endoplasmic reticulum synthesizes proteins as plasma proteins, while the smooth endoplasmic reticulum contains **microsomes** that play a role in toxin metabolism (e.g. drugs, some carcinogens and chemicals such as thioacetamide), as well as cholesterol and

bile acid synthesis. **Peroxisomes** perform oxidative reactions using molecular oxygen, involve in the fatty acids oxidation and participate in the metabolism of alcohol. **Mitochondria** are numerous and represent the site of oxidative phosphorylation and energy production. Their number, size and enzymatic properties depend on the position of cell within the hepatic acinus. **Lysosomes** contain scavenging enzymes besides its role in deposition of iron, lipofuscin, bile pigments and copper. **Golgi apparatus** plays a role in secretion of bile acids and albumin (Solter, 2005).

Endothelial cells are fenestrated cells lining the sinusoids. They allow the passage of large protein molecules and prevent the passage of blood cells and some chylomicrons to the perisinusoidal space. In addition, they share with macrophages in scavenging macromolecules.

Kupffer cells are special macrophages having phagocytic function located on the walls of sinusoids and contain lysosomes to break down phagocytized bacteria. They are responsible for clearing antigen-antibody complexes from blood (Solter, 2005).

Hepatic stellate cells (Ito cells) are found between the endothelial lining of sinusoids and the hepatocytes in the **space of Disse**. In quiescent state, they store vitamin A, but on stimulation, they produce collagen fibers and extracellular matrix that is responsible for liver fibrosis then cirrhosis (Dancygier, 2010). They are considered as a major regulator of normal liver homeostasis (Dancygier, 2010).

Pit cells are large granular lymphocytes found within the lumen of sinusoids adjacent to kupffer cells. They have natural killer activity, so they play a role as antitumor and antiviral defense (Nakatani *et al*., 2004).

2.1.4 Biochemical Functions of the Liver

Inside the human body, the liver represents an important regulator (Koek, *et al*., 2007). It is a distinctive organ which functions as a metabolic and biochemical transformation factory (Bacon, 2006). It is essential in maintaining the homeostasis via processing carbohydrates, amino acids, lipids and vitamins; metabolism of toxins and cholesterol; production of clotting factors and storage of glycogen (Heidelbaugh & Bruderly, 2006).

The liver receives substances contained in the blood after being absorbed or secreted by the gastrointestinal organs including the stomach, pancreas, spleen, and the intestine via the hepatic portal vein (Standring, 2008). Through the hepatic artery, the liver receives oxygenated blood. The substances that enter the liver are then modified or re-synthesized completely into new chemicals which are taken back to the blood or to bile to be excreted.

2.1.4.1. Excretory Function

Organic anions such as bilirubin and bile acids found in the sinusoidal blood are extracted, biotransformed and excreted into bile or urine. Haemoglobin metabolism results in the formation of bilivirdin by the action of heme oxygenase and then converted into bilirubin. It is water insoluble, so it is transported in blood attached to serum albumin as unconjugated bilirubin. These organic anions can be assessed by measuring their concentration in blood plasma by special tests (Dancygier, 2010).

2.1.4.2. Synthetic Function

About 48 g of protein is synthesized daily by the liver (Marieb & Hoehn, 2007). The most constituent protein in the blood plasma is **Albumin**. It is responsible for maintaining colloidal osmotic pressure (oncotic pressure) in vascular and extracellular spaces, transporting phospholipids, free fatty acids, amino acids, metallic ions, drugs, bilirubin and hormones (Marieb & Hoehn, 2007). Toxins and alcohol inhibit synthesis of albumin in the liver, so its concentration decreases in the plasma when the liver is injured. **Alpha-1 antitrypsin** is a protein that inhibits leukocyte elastase and protects the tissue from enzymes released by inflammatory cells. Its concentration in plasma decreases in liver diseases. **Transthyretin** is synthesized mainly in the liver to transport thyroxine and retinol. All **clotting factors** and their inhibitors are synthesized in the liver (Mandato *et al*., 2005). Liver diseases inhibit the formation of Transthyretin in the liver. The concentration of a number of proteins changes as a response to the injury of the liver tissue or viruses. The synthetic ability of the liver can be detected by prothrombin time (PT) as it depends on the ability of the liver to produce clotting factors. The degree of liver failure can be detected by the degree of prolongation of PT (Marieb & Hoehn, 2007).

2.1.4.3. Metabolic Function

The liver plays an important role in **carbohydrate metabolism.** In strenuous activities, glycogen is degraded into glucose (glycogenolysis). Hormones and genes as recently

reported control carbohydrate metabolism (Ptitsyn *et al*., 2006). In **fat metabolism,** the liver oxidizes fatty acids to supply energy, synthesize cholesterol, phospholipids and lipoproteins, and synthesize fats from carbohydrates and proteins.

In **protein metabolism**, hepatocytes de-aminate amino acids to be used in ATP production, or converting them into carbohydrates or fats (Tortora & Derrickson, 2009). The removed ammonia from de-aminated amino acids is converted into less toxic urea, which is excreted in urine. The liver keeps constant equilibrium between cellular amino acids and proteins in cells and cellular proteins. In both acute and chronic liver diseases, serum ammonia rises above normal levels (Tortora & Derrickson, 2009).

2.1.4.4. Exocrine Function

Exocrine function of the liver is represented in bile secretion. Hepatocytes secrete daily about 500 ml of bile into biliary canaliculi. Bile is composed of inorganic electrolytes, water in addition to some solutes such as sodium and potassium salts (Marieb & Hoehn, 2007). Secretion of bile results from excretion of bile pigments, steroids, cholesterol and some drugs. Therefore, patients of jaundice have high cholesterol as well as alkaline phosphatase blood level.

2.1.4.5. Storage Function

Vitamin A, $B_{12,}$ D, E and K are stored in large quantities in hepatic stellate cells (Marieb & Hoehn, 2007). Also the liver stores minerals (iron and copper) which are released from the liver when needed by the body.

2.1.4.6. Drug and Xenobiotics' Processing

Xenobiotics are toxic substances to the body such as alcohol and drugs. The body eliminates most of these substances that are water-soluble xenobiotics through the kidneys. Some of these substances are secreted such as penicillin; erythromycin and sulfonamides are secreted into bile (Tortora & Derrickson, 2009). The liver metabolizes lipophylic xenobiotics by two kinds of biochemical reactions. The first phase of reactions involves hepatic **cytochrome P450 enzymes** which metabolize many different drugs. In phase II reactions, a big molecule is attached to the substance to make it less lipophylic and more water soluble to be easily excreted by the body. The elimination of hormones such as thyroid and steroid hormones is one of the common roles of the liver.

2.1.4.7. Phagocytosis Function

Blood cleansing is also one of the crucial roles played by the liver. Cells of the liver phagocytize aged blood cells as well as bacteria leaving the gut and entering the blood.

2.1.5 Liver Cirrhosis

In liver fibrosis, a substantial increase in most matrix proteins are observed especially the interstitial **collagens type I** and **III**. They are not only present in greater amounts, but are deposited in abnormal sites within the liver microanatomy (Dancygier, 2010). Hepatic stellate cells found within the space of Disse and the portal fibroblasts embedded in the connective tissue are the major cell types associated with the formation of scar tissue as a response to liver damage (Antoine *et al*., 2007). The scar tissue replaces the damaged liver cells reducing blood supply and preventing the proper liver function.

2.1.5.1. Role of Stellate Cells and Portal Fibroblasts in Fibrosis of the Liver

Stellate cells activation is the basic event in liver fibrosis which includes two major stages, initiation (pre-inflammatory stage) and perpetuation stage (Friedman, 2002). Stellate cells are initially changed by paracrine stimulation derived by all the surrounding cells including kupffer cells, hepatocytes, platelets, leukocytes and sinusoidal epithelium. Kupffer cells play a major role in the activation process by releasing transforming growth factor TGF-α which stimulates stellate cell proliferation (Friedman, 2002) and TGF-β which stimulates stellate cell extracellular matrix ECM synthesis (Gressner et al., 2007). In addition, kupffer cells secrete matrix metalloproteinase 9 (MMP-9) which activates TGF-β that in turn induces the formation of stellate cell collagen (Li *et al*., 2008). Hepatocytes which are the most abundant types of cells in the liver, share in liver fibrosis by releasing fibrogenic lipid peroxides. Platelets found in the injured liver are powerful source of growth factors (Tsukada *et al.*, 2006) such as platelet growth factor PDGF, TGF-β and

epidermal growth factor EGF. During liver injury, leukocytes also play a role in activating stellate cells by joining with kupffer cells and produce compounds that change the behavior of stellate cells. One of these leukocytes are neutrophils which when activated, act as a specific stimulus to stellate cells collagen synthesis by producing reactive oxygen species ROS (Tsukada *et al*., 2006).

Perpetuation stage of stellate cell activation includes many changes in the cell behavior. Stellate cells start proliferation when induced by PDGF receptors (Iredale, 2007). Cytokine chemo-attractors can stimulate stellate cells to migrate towards them (Kumar & Sarin, 2007). Stellate cell activation by TGF-β generates hepatic fibrosis through increased matrix production. Lipid peroxidation can stimulate ECM production and the effect of these products becomes stronger when there is lack of antioxidants (Brunati *et al*., 2010).

On mechanical stress and repeated injury to hepatic cells or the epithelia of the bile duct, the HSCs together with the portal perivenular fibroblasts become active and transdifferenciate into myofibroblasts. Microfibroblast acitivation is derived mainly by growth factors and fibrogenic cytokines released from Kupffer cells when they are activated. The most prominent pro-fibrogenic cytokine is TGF-β (Rockey, 2005; Schuppan & Afdhal, 2008). When myofibroblasts are activated, they produce excessive amount of collagens, suppress matrix metallproteinases (MMPs) production and overexpression of MMPs inhibitors (TIMP-2 and TIMP-1). TIMP-1 can enhance proliferation of myofibroblasts and inhibit their apoptosis (Schuppan & Afdhal, 2008).

2.1.5.2. The Pathogenic Changes of Fibrosis in Various Liver Diseases

In liver disease induced by alcohol, alcohol changes the bacteria of the gut resulting in an increase in the bacterial flora growth. Lipopolysaccharide increases in portal blood activating Kupffer cells to produce reactive oxygen species through NADPH oxidase (Bataller & Brenner, 2005). The free radicals especially hydroxyl radical which is the most dangerous oxygen radical, may attack and mutate DNA. In addition, free it initiates lipid peroxidation, leads to modifications of amino acids and carbohydrates, oxidizes nucleobases and reduces the level of antioxidants which eliminate ROS and stimulate the activity of cytochrome P450s producing more ROS. Oxidants activate Kupffer cells producing more TNF-α which enhances infiltration of neutrophils in addition to the production of oxidants by the mitochondria of hepatic cells and induces their apoptosis. Acetaldehyde, the main product of alcohol metabolism, activates HSCs and stimulates inflammatory and fibrogenic signal (Purohit & Brenner, 2006).

Hepatitis C virus causes oxidative stress and recruits the inflammatory cells that activate HSC and collagen deposition (Kisseleva & Brenner, 2007). In chronic viral hepatitis, reactive oxygen species develops pathogenic effects through cell signaling which modulate gene expression, cell metabolism and cell death (Choi & Ou, 2006). In addition, oxidative stress enhances proliferation of HSCs increasing their production of matrix and collagen synthesis (Gressner & Weiskirchen, 2007).

In chronic cholestatic disorders, cytokines damage bile duct (Bataller & Brenner, 2005). Biliary cells secrete fibrogenic mediators, which activate portal myofibroblasts as well as perisinusoidal HSCs to secrete ECM. Metals such as iron, chromium and copper

undergo redox cycling and produce reactive oxygen species. Most enzymes that produce ROS contain one of these metals. The presence of such metals in the biological systems in their complex form can increase oxidative stress. For example, accumulation of iron in tissues causes hemochromatosis, which in turn leads to liver cirrhosis as one of its clinical syndromes. Moreover, Oxidative stress leads to mitochondrial DNA mutations that cause abnormal respiratory enzymatic reactions and further oxidative stress (Sligte *et al*., 2004).

In Nonalcoholic fatty liver disease (NAFLD) caused by obesity and increase of blood sugar level, insulin resistance and hyperglycemia elevates the serum level of fatty acids, causing hepatic steatosis. The receptors which activate proliferation of peroxisome and sterol that regulates enzymes responsible for the oxidation and synthesis of fatty acids are inhibited causing accumulation of fats in the liver. Hepatocyte necrosis occurs at this stage accompanied by hepatocytes death and inflammatory mediators that lead to the activation of stellate cells.

2.1.5.3. Symptoms and Complications of Liver Cirrhosis

In early stages of liver cirrhosis many patients are asymptomatic until the complications of the disease appear where approximately 80% - 90% of liver parenchyma is destroyed before liver failure is clinically manifested. However when the liver is distorted and loses its functions, symptoms become apparent. The symptoms are anorexia, loss of weight, itching, feeling fatigue and osteoporosis due to malabsorption of vitamin D and subsequent calcium deficiency (Heidelbaugh & Bruderly, 2006).

With the development of the disease, many complications appear. **Jaundice** is the most specific clinical manifestation of liver dysfunction that is characterized by deposition of bilirubin causing yellow skin, mucous membranes and sclera. In acute hepatitis and bile duct obstruction, bilirubin leaks from the liver to the intestinal tract showing tea-colored urine (Dancygier, 2010). **Portal hypertension** occurs when the portal blood flow is obstructed along its course. Sinusoidal hypertension is caused by liver cirrhosis due to HSCs, myofibroblasts and vascular smooth-muscle cells contraction when they are activated. When portal pressure increases, the metabolic and the synthetic functions of the liver are impaired. **Bleeding esophageal varices** result from the inability of blood to flow through the liver resulting in, more blood flowing through the veins of the esophagus and causing the veins of the esophagus to balloon outward as a result, they rupture causing severe bleeding (Chow & Chow, 2006). **Ascites** that is accumulation of fluid in the peritoneal cavity results from portal hypertension and low serum albumen level (Cárdenas & Chopra, 2002). **Spontaneous bacterial peritonitis** results from intrahepatic obstruction of blood and compromised host defenses leading to prolonged bacteremia, gram-negative bacteria that infect the ascitic fluid (Dourakis & Sevastianos, 2007). Accumulation of toxic substances in the blood stream causes **Hepatic encephalopathy** as a result of liver failure. Toxins such as manganese and ammonia accumulate in the blood and passes to the brain causing damage of neurons. In addition, accumulation of ammonia and glutamine may contribute to brain edema and can alter the expression of various important brain genes (Lemberg & Fernández, 2009). **Hepatorenal syndrome** constricts the blood vessels of the kidneys and dilates blood vessels in the splanchnic circulation, which supplies the intestines (Fernández *et al*., 2007). Kidney function deterioration elevates the creatinine

level of the blood, or slows down the clearance of creatinine in the urine (Levey *et al*., 2003). **Hepatic carcinoma** takes place due to mutation of the hepatic cellular machinery by many factors as viruses and alcohol (Gurtsevitch, 2008).

Cirrhotic cases are usually associated with infertility, so pregnancy is rarely considered in liver cirrhosis. Approximately 15-20 % of pregnant women with Chronic liver disease suffer spontaneous abortion and Variceal bleeding may also occur during labor (Tiribelli & Rigato, 2006). In male patients, gynecomastia and loss of male hair can be seen as a result of the formation of oestrone and oestradiol, and the suppression of degradation of oestradiol in the liver (Schuppan & Afdhal, 2008).

2.1.5.4. Diagnostic Strategies of Liver Cirrhosis

Liver function tests are useful in detecting, diagnosing, evaluating severity and assessing the prognosis of liver dysfunction.

a. Serum liver enzymes

Hepatocyte inflammation causes increase in the enzymes of the liver, alanine aminotransferase (ALT), and aspartate aminotransferase (AST). When the liver cell is damaged, ALT which is a sensitive marker for liver cell damage, leaks into the blood stream showing high ALT blood level. AST is less specific in reflecting liver injury because it is also present in other cells of the body. However, the ratio between ALT and AST blood levels are useful in assessing the etiology of liver enzyme abnormalities in patients (Crosignani *et al*., 2005). Alkaline phosphatase is (AP) an enzyme found in the

cells lining the biliary ducts of the liver, it is also synthesized in bone, intestine and kidneys. High levels of AP may indicate bone or liver damage, so it is necessary to confirm the source of AP if is of hepatobiliary origin or not by measuring another canalicular enzyme such as gamma glutamyl transpeptidase (GGT) which should be normal if the liver is not the source of increased ALP (Dancygier, 2010).

b. Serum bilirubin

Bilirubin metabolism occurs mainly in the liver. Bilirubin is taken up by liver parenchyma, conjugated in the smooth endoplasmic reticulum by being water-soluble (direct) and secreted into the bile. In hepatic injury, the liver does not process enough bilirubin, so it remains attached to albumin in the plasma as unconjugated bilirubin (indirect) (Mukai *et al*., 2012). Total bilirubin measures the amount of both conjugated and unconjugated biliurubin.

c. Complete blood count

Thrombocytopenia that is decrease in blood platelets intensifies the damage and fibrosis of liver tissues. Thrombocytopenia in Liver Cirrhosis results from the utilization of platelets in aggregates with other cells as monocytes. Complete blood count shows the level of platelets depending on the severity of the disease (Panasiuk *et al*., 2007).

d. Prothrombin time

Measurements of prothrombin time determine the synthetic liver function. It is the most prognostic marker in acute liver disease (Giannini *et al*., 2005). Prolonged

prothrombin time reflects deficiency in VII, X, or V prothrombin or fibrinogen, which is usually observed in cases of vitamin K deficiency and liver diseases.

e. Total protein

Total serum protein test determines the total protein content of the blood including albumin and globulin (Higuchi *et al*., 2003). Low serum albumin indicates liver malfunction which usually characterized by ascites. Globulin consists of different proteins and some globulins are formed in the liver, while others are produced by the immune system. The normal ratio of albumin/globulin is greater than 1 because normally albumin is greater than globulin, so less or more ratio than 1 can give clues about problems in the body including liver cirrhosis (Wallach, 2006).

f. Serum cholesterol

The normal total serum cholesterol depends on normal hepatocellular enzymatic activities. In hepatic biliary obstruction, there is a significant rise in the total serum cholesterol, while in hepatocellular diseases, the total cholesterol concentration of the serum may be normal or slightly reduced (Wallach, 2006).

g. Liver biopsy

Liver biopsy is the isolation of tiny samples of liver via percutaneous, transjugular, laparoscopic, operation or CT-guided fine-needle or ultrasonography. The tissue is then processed, stained and examined under the microscope for histological signs of damage or disease (Avunduk, 2008).

2.2 Thioacetamide (TAA)

2.2.1. Properties of Thioacetamide

Thioacetamide (TAA), is an organic compound with the formula CH_3CSNH_2 (Figure **2.3**). It has other IUPAC names, acetothioamide, ethanethioamide and thioacetamidic acid. It is in the form of white crystals under standard conditions, dissolves easily in ethanol and water, has melting point between 110 and 115^{o} C. It is stable compound at room temperature (Cinghită *et al*., 2008).

In laboratories, TAA serves as a source of sulphur in the synthesis of organic compounds such as rubber chemicals, curing agents, cross linking agents, metallurgy, pesticides and pharmaceuticals. In addition, it is used as a stabilizer of motor fuels, in purification of hydrochloric and sulphuric acids and in leather processing (Cinghită, *et al*., 2008). TAA was first used in controlling oranges' decay and then as a fungicide (Madani *et al*., 2008). TAA is still widely used in qualitative inorganic analysis as a substitute for hydrogen sulphide gas (Shen *et al*., 2012).

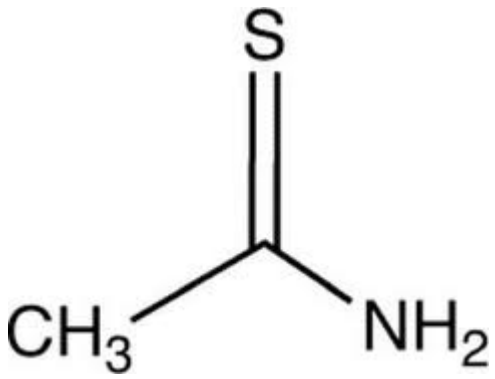

Figure 2.3 Structure of TAA (Cinghită, *et al*., 2008)

Medically, thioacetamide (CH_3-C(S) NH_2) is a hepatotoxin and hepatocarcinogenic, when administered to experimental animals in their diet inducing hepatocellular neoplasms in male rats (Heindryckx *et al*., 2009).

2.2.2 Mechanism of TAA-Induced Liver Cirrhosis

Thioacetamide is broadly used by researchers as a chemical model for inducing acute and chronic liver damage (Muriel & Rivera-Espinoza, 2008). Because of its short half-life, many researchers used TAA to study mechanisms of hepatic necrosis (Murayama *et al*., 2007), it induces a cirrhotic state in the liver that resembles the case in humans (Zimmermann *et al*., 1987), has wide time range between necrogenesis and liver failure. Besides, it has short half-life inside the body (Chilakapati *et al*., 2005).

Inside the body, TAA is metabolized to acetate and excreted via urine within 24 hours. Short time after TAA administration into the diet of the animal, it is turned into TAA-S-Oxide (TASO) by microsomal enzymes CYP2E1 of the hepatocytes, and then converted

into the toxic metabolite thioacetamide S, S-Dioxide ($TASO_2$) **(**Figure **2.4**). $TASO_2$ is then distributed among body organs including plasma, liver, kidney, bone marrow, adrenals and other tissues. During biotransformation of TAA, both Cytochrome P450 (CYP) and Flavin-containing Monooxygenase release superoxide anion, which is changed into the toxic Hydrogen peroxide (Sindhu *et al*., 2006). TAA-induced liver fibrosis is caused by free radical-mediated lipid peroxidation. TAA-induced hepatotoxicity occurs due to the binding of highly reactive $TASO_2$ covalently to the hepatocyte macromolecules (Sindhu, *et al*., 2006) such as lipids, proteins and DNA molecules resulting in hepatocyte necrosis and death. Dead hepatocytes release the pro-fibrogenic cytokine TGF-β and also activate kuppfer cells which consequently release TGF-β and pro-inflammatory cytokines TNF-α and IL-6 (Reeves & Friedman, 2002). These mediators activate HSCs which start proliferation expressing ECM especially type-I collagen (Bassiouny *et al*., 2011). Meanwhile, expression of metalloproteinases together with over-expression of their tissue inhibitors, increase the deposition of ECM (Park *et al*., 2010) (Figure **2.5**).

In chronic TAA-induced toxicity, significant liver fibrosis and common regenerative developing nodules are accompanied by increase in the pressure of the blood in the portal vein and the hyperdynamic circulation attribute of liver cirrhosis (Fan & Weng, 2005).

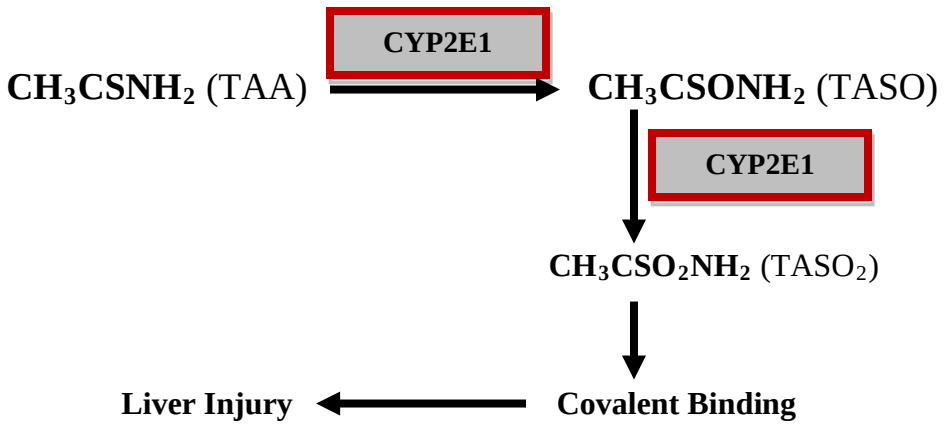

Figure **2.4**: TAA metabolism to $TASO_2$ mediated by CYP2E1 (Chilakapati, *et al*., 2005)

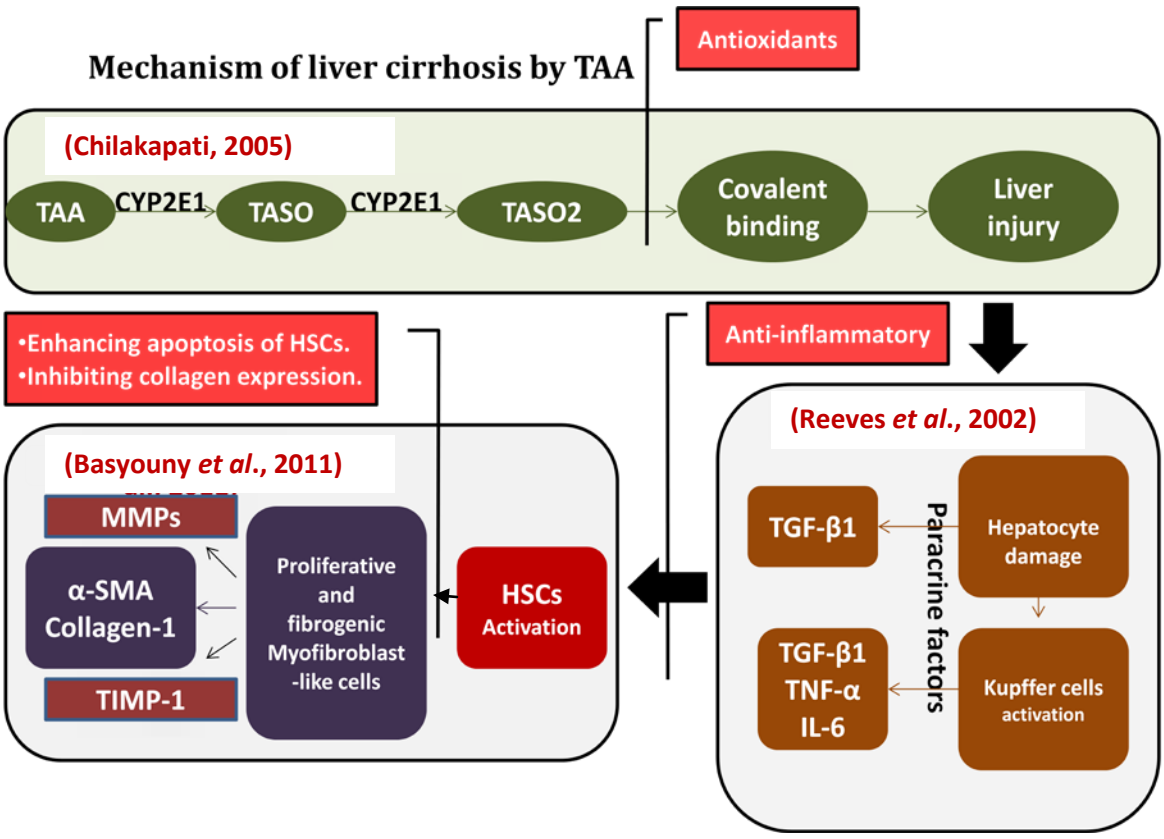

Figure **2.5:** Diagram showing the possible mechanism of TAA-induced liver injury. TAA, thioacetamide; TASO, thioacetamide sulphur oxide; $TASO_2$, thioacetamide sulphur dioxide; TNF-α, tumor necrosis factor α; TGF-β1, transforming growth factor-β1; IL-6, interlukin-6; HSCs, hepatic stellate cells; MMPs, matrix metalloproteinases; α-SMA; alpha smooth muscle actin; TIMP-1, tissue inhibitor of metalloproteinase-1.

2.3. Medicinal Plants

2.3.1. Antioxidant Properties of Medicinal Plants

Synthesized antioxidants such as butylate hydroxyl toluene (BHT) and terbutyl hydroquinone (TBHQ) have been prevented as food additives due to their toxic effect (Damiani *et al.*, 2003). Therefore, the modern strategy is directed towards natural

antioxidants which can be extracted from medicinal plants by the modern techniques of fractionation. These natural antioxidants also should be used with great care due to the possible adverse affects of some of them such as some flavonoids (Cook & Samman, 1996). Antioxidants have different compositions; they may be phenolic compounds such as flavonoids and flavonones or may be nitrogen containing compounds such as chlorophyll derivatives and alkaloids. These compounds play a crucial role in many diseases as cancer (Dimitrios, 2006) and liver cirrhosis such as Silymarin which is a very well recorded antioxidant extracted from the seeds of *Silybum marinum* and it was reported as a highly hepatoprotectant (Girish & Pradhan, 2008).

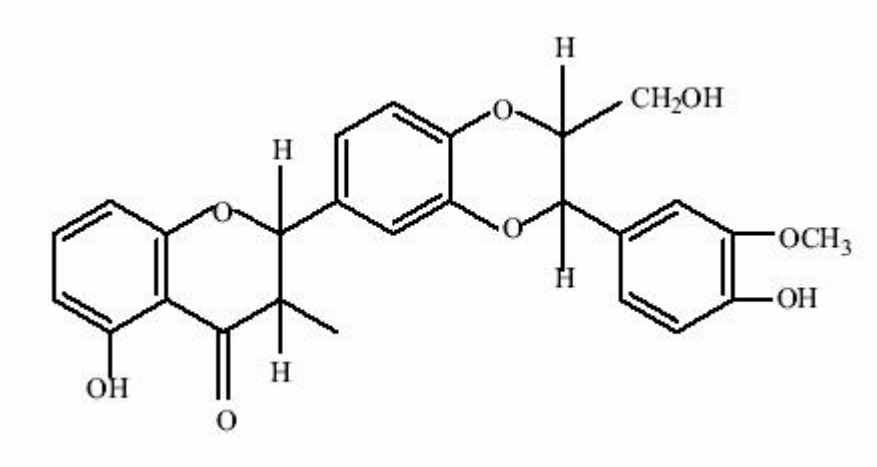

Figure **2.6:** The structure of Silymarin (Singh, 2004)

Many studies have been conducted on Silymarin and reported that it is highly anti-inflammatory antioxidant (Ramasamy & Agarwal, 2008) enhancing the activity of RNA polymerase I that plays a role in blocking the uptake of toxins (Yadav *et al*., 2008). Furthermore, Silymarin has high scavenging capacity to free radicals and strongly inhibit lipid peroxidation (Fraschini *et al*., 2002).

2.3.2. Medicinal Plants and Liver Diseases

Recently, many compounds have been isolated from different medicinal plants and reported to have hepatoprotective activities. The herbal mixture 861 contains mixed chinese herbs and was proved to regulate mRNA expression of α-SMA in HSCs *In vitro* (Wang *et al*., 2008). Rosmarinic acid was proved to enhance apoptosis of HSCs (Zhang *et al*., 2011). Silymarin is a natural product that contains three polyphenol compounds, silybinin, silychristin and silydianin was reported to have high antioxidant power and inhibit HSC activation into myofibroblast (Pradhan & Girish, 2006). Curcumin is a natural product isolated from *C. longa* rhizomes and was shown to have anti-inflammatory properties and inhibit NF-kB (Bruck *et al*., 2007).

2.4 Zingiberaceae Family

2.4.1 Morphology and Distribution

Family Zingiberaceae is one of the largest families from the order Zingiberales. Zingiberaceae species grow naturally scattered in moist, shaded parts of lowland areas and slopes of hills, where the leaves and fleshy rhizomes of most members of the family have aromatic characters when they are both crushed. Several studies showed that the members of the zingiberacae family consist of different active phytochemicals in addition to antioxidative, anti-inflammatory, anticancer and anti-tumour promoting activity (Basak *et al*., 2010).

2.4.2. *Boesenbergia rotunda* (L.)

Figure **2.7**: *Boesenbergia rotunda* rhizomes (http://www.indonesian-culinary.com 2010)

Table **2.1:** Taxonomy of *Boesenbergia rotunda* (L.)

Kingdom	Plantae
Subkingdom	Trachiobionta
Division	Magnoliophyta
Class	Liliopsida
Order	Zingiberales
Family	Zingiberaceae
Genus	*Boesenbergia*
Species	*rotunda*

One of the species of family Zingiberaceae is *Boesenbergia rotunda* (L.), (Figure **2.7**), (Table **2.1**), which is a perennial herb locally known as “Kra-chai” in Thai, “temu kunchi” in Malaysia, Chinese ginger in China and in English, it is traditionally called Fingerroot because of its finger-like rhizomes. It is used commonly in Southeast Asia as folk medicine for treating several diseases such as, stomach discomfort, dysentery and leucorrhea. Moreover, the fresh rhizomes of *Boesenbergia rotunda* is commonly used by natives of Southeast Asia in cooking and its tonics are added to lotions to treat rheumatism and muscle pain (Ching *et al*., 2007).

In Malaysia, Fingerroot plant is popularly known as cekur which is used by almost all households in the Malay custom as culinary plant as well as medication purposes. Drinking the water in which the fresh edible roots are boiled, has a good effect in rejuvenating women after giving birth and the regular drinking of this water can also be anti-aging. It is believed that chewing the bulbous roots helps to treat sore throat. Malay can identify the types of cekur species by a simple practice, rubbing the bulbous roots against the core of banana tree, turning reddish indicates the right species that has good medical properties.

Hexane and chloroform extracts of rhizomes of *Boesenbergia rotunda* (L.) separated three flavanones, pinostrobin, alpinetin and pinocembrin, and the chalcones, boesenbergin A and cardamonin (Ching *et al*., 2007). The ethanolic extract of leaves, stems and rhizomes of B. rotunda showed high contents of Kaempferol and Quercetin (Figure **2.8**), (Yob *et al*., 2011).

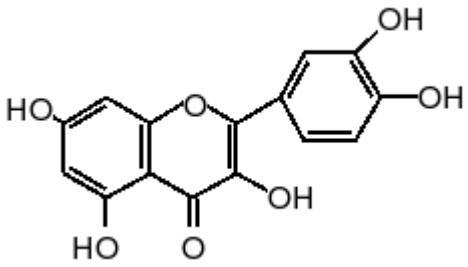

Quercetin (3,3',4'5,7-pentahydroxy flavone)

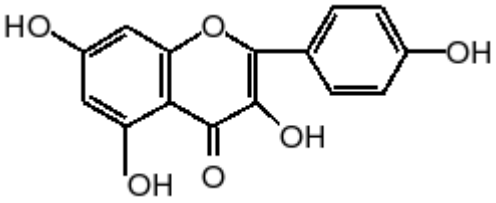

Kaempferol (3,4',5,7-tetrahydroxyflavone)

Figure **2.8:** Chemical structures of Quercetin and Kaempferol (Škerget *et al*., 2005)

Panduratin A is cyclohexenyl chalcone from *Boesenbergia rotunda* rhizomes exhibited many activities *in vitro* and *in vivo* studies such as anticancer (Cheah *et al*., 2011), proapoptosis, antiproliferative, anti-inflammatory, and antioxidant. It has been reported to stimulate anti-inflammatory activity in animals experiment. The bactericidal activity of Panduratin A against biofilm organisms has been reported (Rukayadi *et al*., 2009). It showed suppressive activity to COX-2 in laboratory animal peritoneal macrophages (Yun *et al*., 2006). Cheah, *et al*, (2011) reported that Panduratin A inhibited NF-kB in A549 cells. In addition, Panduratin A provides the protected hepatoma cells

against *t*-BHP-induced damage (Sohn *et al*., 2005). Furthermore, recent studies showed that Panduratin A has Antiangiogenic activity *in vivo* and *in vitro* (Orlikova *et al*., 2011)

2.4.3 *Curcuma longa* (L.)

Figure **2.9:** *Curcuma longa* rhizomes (http://www.ramuantaufiq.com 2011)

Table **2.2**: Taxonomy of *Curcuma longa*

Kingdom	Plantae
Subkingdom	Trachiobionta
Division	Magnoliophyta
Class	Liliopsida
Order	Zingiberales
Family	Zingiberaceae
Genus	*Curcuma*
Species	*longa*

Curcuma longa is another rhizomatous perennial plant species **(**Figure **2.9)** that belongs to the family Zingiberaceae (Table **2.2)**, originally found in South Asia and commonly known as turmeric, indian saffron and curcumin (Bhowmik *et al*., 2009). Recently, studies suggest that it reduces the symptoms of irritable bowel syndrome, ulcerative colitis, and osteoarthritis (Fischer & Mullin, 2012). In Okinawa and Japan, turmeric is used as a Tea, in Pakistan, as a medicine for treating digestive disorders and anti-inflammatory, in Afghanistan and Northwest Pakistan, applied to wounds for cleansing and fast recovery, and in India used in skin creams. Currently, 19 clinical trials have been registered by the U.S. National Institutes to study the effect of turmeric on many clinical disorders (Shehzad *et al*., 2010).

In Malaysia, kunyit is the popular name of Turmeric plant and considered as a common plant for culinary dishes. In addition, it is used as a herbal medicine because people believe in its different medicinal properties. The concoction from boiling turmeric is used to treat irritation in the eyes. Concentrated turmeric oil is used to treat arthritis. The liquid obtained from scraped and pressed turmeric is mixed with egg yolk to treat gastric disorders. Moreover, a published Malaysian article had described the effective use of Kunyit in strengthening gall bladder, degrading blood clot and reducing toxin in liver (Bruck *et al*., 2007).

High Performance Liquid Chromatography of *Curcuma longa* showed that it contains Curcumin, demethoxycurcumin, bisdemethoxycurcumin, ar-turmerone and curlone. Curcumin which is the coloring substance in *Curcuma longa* together with demethoxycurcumin, bisdemethoxycurcumin are known as curcuminoids (Dandekar &

Gaikar, 2003), (Figure **2.10**). Curcuminoids together with sesquiterpenoids were found to decrease blood glucose level in diabetic mice (Nishiyama *et al*., 2005). Curcuminoids also have anticancer activity (Jankun *et al*., 2006) and are inhibitors of HIV-2 and HIV-1 proteases (Itokawa *et al*., 2008). In addition, the oil isolated from of *C. longa* was found to contain many components, ar-turmerone (51.8%), ar-turmerol (11.9%). These studies indicated that *C. longa* is an effective antifungal material (Singh *et al*., 2002).

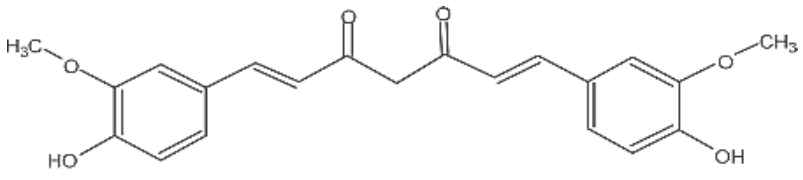

Curcumin

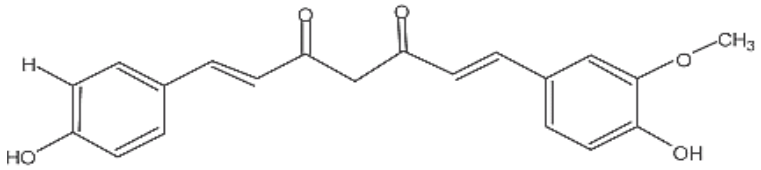

de-Methoxy curcumin

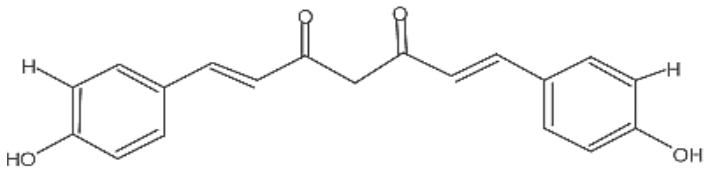

Bis de-methoxy curcumin

Figure **2.10** Chemical structures of Curcuminoids (Dandekar & Gaikar, 2003)

.

Germacrone, is a sesquiterpene component of *C. longa* rhizomes (Jayaprakasha *et al.,* 2005). After 2006, it was found that it significantly enhances the release of cytochrome C and Bok expression out of mitochondria (Liu *et al*., 2012). Researchers reported, germacrone might protect animals against inducers such as D-galactosamine and lipo polysaccharide in liver injury in mice (Yoshikawa *et al*., 2006). It was suggested that germacrone might be a new potent chemopreventive drug candidate for liver cancer *by* regulating protein expression related to the cycle of cell and apoptosis which may be important in the inhibition of human liver cancer cells (Liu *et al*., 2012).

CHAPTER III

METHODOLOGY

3.1. Plant Preparation and Extraction

Plant extraction using solvents with different polar properties have been used in research. Researchers suggested that ethanol is capable of yielding high quantity of the crude extract compared to aqueous extraction due to its polar solvent property, high volatility and higher penetration susceptibility (Pinelo *et al*., 2005). Moreover, the type of the solvent used affects the concentration of the antioxidant compound constituents of the crude extract (Turkmen *et al*., 2006) Therefore, ethanol was selected for plant extraction in the present study. Fresh rhizomes of the plants *Boesenbergia rotunda* and *Curcuma longa* were purchased from a commercial company (Ethno Resources Sdn Bhd, Selangor Malaysia), and identified by comparing them with the voucher specimen deposited at the Herbarium of Rimba Ilmu, Institute of Science Biology, University of Malaya, Kuala Lumpur. After initial washing with tap water followed by distilled water, the rhizomes were sliced and left in the shade for a duration of 10 days to dry. The dried samples were then grounded finely and 100 g of the resulting powder was mixed in 1000 mL 95 % ethanol for 7 days at room temperature. The ethanol extract was distilled under a reduced pressure in Rotary Evaporator (Rotavapor, Buchi R-215, Switzerland), and dried at 40^{o}C in an incubator for 3 days giving a gummy yield of 9.49 % (w/w) for *B. rotunda* and dark yellow gummy yield (7%, w/w) for *C. longa*.

3.2. Evaluation of the Antioxidant Capacity of the Crude Extracts

3.2.1. The Activity of Scavenging DPPH

The scavenging activity of the *B. rotunda* and *C. longa* crude extracts was determined using 1,1-diphenyl-2-picrylhydrazyl radical (DPPH) stable free radical scavenging assay. The purple hue which is usual for free DPPH radical decays and the decrease in the reading of the spectrophotometer at 517 nm can be recorded. This assay evaluates the free radical scavenging capability of the crude extract. The assay was conveyed out according to the procedure explained by (Gorinstein *et al.*, 2003) with little modification. In brief, 1 ml of dimethyl sulfoxide was used to dissolve 1 mg from each ethanolic extract and then diluted to the concentrations (50, 25, 12.5, 6.25 and 3.125 μg/mL), Ascorbic acid and Trolox were utilized as antioxidant standards. An amount of 195 μL of 100 μM DPPH was added to 5 μL from each plant extract and the standards in triplicate. The resulting decrease in the spectrophotometer reading was assessed at 517 nm by UV 1601 spectrophotometer for two hours with twenty minutes gaps. The power of scavenging DPPH radical was determined from the following formula and the analysis of the results was recorded as Mean ± SEM:

% of fundamental scavenging activity = (Abs blank – Abs sample) /Abs blank X100

3.2.2. Ferric Reducing Antioxidant Capacity (FRAP)

The anti-oxidant power of *B. rotunda* and *C. longa* crude extracts was also determined using a test sensitive to its scavenging ability towards reactive oxygen species or reagents containing iron. In this regard, the ferric reducing anti-oxidant power (FRAP)

of both plant extracts was determined using an assay by following the method described in (Benzie & Strain, 1996), with a slight modification. The FRAP reagent was prepared by mixing 300 mM acetate buffer (3.1 mg sodium acetate/ml, pH 3.6), 10 mM 2,4,6-tripyridyl-S-triazine (TPTZ) (Merck, Darmstadt-Germany) solution and 20 mM $FeCl_3.H_2O$ (5.4 mg/mL). The *B. rotunda* and *C. longa* crude extracts, and the standards Ascorbic acid were sampled in amounts of 10 µL of 1mg/mL along with 10 µL of 0.1mg/mL silymarin and added into 300 µL of the reagent TPTZ separately in triplicate. The absorbancies of the resulting mixtures were read using ELISA reader (UV 1601 spectrophotometer, Shimadzu, Kyoto, Japan) at 593 nm wavelength at 0 minute and after 4 minutes. We note that the dynamic range of the instrument was limited to read the dose amounts of 500 mg/kg for the *B. rotunda* and *C. longa* crude extracts and 50 mg/kg dose for silymarin administered to the rats daily, as described below. To compensate this deficiency, we performed the measurements in equivalent amounts obtained by scaling the administered doses up by 20 times, respectively. The purpose of adding Silymarin was to compare the iron chelating power of the plant extracts to Silymarin as a hepatoprotectant compound recently proved for this property (Moayedi *et al*., 2013) The readings from both plant extracts and silymarin were compared against the standards Ascorbic acid and Trolox (Asghar & Masood, 2008).

3.2.3. Total Phenolic Content (TPC) Evaluation

The colorimetric method of Folin Denis using the reagent Folin-Ciocalteau (Merck, Darmstadt, Germany) was performed to measure the total phenolic content of the *B. rotunda* and *C. longa* crude extracts and the result was expressed equivalent to gallic acid (µg GAE/mg extract) (Cunniff, 1995). An amount of I mL DMSO was used to dissole 1 mg

of each crude extract or 0.1 mg of Silymarin was. Next, 20 µL of the extract or Silymarin was added to 100 µL of Folin-Ciocalteau reagent, followed by 3 minutes incubation of the mixture in the dark. Then, the resulting mixture was mixed with 100 µL of Na_2CO_3 solution (1g/10 mL). The final mixture was re-incubated in the dark for 1 h and the spectrophotometer was read at 750 nm wavelength. All procedures were carried out in triplicate. Serial dilution of gallic acid (1 mg/mL DMSO) was used to produce linear standard curve and the absorbance was read at 750 nm.

3.3. Animal Experiments

3.3.1. Animals

One hundred and two wholesome rats of the species *Sprague Dawley* (180-250 g) were used in the experiments on the crude extracts. All the experimental rats were placed in special cages at 25 ± 2°C, given pellet and water and the 12-h light/dark circuits was adjusted to be in a special room prepared for animals at 50–60% humidity. Throughout all the experiments, all animals obtained human care according to the criteria delineated in the "Guide for the Care and Use of lab Animals" prepared by the National Academy of Sciences and released by the National institute of Health. Animal protocols governing all experiments were approved by the Ethics Committee for Animal Experimentation, Faculty of Medicine, University of Malaya, Malaysia PM/07/05/2008/MMA (a) (R) (Appendix I).

3.3.2. Acute Toxicity Study of Crude Extracts

The toxicity of the *B. rotunda* and *C. longa* crude extracts was evaluated in 60 normal healthy *Sprague Dawley* rats by subjecting them significantly to low and high doses of the extract. Rats were assigned equally into 5 groups, each with 6 males and 6 females, labelled as vehicle (5 mL/kg, 10% Tween-20), and 2 g/kg and 5 g/kg for each rhizome extract preparation, respectively (Table **3.1**). The rats were deprived of food but not water prior to the dosing. Food was withheld for another 3-4 hours after the dosing. The animals were observed at 30 min and 2, 4, 8, 24 and 48 hours after the oral administration to detect the onset of clinical or toxicological symptoms. The animals were sacrificed on day 15. Through the jugular vein, blood was collected directly at the time of the sacrifice. Histological and serum biochemical parameters (liver enzymes, lipid profile, plasma protein and Prothrombin time) were determined following the standard methods (Mahmood *et al*., 2010).

Table 3.1 Experimental design of the acute toxicity test of *B. rotunda* and *C. longa* crude extracts

Species	*Sprague Dawley* rats		
Age	6 – 8 weeks		
Number of animals	6 of each sex per dose level, for each rhizome extract		
Dosage	**Low dose groups** 2g/kg *B. rotunda* 2 g/kg *C. longa*	**High dose groups** 5g/kg *B. rotunda* 5g/kg *C. longa*	**Vehicle group** 10% Tween 20
Observation period	14 days		

3.3.3. *In vivo* Hepatoprotective Activity of the Crude Extracts and Silymarin against TAA Toxicity

A set of experiments were carried out to test the therapeutic effects of the *B. rotunda* and *C. longa* crude extracts on liver cirrhosis. For this purpose, 42 male *Sprague Dawley* rats were randomly divided into 7 groups of 6 rats each. The plant extracts and the Silymarin that is used as a standard drug (International Laboratory, USA) were prepared by completely dissolving in 10% Tween 20 and sterile distilled water to be orally administered to animals (5 mL/ kg body weight). The oral acute toxicity test of the ethanol extract of *B. rotunda* and *C. longa* showed no mortality at the highest dose 5 g/kg. Therefore, 5 g/kg was considered LD_{50} cut off dose and 1/10 and 1/20 of LD_{50} were selected (500 mg/kg and 250 mg/kg) for the experiment. The preparation of TAA was done by complete dissolving of its crystals (Sigma-Aldrich, St Louis, MO, USA) in sterile distilled water (Aydın *et al.*, 2010). **Group 1** rats (normal control group) were given oral administration of 10% Tween-20 (5 mL/kg) daily and intraperitoneal injection of sterile distilled water (1 mL/kg) thrice weekly. To induce liver cirrhosis, groups 2–7 were intraperitoneally injected by TAA (200 mg/kg) three times a week. The pathological changes induced by constant exposure of this concentration of TAA were reported to be comparable to the etiology of cirrhosis in humans (Beale *et al.*, 2008). **Group 2** rats (group of cirrhosis control) were by mouth administered 5 ml/kg 10% Tween-20 daily. Rats of **Group 3** (group treated with Silymarin) were by mouth administered a daily dose (50 mg/kg) of Silymarin. Rats of **Groups 4** and **5** were by mouth administered *B. rotunda* extract at daily doses of 250 mg/kg and 500 mg/kg, respectively. Rats of **Groups 6** and **7** were by mouth administered *C. longa* extract at daily doses of 250 mg/kg and 500 mg/kg, respectively. This treatment protocol for rats over an 8 week period with Silymarin or *B. rotunda* extract or *C. longa* extract in parallel; slows

down progression of liver fibrosis and protects the liver from further damage and therefore is considered preventive. At the end of the 8-weeks period of the experiment and after the last treatment, the rats were allowed to fast for 24 hours and sacrificed under ketamine (30 mg/kg, 100 mg/mL) and xylazil (3 mg/kg, 100 mg/mL) anesthesia (Fatemi *et al*., 2010). The blood of the jugular vein from all animals was collected for biochemical tests, prothrombin time, cytokines and apoptotic proteins assessment. Ice cold normal saline was used to wash liver tissues after being excised. Following blotting on filter paper, liver tissues were then weighed, examined for gross pathology and eventually collected for the assessment of cellular damage and histopathology.

Table 3.2: Experimental design of the hepatoprotective effect of *B. rotunda* and *C. longa* crude extracts

Group	Number of animals	Intraperitoneal injection (three times/week)	Oral administration (5mL/kg)	Durations (weeks)
Normal control	6	Sterile Distilled Water (1mL/kg)	10% Tween 20	8
Cirrhosis control	6	TAA	10% Tween 20	8
Reference control	6	TAA	Silymarin 50mg/kg	8
Low dose *B. rotunda*	6	TAA	*B. rotunda* 250mg/Kg	8
High dose *B. rotunda*	6	TAA	*B. rotunda* 500mg/kg	8
Low dose *C. longa*	6	TAA	*C. longa* 250mg/kg	8
High dose *C. longa*	6	TAA	*C. longa* 500mg/kg	8

3.3.3.1. Postmortem Liver Tissue Analysis

For histopathological analysis, the liver specimens were fixed in 10 % buffered formaldehyde, processed by automated tissue processing machine (Leica, Germany) and then embedded in paraffin wax. Sections were prepared in 5 μm-thicknesses, stained with hematoxylin-eosin (H&E) (Budak *et al.*, 2011) and examined under the light microscope. For determining the normality of hepotocytes, the number of normal cells were counted at the center of the cirrhotic area as well as the normal areas adjacent to both sides of the

cirrhotic area using a light microscope with an oil immersion objective (x40) covering 0.15 mm^2 (Al Bayaty *et al*., 2010). Dead hepatocytes could be differentiated by having no or small dark-stained or big dark-stained nucleus, while normal hepatocytes acquired big light-stained nucleus with clear chromatin. Percentage of the normal cells was calculated by using the formula:

% Normal cells = [(Normal cells/ (Normal + dead cells) x 100].

3.3.3.2. Histopathological Analysis

Five µm-thick sections of liver samples were prepared and divided into two groups of slides. One group of slides was stained with hematoxylin and eosin (H&E, Appendix II, P. 182) for routine examination of the liver tissue histopathology and architecture. The second group of slides was stained with Masson's Trichrome (Sigma, USA, Appendix II, P. 184) as a marker for detecting the degree of fibrosis (Zeisberg *et al.*, 2007) and identifying collagen fibers in liver tissues (Edgtton *et al*., 2004). The tissue slides were examined under light microscope and Nikon microscope (Y-THS, Japan) was used to capture digital images (magnification ×20).

3.3.3.3. Biochemical Analysis

For the assessment of specific liver markers, blood samples were collected from all rats into carefully labelled gel-activated tubes. Sodium citrate tubes were used to collect another group of blood samples to determine prothrombin time. After leaving the blood to clot, the gel-activated tubes were transferred to the centrifuge which was adjusted at 3400

rpm for 10 min at 4°C. The resulting samples of serum were collected and divided into aliquots and then kept at -80^{o}C. For measuring the liver markers, alkaline phosphatase (AP), alanine aminotransferase (ALT), aspartate aminotransferase (AST), gamma-glutamyl tranferase (GGT) lactate dehydrogenase (LDH), total protein, albumen and bilirubin and lipid profile, aliquots were sent to the Medical Center of University of Malaya where the samples were spectrophotometrically assayed by standard automated techniques of the Central Diagnostic Laboratory (CDL).

3.3.3.4. Protein Content Assay

Liver tissues from all experimental animals were collected and washed in ice-cold PBS (0.02 mol/L, pH 7.0-7.2) to remove excess blood. One gram of each liver was sampled, mixed with 10 mL PBS (pH 7.2) and then homogenized using HG 15A homgenizer (DAIHAN Sci., Seoul, Korea). The resulting tissue homogenate was centrifuged at 5000 xg for 5 minutes using Rotofix 32 centrifuge (Hettich Zentrifugen, Germany). The supernatant was collected and divided into aliquots and then kept at -80^{o}C till being assayed. The protein content in the liver tissue homogenate collected from all animals was assayed by using bovine serum albumin (BSA) according to (Lowry *et al*., 1951) with slight modification. In brief, 10 serial dilutions of BSA were prepared to the final concentration 100 mg/L. 700 µL of Lowry solution was added to 500 µL of each sample or standard. All samples were designed in triplicate and incubated at room temperature in the dark. After 20 minutes of incubation, 100 µL of diluted 2N Folin-

Ciocalteau's Phenol Reagent (1:1) was added and incubated for 35 minutes followed by reading the optical density at 750 nm.

3.3.3.5. Assessment of Hepatic CYP2E1 Levels

To demonstrate the effect of the crude extracts of *B. rotunda* and *C. longa* rhizomes on the level of CYP2E1 as an important enzyme in the biotransformation of TAA in the liver microsome (Amali *et al*., 2006), the tissue homogenate from all rats was tested for the level of CYP2E1 enzyme by following the instructions of Uscn Life Science sandwich enzyme immunoassay (E90988Ra, China, Appendix II p. 185). Briefly, 100 µL of the sample was incubated with pre-coated capture antibody specific to CYP2E1 in duplicate in 96-well plate for 2 hours at 37^{o}C. After brief rinsing, the sample was incubated for 1 hour at 37^{o}C with 100 µL of biotin-conjugated secondary antibody followed by three times washing using 350 µL washing buffer (1x). 100 µL Streptavidin-Horse radish peroxidase (HRP) was added to the sample and incubated for 30 minutes at 37^{o}C followed by 5 repeated washes. 90 µL Tetramethylbenzidine (TMB) was added to the sample as a colorimetric reagent and incubated for 20 minutes. Finally, the reaction was stopped using 50 µL of H_2SO_4 and the absorbance was read at 450 nm.

3.3.3.6. Evaluation of Oxidative Stress Markers

(a) Urine 8 Hydroxy Deoxyguanosine (8-OH-dG)

Oxidative damage of DNA due to free radicals-induced oxidative stress, produces (8-OH-dG) (Valavanidis *et al*., 2009) and therefore it serves as an established oxidative stress marker (Beckman & Ames, 1997). For this purpose, clean urine samples from all

animals were collected 24 h before sacrifice by tickling the back of the animal gently while holding its tail and collecting the urine in 5 mL clean polystyrene disposable beakers after cleaning the periurethral area of the animal (Kurien *et al*., 2004). Collected urine samples were kept at –80°C before assaying for OH-dG levels following the instructions of the manuals (Genox KOG-HS10E, USA, Appendix II, p. 190). Briefly, in triplicate in a 96-well microtiter plate, pre-coated with monoclonal antibody specific for 8-OH-dG, 50 µL of clear urine sample was incubated at 4^{o}C overnight. The plate was then washed 5 times with concentrated buffered saline (pH=7.4). 100 µL of biotinylated secondary antibody was added to the sample and incubated for one hour at room temperature followed by 3 times washes. 100 µL of the chromatic solution tetramethylbenzidine (TMB) was added and incubated at room temperature for 15 minutes in the dark. 100 µL of the reaction terminating solution (1M phosphoric acid) was added and the plate was read at 450 nm.

(b) Hepatic Nitrotyrosine

Nitrotyrosine, as a marker of protein oxidation (Bruck, *et al*., 2007) was assessed in the liver of animals by ELISA immunoassay guided by the manufacturer's instructions (MyBiosource MBS722419, USA, Appendix II, p. 193). Succinctly, 100 µL of the sample was incubated with monoclonal Nitrotyrosine-HRP conjugate in duplicate in a microtiter plate. After one hour of incubation, the plate was washed 5 times using 350 µL wash solution (x1). 100 µL of substrate specific to HRP enzyme was added to the sample followed by 50 µL stop solution and the intensity of the produced colour was measured spectrophotometrically at 450 nm.

(c) Hepatic Malondialdehyde (MDA)

Malondialdehyde levels were measured in the liver tissue homogenate of all experimental groups as a measure for lipid peroxidation (Del Rio *et al.*, 2005) using thiobarbituric acid according to the manufacturer's instructions (Cayman Cat. # 10009055, Appendix II, p. 199). To 100 µL sample or standard, 100 µl of the provided SDS solution was added followed by the addition of 4 mL of the colour reagent. Samples and standard solutions vials were kept in boiling water for 1 hour and the reaction was stopped by immediate incubation in ice bath for 10 minutes. All vials were then centrifuged at 1600 xg for 10 minutes at 4^{o}C and 150 µL of each sample or standard was loaded onto 96-well plate in duplicate, and then the absorbance was read at 532 nm.

3.3.3.7. Antioxidant Enzyme Assessment

Superoxide dismutase (SOD) catalase (CAT) and glutathione peroxidase (GPx) enzymes were determined in the liver homogenates collected from all animal groups using Cayman kits according to the manual's instructions (Cayman Cat. # 706002, # 707002 and # 703102 respectively, Appendix II, PP. 205, 212 and 219). SOD activity was evaluated by tetrazolium salt detecting superoxide radicals produced by the action of xanthine oxidase on hypxanthine. Bovine erythrocyte SOD was used to represent SOD standard curve. Tetrazolium salt solution (200 µL) was added to 10 µL standard or sample followed by fast addition of 20 µL of 8 xanthine oxidase to initiate the reaction. The plate was covered and incubated for 20 minutes on a plate shaker (Barnstead Dubuque, USA) and the reading of

the spectrophotometer was recorded at 450 nm. CAT activity was evaluated by the chromagen, 4-amino-3 hydrazino-5-mercapto-1,2,4-triazole which measures the formaldehyde produced by the reaction of CAT enzyme with methanol in the presence of H_2O_2. The standard curve was obtained by catalase formaldehyde standard. 100 µL of assay buffer and 30 µL of methanol were added to 20 µL of standards/samples and the reaction was initiated by fast addition of 20 µL of H_2O_2. The plate was incubated in the dark at room temperature for 20 minutes, followed by the addition of 30 µL of potassium phosphate buffer to terminate the reaction. An amount of 30 µL of the chromagen was added and the plate incubated on the shaker at room temperature in the dark. After 10 minutes of incubation, 10 µL of catalase potassium periodate was added and the plate covered and then left for five minutes on the shaker at room temperature before recording the reading of the spectrophotometer at 540 nm. The principle of GPx assay depends on the indirect measure of GPx activity by a coupled reaction. GPx reduces hydroperoxide into the oxidized form glutathione (GSSG) which is recycled by NADPH into its reduced form glutathione reductase (GR). All assays where performed in triplicate.

3.3.3.8. Assessment of Cytokines

Sera aliquots collected from all rats were assayed for transforming growth factor-beta (TGF-β1) as a fibrogenesis-driving cytokine (Gressner *et al*., 2007) by ELISA as per the manufacturers' instructions (Abnova, KA0416, USA, Appendix II, P. 225). Briefly, the capture antibody was diluted with the sample buffer provided and added onto 96-plate pre-coated with anti-rat antibody specific to TGF-β After the recommended incubation period,

biotinylated anti-rat specific antibody was added and left incubated at 37^{o}C in the dark. Following 3 washes with the provided wash buffer, the samples and the standards were incubated in with streptavidin-HRP conjugate which was finally removed by 5 washes with the wash buffer. The wells were then incubated with the colorimetric reagent TMB and the reaction was stopped so that to read the absorbance at 450 nm. The concentrations were calculated by the optical density measurements from the obtained standard curve. The nuclear transcription factor NF-κB and the pro-inflammatory cytokine interlukin IL-6 as important signals in liver injury (Mandrekar & Szabo, 2009) were assayed in the sera aliquots by enzyme-linked immunosorbent assay in duplicate following the instructions of the manufacturer (Uscn Life Science, China E91824Ra, for NF-κB and E90079Ra for IL-6, Appendix II, P. 230 and 235).

3.3.3.9. Pro-apoptotic Bax, Anti-apoptotic Bcl-2 and caspase-3 Assessment

Based on many studies, it was found that the triad Bax, Bcl-2 and caspase-3 are involved in the apoptosis of hepatocytes during liver injury (Elsharkawy *et al*., 2005) To demonstrate the effect of *B. rotunda* and *C. longa* rhizome extracts on the apoptosis of liver cells, rat Bax ELISA kit (Uscn Life Science E91824Ra, China), rat Bcl-2 ELISA kit (Uscn Life Science E90778Ra, China), and rat caspase-3 ELISA kit (Uscn Life Science E90626Ra, China) (Appendix II, PP. 238, 241 and 244) were used to evaluate the expression of Bax, Bcl-2 and caspase-3 in the sera aliquots collected from all rats. Prior to use, sera samples stored at -80^{o}C were warmed up in 37^{o}C bath and then assayed in duplicate according to the instructions supplied by the company. The absorbance was read at 450 nm and the concentration ratio of Bax/Bcl-2 was calculated.

3.3.3.10. Evaluation of Matrix Metalloproteinase enzymes (MMP-2 and MMP-9) and TIMP-1

Matrix metalloproteinase enzymes (MMP-2 and MMP-9) and their partial regulator tissue inhibitor of metalloproteinase (TIMP-1) play a role in liver damage (Okazaki *et al*., 2003). For this purpose, the following assay was conducted to perform the effect of *B.* rotunda and *C. longa* rhizome extracts on these enzymes in the liver tissue homogenate collected from the rats of all groups as mentioned previously and assayed in duplicate by enzyme-linked immunosorbent assay kit following the kits' manuals (Uscn Life Science E90100Ra, E90553Ra and E90552Ra, China, Appendix II, PP. 247, 250 and 253).

3.3.3.11. Immunohistochemistry

Using poly-L-lysine-coated slides, liver sections were prepared and heated in an oven (Venticell, MMM, Einrichtungen, Germany) for 25 minutes at 60^{o}C. After heating, xylene was used to deparaffinize and graded alcohol to rehydrate liver sections. Sodium citrate buffer was used for antigen retrieval. The steps of immunohistochemistry staining were performed following the manual's instructions (DakoCytomation, USA, Appendix II, P. 256). In brief, 0.03% hydrogen peroxide sodium azide was used to block the endogenous peroxidase for 5 min followed by washing the tissue sections gently with wash buffer and then incubated with Bcl-2–associated X protein (Bax) (1:500), Proliferating Cell Nuclear Antigen (PCNA) (1:200) and anti-apoptotic protein Bcl2 (1:50) (Santa Cruz Biotechnology Inc, California, USA) biotinylated primary antibodies for 15 minutes. After incubation, sections were re-washed gently using wash buffer and kept in the buffer bath in a humid

chamber. Sections were then incubated for 15 min with Streptavidin-HRP followed by washing. Further, sections were incubated with diaminobenzidine-substrate chromagen for over 7 min followed by washing and hematoxylin counterstaining for a period of 5 seconds. A solution of weak ammonia (0.037 mol/L) was used in dipping the sections 10 times. The sections were then washed and cover slipped. Light microscopy was used to examine the brown-stained positive antigens. Light microscopy was used to examine the brown-stained positive antigens.

3.3.4. Isolation of Compounds from their Crude Extracts

3.3.4.1. Instrumentation

(a) Column Chromatography

Agilent XDB C-18 Reversed phased column, dimensions 4.6 x 250 mm and Particle size, 5.0 μm.

(b) HPLC Components

Agilent 1100 Series Diode Array and Multiple Wavelength Detectors

HPLC parameters

Volume of injection: 100 μL

Solvents: A: Acetonitrile **,** B: Milli-Q Water (Millipore, USA) (0.25% acetic acid)

Flow rate: 1.2 mL/ min

Post run: 2 minutes

Table 3.3: HPLC gradient conditions

Time	A%	B%
0	45	55
10	45	55
15	60	40
20	60	40
25	80	20
30	45	55
32	45	55

(c) LCMS components

Instrument: Agilent 1200 Series HPLC system with Capillary pump and degasser, micro-well plate sampler with thermostat, and Agilent 6520 Accurate-Mass Q-TOF mass spectrometer with dual ESI source.

LC Parameters:

Column Used: UHC small molecule chip with 500 nL enrichment column and 75 µm x 150 mm separation column packed with Zorbax 80SB-C-18 5µm material.

Solvents for capillary pump: (A) 0.1% formic acid in water (B) 90% acetonitrile in water with 0.1% formic acid.

Solvents for Nano pump: (A) 0.1% formic acid in water (B) 100% acetonitrile in water with 0.1% formic acid.

Injection Volume: 1µL.

Flow Rate: Capillary pump 4 µL/min and Nano pump 0.4 µL/min.

Table 3.4: LC gradient conditions

Time (min)	A%
Initial	95
10	95
17	95
17.1	40

Sample Analysis: Isocratic run with Acetonitrile + 0.1% Formic acid for 30 minutes

MS Parameters:

Ion Polarity: Positive & Negative

Vcap: 3500V

Fragmentor Voltage: 125V

Skimmer: 65 V

OCT 1 RF Vpp: 750 V

Drying Gas: 5L/ min

Gas Temperature: 300°C

Nebulizer: 30 psig

Ref nebulizer: 1 psig

Data Acquisition: MS only mode. For Positive Polarity: range 103-1500 m/z

For Negative Polarity: Range 115-1000 m/z

3.3.4.2. Isolation of Panduratin A Compound from *B. rotunda* Crude Extract

A quantity of 2.67 g *B. rotunda* crude (BR) was dissolved in 1 mL acetone (Merck AR Grade, Malaysia), solvent. The resulting concentrated crude alcoholic extract solution was then mixed with 5 g silica gel (Silicycle, Ultrapure Silica Gel, Canada) and dried using rotary evaporator to form sample powder. The sample powder obtained was subjected to dry-pack column chromatography (CC) containing 47 g of silica gel. The fractionation/isolation step was based on gradient elution method and the solvent system used was Hexane-Ethyl acetate (Fisher Scientific AR Grade, UK). A total of 11 fractions afforded (Figure **1**). A Thin Layer Chromatography (Merck, Silica gel 60 F254, Japan) experiment of the 11 fractions versus Paduratin A standard (98% purity, China) was carried out using Hexane-Ethyl acetate (Fisher Scientific AR Grade, UK) at ratio 95:5. Fraction BR-3 was prepared in high and low concentrations (10 and 1 mg/ml respectively) using acetone solvent (AR grade, Merck) for TLC profiling. Pure crystals (96.6%) of Panduratin A were obtained as confirmed by High Performance Liquid Chromatography (HPLC) report according to the following formula,

% Purity = Peak Area of Panduratin A/ (Total Peak Area-Peak Area of solvent)

The mass of the isolated panduratin A was determined by LCMS using METLIN DATABASE.

3.3.4.3. Yield of Panduratin A compound

A quantity of 28 g of *B. rotunda* alcoholic extract was fractionated by dry packed column chromatography as previously mentioned. A column of 5 cm was used to fractionate 10 g of the crude extract giving a yield of 2.87g. Pale yellow crystals of pure panduratin A were obtained and prepared for evaluating the hepatoprotective activity of Panduratin A *in vivo*.

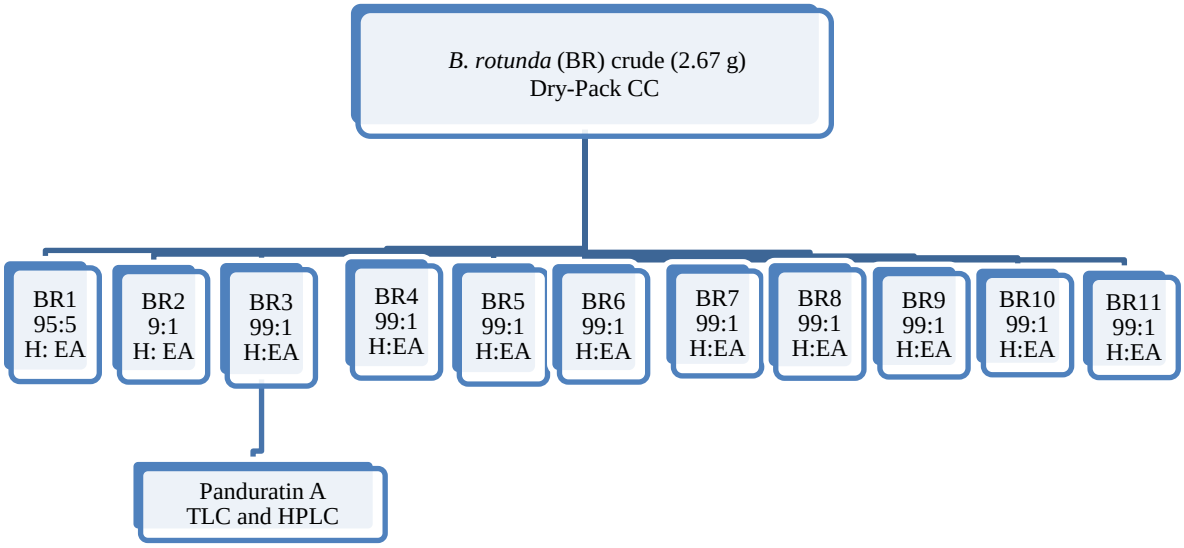

Figure 3.1: Flow Chart fractionation of *B. rotunda* (BR) crude extract using dry pack column chromatography (CC). H: Hexane, EA: Ethyl acetate, TLC: Thin Layer Chromatography, HPLC: High Performance Liquid Chromatography.

3.3.4.4. Isolation of Germacrone Compound from *C. longa* Crude Extract

A quantity of 9.5 g of *C. longa* crude sample was dissolved in 1 ml acetone solvent (Merck AR Grade, Malaysia). The resulting solution was mixed with 50 g of silica gel (Silicycle, Ultrapure Silica Gel, Canada) and dried using rotary evaporator to form sample powder.

The sample powder obtained was subjected to column chromatography (CC) containing silica gel. The amount of silica gel (150 g) used was based on the ratio of 1 g of crude extract to 15 g of silica gel. The fractionation/ isolation step was based on gradient elution method and the solvent system used was Petroleum ether- Ethyl acetate (Fisher Scientific AR Grade, UK). A total of 18 fractions afforded (Figure **3-2)**. A Thin Layer Chromatography (TLC) (Merck, Silica gel 60 F254, Japan) experiment of the 18 fractions versus Germacrone standard was carried out using Hexane- Ethyl acetate (Fisher Scientific AR Grade, UK) at ratio 95: 5. Fractions 1-4 (CL-1-4) were combined and dried using rotary evaporator and weighed using analytical balance.

Purification of Germacrone from CL-1-4

2.65 g of the combined fraction sample (CL-1-4) was dissolved in 1 ml hexane solvent (Fisher Scientific AR Grade, UK). The sample was subjected to column chromatography (CC) containing silica gel (Silicycle, Ultrapure Silica Gel, Canada). The amount of silica gel (27 g) was based on the ratio of 1 g of crude extract to 10 g of silica gel. Hexane- Ethyl acetate solvent system was used. A total of 21 fractions were afforded (Figure **3-2**) from the fractionation. A thin Layer Chromatography (TLC) experiment was performed using Hexane- Ethyl acetate (Fisher Scientific AR Grade, UK) at ratio 95: 5 on all the fractions. TLC was observed under UV light at 254 nm and was stained with 15% Concentrated Sulphuric acid (Fisher Scientific AR Grade, UK) in ethanol (Fisher Scientific 96%, Malaysia) to confirm the presence of Germacrone. The mass of the isolated Germacrone was determined by LCMS and the library used in identification was METLIN DATABAS.

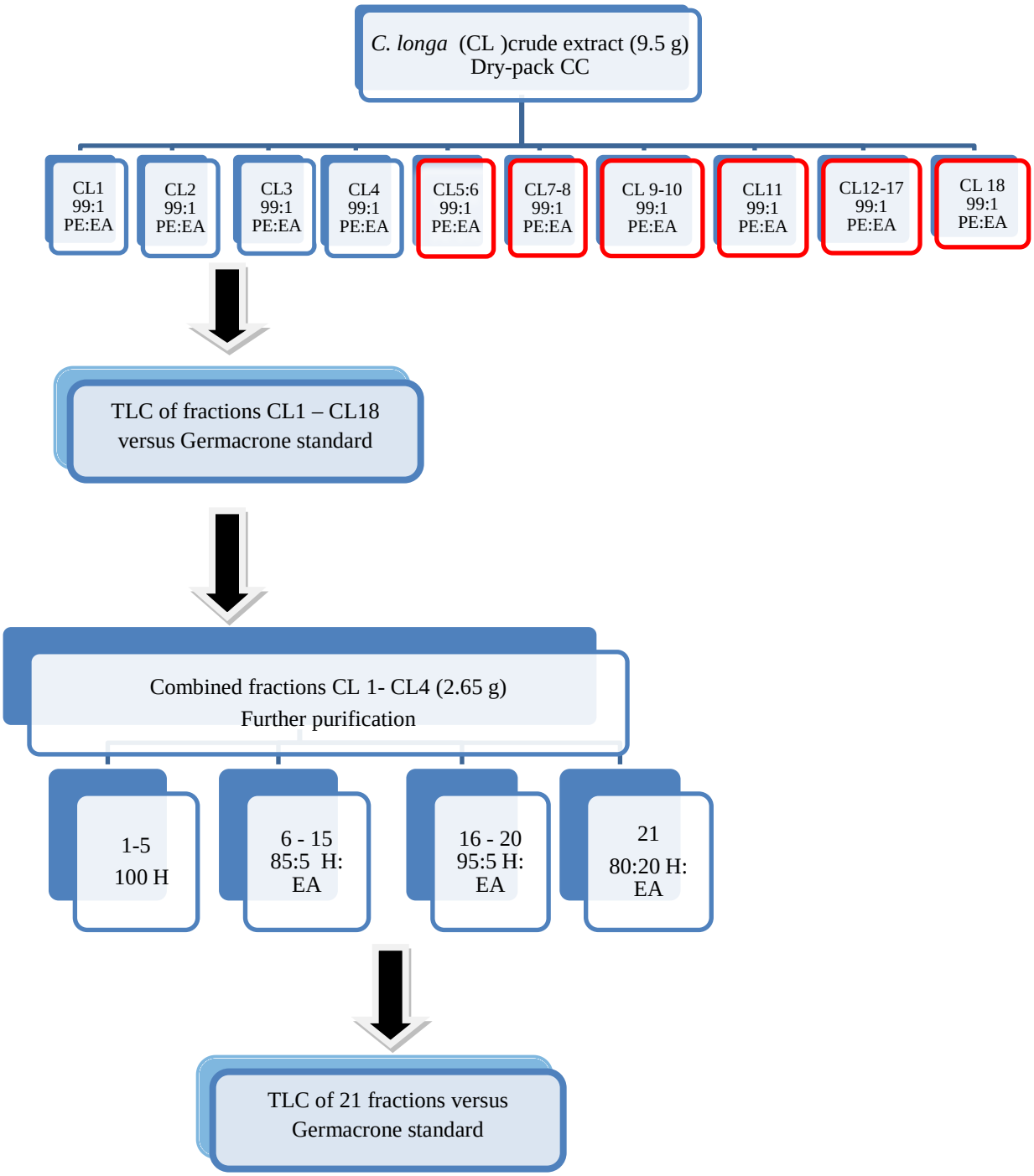

Figure 3.2: Flow Chart fractionation of *C. longa* (CL) crude extract. CC: Column Chromatography. H: Hexane, EA: Ethyl acetate, PE: Petroleum Ether, EA: Ethyl acetate. TLC: Thin Layer Chromatography.

3.3.5. *In vitro* Protective Activity of Panduratin A and Germacrone against TAA-Induced Oxidative Damage in WRL-68

3.3.5.1. DPPH Scavenging Activity of Panduratin A

The antioxidant capacity of the isolated compound PA was examined first by using 1,1-diphenyl-2-picrylhydrazyl radical (DPPH) stable free radical scavenging assay as previously described in section 3.2.1 compared to Ascorbic acid as a standard.

3.3.5.2. Cell Culture

Human normal liver cell line (WRL-68) was purchased from American Type Culture Collection ATCC (Rockville, MD, USA) and allowed to grow in RPMI-1640 (Sigma-Aldrich, UK) (Sato *et al.*, 2004) formulated with 10 % (v/v) FBS (J R Medical, Inc, USA) and penicillin-streptomycin solution of concentration1% (v/v) (Sigma-Aldrich, UK). WRL-68 cell line was grown and maintained at 37° C, 5 % CO_2 incubator (NuAire, Plymouth, USA).

3.3.5.3. Determination of the IC_{50} Dose of TAA Cytotoxicity

To induce cell oxidative damage by TAA and to determine the dose of TAA that kills 50 % of cells (IC_{50}), WRL-68, normal cells (Passage 24) were seeded onto 96-well sterile plates with flat bottoms (Jet Biofil, China) for tissue culture in 100 µL of RPMI-1640 containing 10% FBS with density 3000 cells/ well. Cells were incubated at 37^{o}C and 5% CO_2 for 24 hours. An amount 10 µL of different concentrations 0.03, 0.04, 0.05 g/mL TAA was added to the cells according to (Sarkar & Sil, 2007) with slight modification. TAA was prepared by dissolving each dose separately in sterile distilled water. The cells

were designed (Table **3.3**) in 4 separate experiments for 30, 60, 90 and 120 minutes, each in triplicate and the cell viability was calculated every time by Trypan blue dye (Sigma, UK) exclusion test MTT (Bove *et al*., 2001) after 30, 60, 90 and 120 minutes of incubation, while the absorbance was read at 570 nm. The percentage of cell viability was calculated by the following formula,

$$\% \text{ Cell viability} = [(O.D_{\text{TAA-treated cells}} / O.D_{\text{Sterile-D.W-treated cells}}) \text{ X } 100]$$

Table 3.5: Experimental design (x4) for determining IC_{50} of TAA

Group	Treatment in 100 µL RPMI-1640		
Control	10 µL sterile D.W	10 µL sterile D.W	10 µL sterile D.W
TAA 0.03 g/mL	10 µL TAA	10 µL TAA	10 µL TAA
TAA 0.04 g/mL	10 µL TAA	10 µL TAA	10 µL TAA
TAA 0.05 g/mL	10 µL TAA	10 µL TAA	10 µL TAA

TAA: Thioacetamide, D.W: Distilled water

3.3.5.4. Evaluation of Cytotoxicity of Panduratin A and Germacrone Compounds

To test Panduratin A and Germacrone compounds for their cytotoxicity in WRL-68, the compounds were prepared in concentrations 1, 10 and 100 µg/ mL (Sarkar & Sil, 2007)

by complete dissolving of each dose separately in 2.5% DMSO and then adjusting the volume to I mL RPMI-1640. Cells were seeded in 200 µL of RPMI-1640 containing 10% FBS and 1% penicillin-streptomycin solution with density 3000 cells/well in 96-well plate and incubated at 37^{o}C and 5% CO_2 for 24 hours. Cells were then treated with 10 µL of the mentioned concentrations and designed in 3 separate experiments for 24, 48 and 72 hours. Twenty four hours after each period, 10 µL of the yellow MTT (3-(4,5-Dimethylthiazol-2-yl)-2,5-diphenyltetrazolium bromide, a tetrazole) was added into each well and re-incubated for 4 hours under the same conditions. The purple formazan colour in the mitochondria of the cells results from the reduced MTT indicating living cells (Liu *et al*., 1997). Directly after incubation, the contents of all the wells were removed followed by the addition of 100 µL of DMSO (Fisher Medical, UK) to each well to read the absorbance at 570 nm using energy trend x340 ELISA Audience (Bio-Tek Equipment, Inc., Winooski, VT, USA). Each experiment was demonstrated in triplicate and the % cell viability was calculated.

3.3.5.5. Evaluation of the Protective Effect of Panduratin A and Germacrone Compounds against TAA-Cytotoxicity in WRL-68 Cell Line

Cells were seeded in 200 µL RPMI-1640 containing 10% FBS and 1% penicillin-streptomycin solution with density 3000 cells/well in 96-well plate and incubated at 37^{o}C and 5% CO_2. After 24 hours, cells were treated with a single dose of 0.04 g/mL TAA (10 µL) except Normal control group cells. All cells were incubated for one hour and then Silymarin as a reference drug, Panduratin A and Germacrone compounds were added in the

prepared concentrations 1, 10 and 100 µg/mL. Each dose of the mentioned compounds and Silymarin was prepared by dissolving the required dose in 2.5% DMSO and adjusting the volume to 1 mL using RPMI-1640. Cells were designed in 3 separate experiments each in triplicate and incubated for 24, 48 and 72 hours. The cell viability test was performed for all the cells and the absorbance was read at 570 nm to calculate the % cell viability.

Table 3.6: Experimental design for the *In vitro* hepatoprotective activity of Panduratin A and Germacrone compounds compared to Silymarin

Group	Toxic substance (TAA 0.04 mg/mL)	Treatment
Normal control	–	–
Toxin control	10 µL	–
Si1 1µg/mL Silymarin	10 µL	10 µL
Si10 10 µg/mL Silymarin	10 µL	10 µL
Si100 100 µg/mL Silymarin	10 µL	10 µL
Pa1 1 µg/mL Panduratin A	10 µL	10 µL
Pa10 10 µg/mL Panduratin A	10 µL	10 µL
Pa100 100 µg/mL Panduratin A	10 µL	10 µL
Ge1 1 µg/mL Germacrone	10 µL	10 µL
Ge10 10 µg/mL Germacrone	10 µL	10 µL
Ge100 100 µg/mL Germacrone	10 µL	10 µL

3.3.5.6. Assessment of MDA and SOD

To evaluate the protective effect of Panduratin A and Germacrone against TAA-induced oxidative damage, the following experiment was conducted to assess the level of the antioxidant enzyme SOD and MDA resulting from oxidative damage in the cell lysate collected from all samples. WRL-68 cells were seeded and incubated with 10 µL TAA (0.04 g/mL) and then 10 µL of Silymarin, Panduratin A and Germacrone compounds was added, each in the concentrations (1, 10, 100 µg/mL) as mentioned previously. After 72 hours of incubation at 37^{o}C and 5% CO_2, all the cells were washed twice with 300 µL Phosphate Buffered Saline (PBS), pH 7.4. The cells were detached using a sterilized scrapper, lysed in 25 mmol/L Tris-HCl lysis buffer, sonicated on ice (10 seconds pulse) and then centrifuged at 13000 x g for 15 minutes to remove the cell debris. The resulting cell lysates were collected and kept at -20^{o}C for assaying SOD and MDA following the instructions in the kit manuals of Cayman kits, USA (Cat. # 706002 for SOD, and # 10009055 for MDA).

3.3.6. *In vivo* Hepatoprotective Effect of Panduratin A against Induced Liver Damage in Rats

3.3.6.1. Animals

Thirty healthy male *Sprague Dawley* rats (180-250 g) were used in the experiment. All rats were kept at 25 ± 3°C in an animal room and the humidity was maintained at 40-60%, the animals were given tap water and standard pellet diet. During the experiments, animals were treated following the criteria outlined in the "Guide for the Care and Use of Laboratory Animals" prepared by the National Academy of Sciences and published by the

national Institute of health. The approval of the study was processed by the Ethics Committee for Animal Experimentation, Faculty of Medicine, University of Malaya, Malaysia PM/28/08/2009/MAA.

3.3.6.2. Evaluation of Hepatoprotective Activity of Panduratin A Compound

Animals were at random separated into 6 groups of 5 rats each. **Group 1** Rats (Normal group) were given 10% Tween-20 daily by oral administration and sterile distilled water (1 mL/kg) by intraperitoneal injection 3 times every week. TAA and Silymarin were prepared as mentioned earlier in our study. Groups 2–5 were intraperitoneally injected by TAA (200 mg/kg) three times per week to induce liver cirrhosis. **Group 2** rats of (group of cirrhosis control) were by mouth administered a daily dose of 5 mL/kg, 10% Tween-20 daily. **Group 3** rats (Silymarin-treated group) were by mouth administrated Silymarin (50 mg/kg) everyday. Rats of **Groups 4, 5** and **6** (groups treated with different doses of Panduratin A) were by mouth administered PA compound at everyday amounts of 5 mg/kg, 10 mg/kg and 50 mg/kg (Hamed *et al.*, 2011; Lee *et al.*, 2003), respectively (Table **3.7**) . At the end of the 4 weeks, the animals were allowed to fast for 24 h after and sacrificed under ketamine (30 mg/kg, 100 mg/mL) and xylazil (3 mg/kg, 100 mg/mL) sedation (Fatemi, *et al*., 2010). Blood was taken out through the jugular vein and gathered for biochemical tests. After excising the livers of animals, they were cleaned in ice normal saline, weighed, properly and analyzed for any possible pathological changes in the gross and then gathered for histopathology study. After normal saline washes, 50 mM cold potassium phosphate buffer (pH 7.4) was used to prepare liver tissue homogenates (10% w/v). Liver samples

were then homogenized using a teflon homogenizer (Polytron, Heidolph RZR 1, Germany). A refrigerated centrifuge (Heraeus, Germany) was used to centrifuge liver tissue homogenates at 4500 rpm for 15 minutes at 4°C and the collected supernatant was divided into aliquots.

Table 3.7: Animal experimental design for the *in vivo* hepatoprotective effect of Panduratin A

Group	Number of animals	Intraperitoneal injection (three times/week)	Oral administration (5mL/kg)	Durations (weeks)
Normal control	5	Sterile distilled water (1mL/kg)	10% Tween 20	4
Cirrhosis control	5	TAA	10% Tween 20	4
Reference control	5	TAA	Silymarin 50mg/kg	4
Low dose PA	5	TAA	Panduratin A 5mg/Kg	4
Medium dose PA	5	TAA	Panduratin A 10mg/kg	4
High dose PA	5	TAA	Panduratin A 50mg/kg	4

3.3.6.3. Biochemical Study

Samples of blood from all animals were collected into gel-activated tubes for the evaluation of particular liver markers as previously explained in section 3.3.3.3.

3.3.6.4. Liver Malondialdehyde (MDA) Level

To evaluate the degree of lipid peroxidation in liver, malondialdehyde level was determined in the liver tissue homogenate of animals using thiobarbituric acid according to the company's guidelines (Cayman packages, Sigma cat # 10009055, Appendex II, p. 199) and protein concentration was assessed by Lowry *et al*. (1951) method as mentioned previously.

3.3.6.5. Antioxidant Enzymes (SOD, CAT and GPx) Assessment

The antioxidant enzymes, superoxide dismutase (SOD), catalase (CAT) and Glutathione peroxidase (GPx) were assayed in the liver tissue homogenates by Cayman packages according to the company's guidelines (Cayman) as previously mentioned (Appendix II, P. 205 and 212)

3.3.6.6. Histopathology

Liver samples collected from all experimental animals were prepared for H&E and Masson’s Trichrome staining as previously mentioned in sections 3.3.3.1 and 3.3.3.2.

3.3.6.7. Immunohistochemistry

Sections of liver tissues were prepared and processed as previously mentioned in section 3.3.3.11.

3.3.7. Statistical Analysis

Statistical analysis of the results was performed by SPSS (Version 18, SPSS Inc., Chicago, IL, USA). Data were analyzed by following one-way ANOVA and Tukey Post-Hoc Test analysis. Statistically, $P<0.05$ value was considered significant on comparing the data between two groups. All values were mentioned as Mean ± SEM.

CHAPTER IV

RESULTS

4.1. Antioxidant Properties of *B. rotunda* and *C. longa* Extracts

4.1.1. The Scavenging Activity of the Crude Extracts to DPPH

The percentage DPPH inhibition of *B. rotunda* (BR) and *C. longa* (CL) extracts are illustrated in Figure **4.1**. Results showed that *B. rotunda* rhizome extract exhibited IC_{50} 68.33 ± 1.67 μg/mL which was significantly higher than that of *C. longa* extract (10.81 ± 0.60 μg/mL) and the standards Ascorbic acid and Trolox (4.07 ± 0.88 and 9.32 ± 0.40 μg/mL respectively). In addition, IC_{50} of CL (10.81 ± 0.60 μg/mL) was found to approach the value of Trolox (9.32 ± 0.40 μg/mL). Results indicate that the ability of BR to scavenge DPPH is lower than that of CL which has better scavenging activity that approaches the capacity of the standard Trolox.

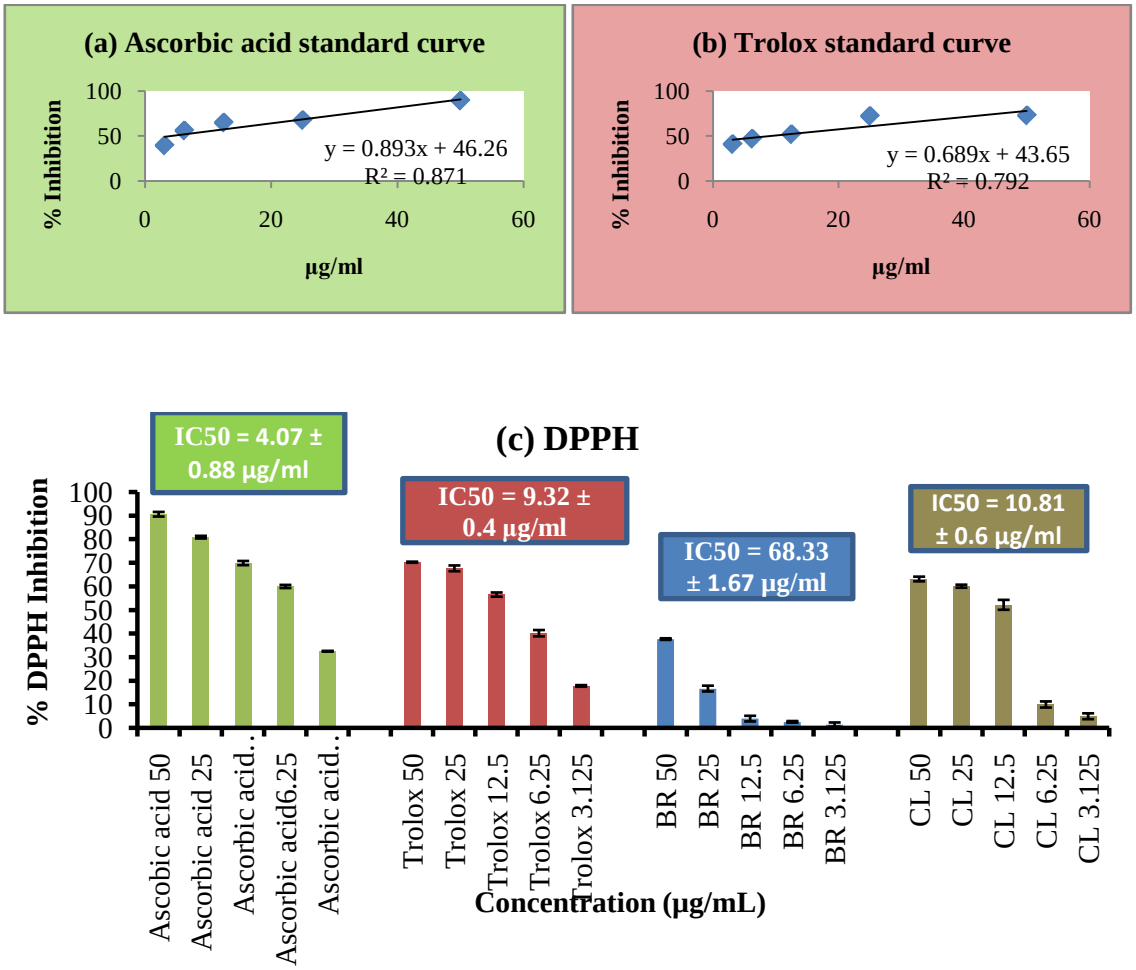

Figure 4.1: (a) Ascorbic acid standard curve **(b)** Trolox standard curve **(c)** Antioxidant activity of the *B. rotunda* (BR) and *C. longa* (CL) extracts compared with the standards, Ascorbic acid, and Trolox.

4.1.2. FRAP capacity of the Crude Extracts

As illustrated in Figure **4.2**, the ferric reducing antioxidant power (FRAP) of *C. longa* extract was significantly higher ($P<0.001$) (1738.22 ± 5.25 mmol FeII/mg) than that of *B. rotunda* (BR) extract which measured 282.30 ± 3.35 mmol FeII/mg. The measured value from both plant extracts were sigificantly lower than the ferric reducing power of the standard Ascorbic acid (1888.33 ± 6.94 mmol FeII/mg respectively) but comparable to the

reference drug silymarin, which read 603.56 ± 4.34 mmol FeII/0.1mg. Based on these readings, it is reasonable to extrapolate that CL extract has high antioxidant activity and BR extract must be containing sufficient acceptable level of anti-oxidant activity, supporting its free radical scavenging property, in helping the liver maintain its status quo.

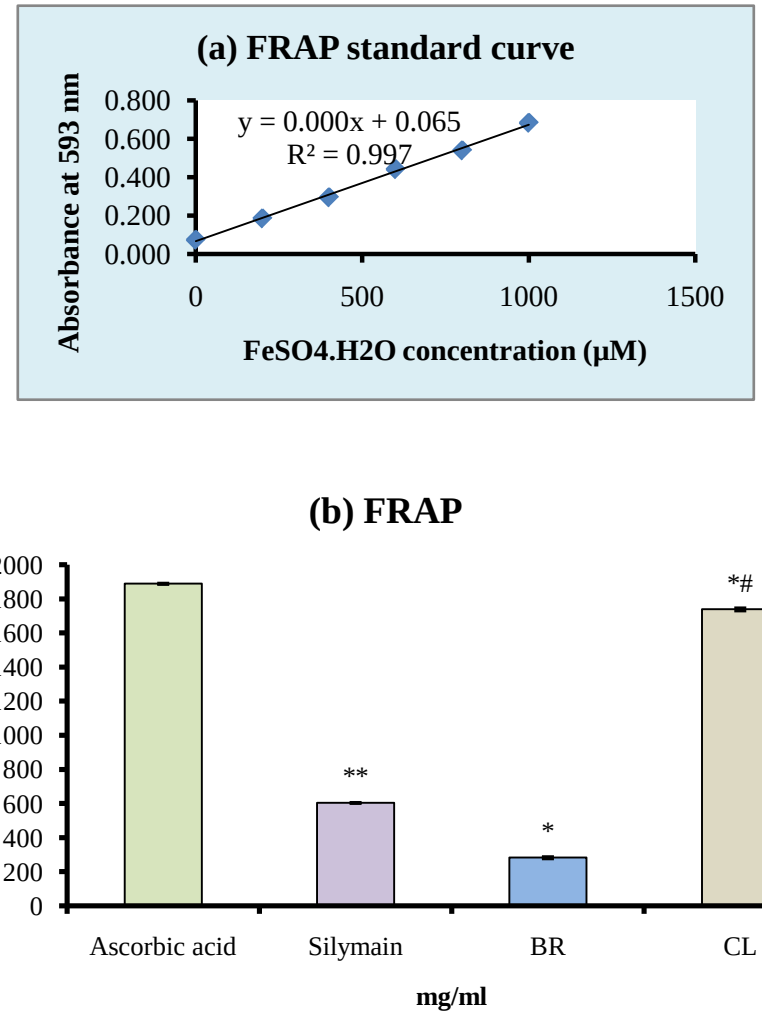

Figure 4.2: (a) FRAP standard curve **(b)** Ferric reducing power (FRAP) of the *B. rotunda* (BR) and *C. longa* (CL) extracts compared with the standard Ascorbic acid as well as the standard drug Silymarin. Values were expressed as Mean ± SEM. $^{*}P< 0.001$ compared to silymarin. $^{\#}P<0.001$ compared to BR. $^{**}P< 0.001$ compared to Ascorbic acid

4.1.3. TPC of Crude Extracts

Figure **4.3** shows the total phenolic content of 1 mg of BR and CL extracts compared to 0.1 mg Silymarin. Results showed that TPC of BR and CL extracts were significantly higher (P<0.001) (338.12 ± 7.51, 485.44 ± 14.30 µg GAE/mg extract respectively) than the TPC of 0.1 mg Silymarin (128.40 ± 2.81 µg GAE/0.1 mg extract). Moreover, there was no significant difference between the TPC value of CL and BR. These results show that both plants extracts have high phenolic content that may explain their hepatoprotective activity.

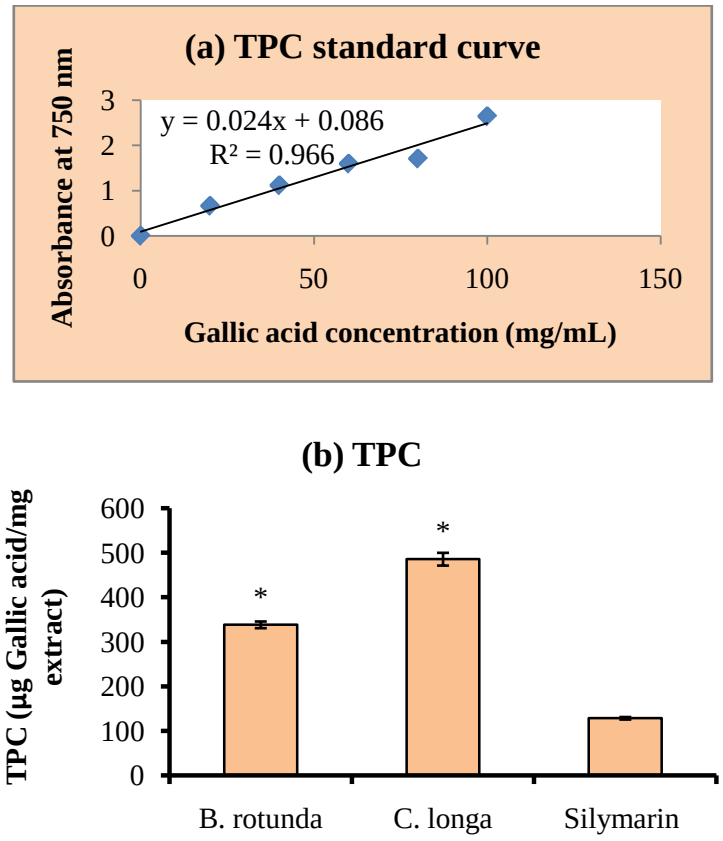

Figure 4.3: Total phenol content (TPC) of the *B. rotunda* and *C. longa* extracts compared with the standard drug Silymarin in gallic acid equivalent. Values were expressed as Mean ± SEM. *P<0.001 compared to Silymarin.

4.2. Acute Toxicity of Crude Extracts

Following administration of *B. rotunda* and *C. longa* crude extracts, all animals were alive and did not show any signs of toxicity even at the highest dose used (5 g/mL). The physical observations indicated no signs of changes in their skins and furs, eyes and mucus membranes, behavior patterns, tremors, salivations, diarrhea occurrences and sleep. The body weight of the treated male and female rats increased gradually but were not significantly different as compared to those of the control rats (Table **4.1**). No significant differences in the clinical observations, serum biochemistry (Tables **4.2** and **4.3**) and histopathology of liver and kidney (Figure **4.**4) were detected between control and treated groups.

Table 4.1: Effect of *B. rotunda* and *C. longa* extracts on the body weights of rats measured from the acute toxicity test

Group	Body weight on Day 0 (g)	Body weight on Day 14 (g)
Vehicle (5 ml/kg)	196.37 ± 7.36	202.21 ± 9.54
Low dose *B. rotunda* (2g/kg)	199.28 ± 10.20	216.12 ± 11.20
High dose *B. rotunda* (5g/kg)	195.10 ± 6.02	214.60 ± 3.63
Low dose *C. longa* (2g/kg)	191.83 ± 3.31	210.33 ± 6.54
High dose *C. longa* (5g/kg)	199.00 ± 5.97	218.33 ± 7.62

Data were recorded as mean ± SEM. No significant changes among the groups. Significant value was at $P<0.05$.

Table 4.2: Effect of *B. rotunda* and *C. longa* extracts on the renal function measured from the acute toxicity test on rats.

Dose	Sodium (mmol/L)	Potassium (mmol/L)	Chloride (mmol/L)	Urea (mmol/L)	Creatinine (µmol/L)
Vehicle (5 ml/kg)	138.25 ± 0.45	5.03 ± 0.19	104.03 ± 0.15	5.63 ± 0.41	50.18 ± 1.34
Low dose *B. rotunda* (2 g/kg)	137.65 ± 0.43	5.21 ± 0.16	102.61 ± 1.22	4.96 ± 0.43	48.97 ± 0.81
High dose *B. rotunda* (5 g/kg)	137.21 ± 0.51	4.89 ± 0.15	102.67 ± 0.76	5.93 ± 0.39	48.60 ± 1.80
Low dose *C. longa* (2 g/kg)	143.31 ± 2.11	5.14 ± 0.39	103.46 ± 2.04	4.97 ± 0.58	39.00 ± 2.71
High dose *C. longa* (5g/kg)	140.67 ± 2.67	5.09 ± 0.40	103.70 ± 1.52	5.27 ± 0.52	38.82 ± 3.14

The values were expressed as mean ± SEM. There were no significant differences between the three groups. Significant value was at $P<0.05$.

Table 4.3: Effect of *B. rotunda* and *C. longa* extracts on the liver function measured from the acute toxicity test on rats.

Dose	Total protein (g/L)	Albumin (g/L)	TB (µmol/L)	AP (IU/L)	ALT (IU/L)	AST (IU/L)	GGT (IU/L)
Vehicle (5 ml/kg)	71.37 ± 1.44	11.36 ± 0.53	1.91 ± 0.17	134.78 ± 9.57	53.05 ± 3.27	153.65 ± 9.35	4.91 ± 0.93
Low dose *B. rotunda* (2 g/kg)	71.47 ± 0.52	11.61 ± 0.34	2.18 ± 0.16	133.37 ± 8.63	51.90 ± 1.33	156.07 ± 3.56	5.00 ± 1.23
High dose *B. rotunda* (5 g/kg)	71.81 ± 1.03	11.72 ± 0.16	1.88 ± 0.21	135.13 ± 6.52	52.27 ± 3.25	155.00 ± 5.35	5.32 ± 1.07
Low dose *C. longa* (2g/kg)	71.17 ± 1.28	12.76 ± 0.58	2.15 ± 0.16	66.90 ± 5.40	39.17 ± 3.16	62.48 ± 2.63	4.08 ± 0..45
High dose *C. longa* (5g/kg)	69.17 ± 1.85	12.26 ± 0.64	1.85 ± 0.46	70.08 ± 11.12	34.50 ± 2.91	55.17 ± 4.83	4.67 ± 0.33

TB: Total bilirubin; AP: Alkaline phosphatase; ALT: Alanine aminotransferase; AST: Aspartate aminotransferase; GGT: Gamma-Glutamyl Transferase. The values were expressed as mean ± SEM. There were no significant differences between the three groups. Significant value was at $P<0.05$.

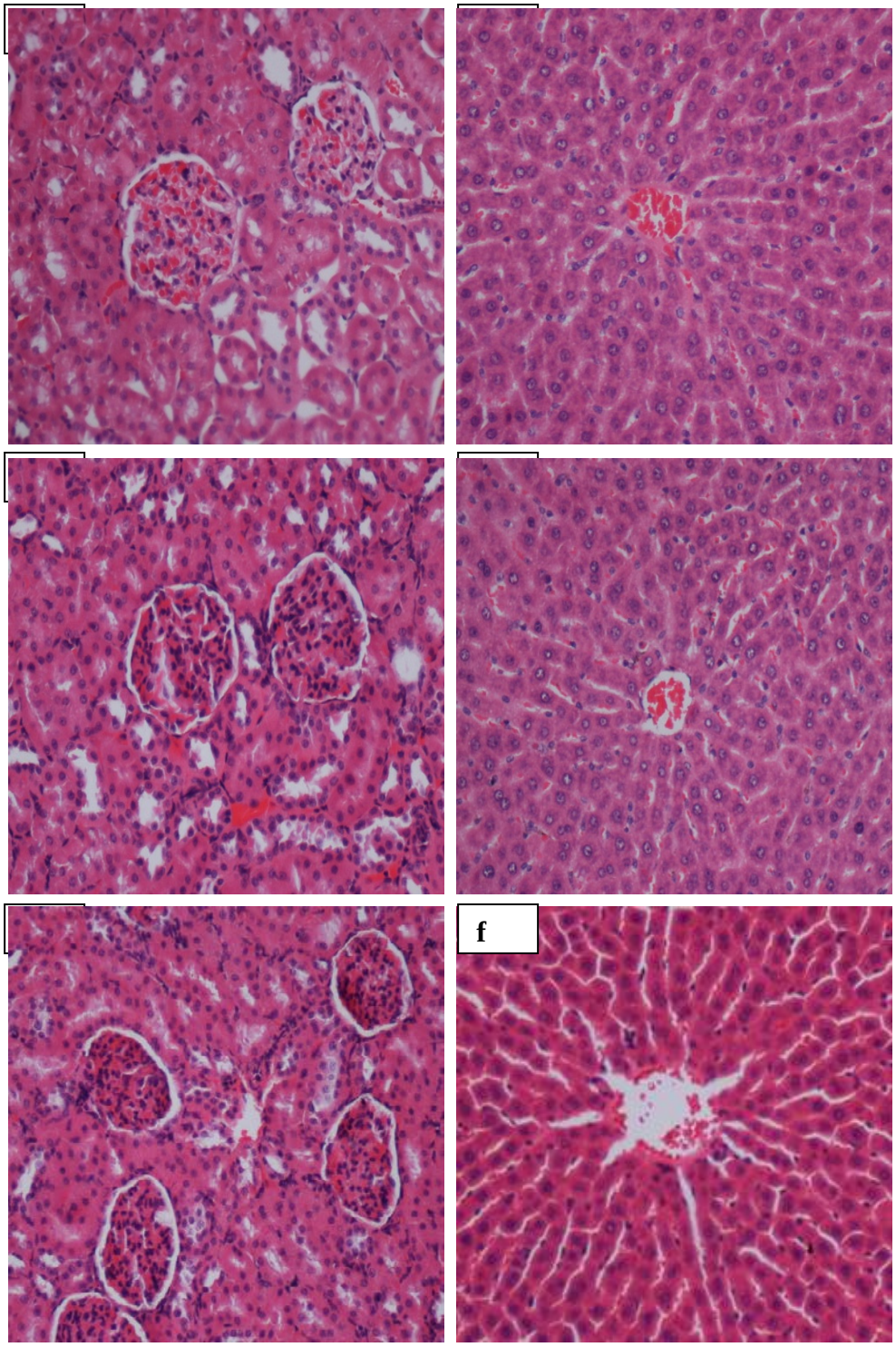
f

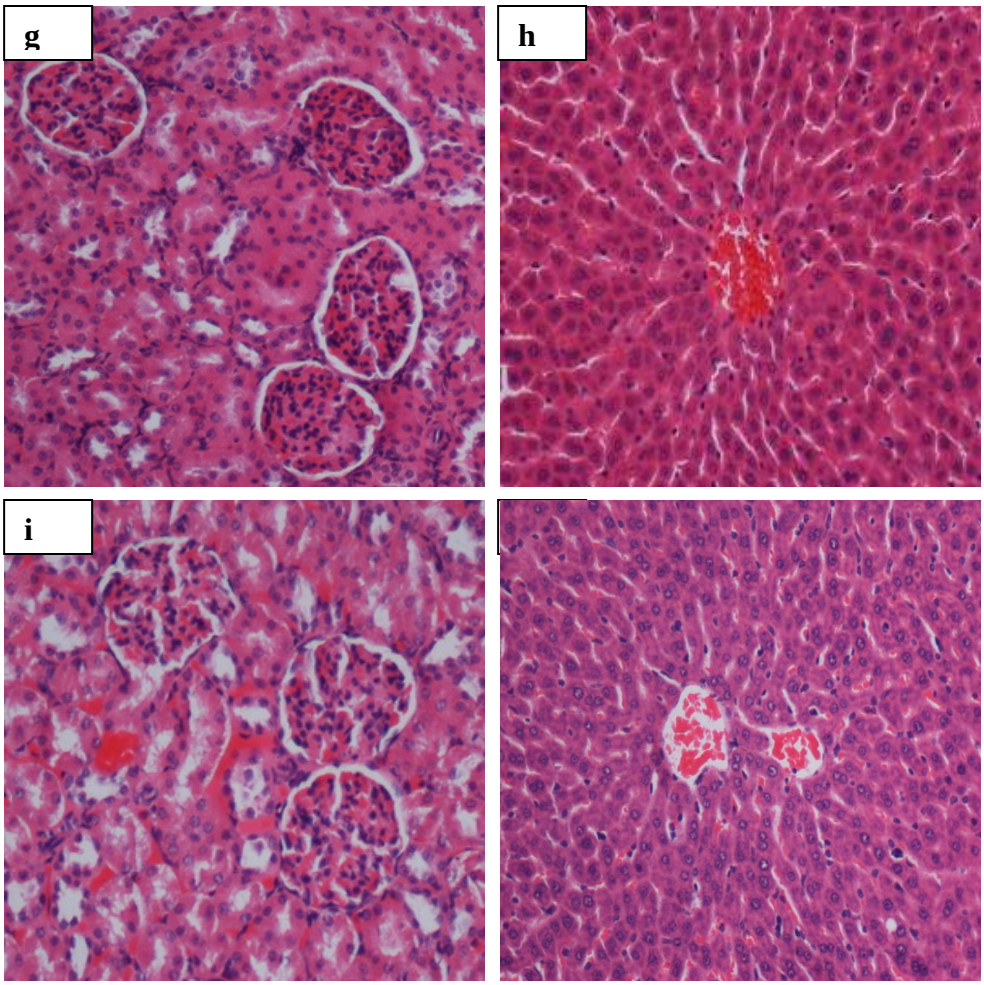

Figure 4.4: Histological sections (H&E) of livers (right column) and kidneys (left column) obtained from the rats in the acute toxicity test. Rat with the kidney and liver shown in **(a)** and **(b)** was treated with 5 ml/kg vehicle (10% Tween 20). Rat with the kidney and liver shown in **(c)** and **(d)** was treated with 2 g/kg (5 ml/kg) dose of the *B. rotunda* extract. Rat with the kidney and liver shown in **(e)** and **(f)** was treated with 5 g/kg (5 ml/kg) dose of the *B. rotunda* extract. Rat with the kidney and liver shown in **(g)** and **(h)** was treated with 2 g/kg (5 ml/kg) dose of the *C. longa* extract. Rat with the kidney and liver shown in **(i)** and **(j)** was treated with 5 g/kg (5 ml/kg) dose of the *C. longa* extract. There was no significant difference in the structures of the liver and kidney between the treatment and control groups. (Original magnification x20)

4.3. Hepatoprotective Effect of *B. rotunda* and *C. longa* Extracts on Liver Cirrhosis

4.3.1. Body Weight and Liver Index

Before sacrifice, the total body weight of each rat was measured. Rats from the normal control group followed a normal growth pattern and obtained a normal weight gain from 184.33 ± 2.08 g on Day 0 reaching 346.51 ± 3.57 g after 8 weeks experimental period. Rats of cirrhosis group had retardation of their growth and their body weight decreased significantly ($P<0.05$) than other groups. When the body weights were factored in, rats from cirrhosis control group measured the highest liver index. The rats treated with high dose of *B. rotunda* extract (500 mg/kg), attained weights equivalent to Silymarin-treated rats, while the rats treated with high dose *C. longa* extract attained weights equivalent to those of normal control group. Further, the rats treated with the low dose (250 mg/kg) *B. rotunda* and *C. longa* acquired increase of body weight more than those of cirrhosis control group but not like those animals of silymarin-treated group and high dose *B. rotunda* or *C. longa*-treated groups (Table **4.4**) which gained better body weight. These findings suggest that high dose *B. rotunda* and *C. longa* could be choicest since their attenuating efficacy to cirrhosis progression was as effective as Silymarin.

Table 4.4 Effect of *B. rotunda* and *C. longa* crude extracts on the liver index measurements from the rats at the end of the 8 week study

Group	Initial Body Weight (gm)	Final Body Weight (gm)	Liver Weight (gm)	Spleen Weight (gm)	Liver Index (%)
Normal control (10% Tween 20, 5ml/kg)	184.33 ± 2.08	346.51 ± 3.57	9.70 ± 0.12	0.57 ± 0.01	2.79 ± 0.15
Cirrhosis control (TAA i.p, 200mg/kg)	180.33 ± 0.33	183.03 ± 1.64**	9.44 ± 0.53	0.54 ± 0.01	5.17 ± 0.04**
Reference control (Silymarin 50 mg/kg)	227.5 ± 9.73	346.70 ± 2.53*	10.28 ± 0.47	0.61 ± 0.17	2.97 ± 0.25*
Low dose *B. rotunda* (250 mg/kg)	186.83 ± 2.70	245.92 ± 2.06*	10.03 ± 0.38	0.53 ± 0.13	3.93 ± 0.38$^{\#}$
High dose *B. rotunda* (500 mg/kg)	256.33 ± 10.81	376.40 ± 4.01*	9.71 ± 0.57	0.60 ± 0.01	2.59 ± 0.25*
Low dose *C. longa* (250 mg/kg)	187.00 ± 2.92	249.17 ± 14.89*	8.80 ± 0.29	0.55 ± 0.01	3.58 ± 0.19*
High dose *C. longa* (500 mg/kg)	216.17 ± 10.08	351.00 ± 19.73*	9.48 ± 0.19	0.68 ± 0.01	2.74 ± 0.15*

Data were expressed as Mean ± SEM. Means among groups (n = 6 rats/group) *P<0.001compared to cirrhosis control. **P<0.001compared to normal control group with. $^{\#}P$<0.01 compared to cirrhosis control group.

4.3.2. Gross anatomy and histopathology

Figures **4.5** and **4.6** respectively depict the gross appearances and the H&E stained sections of liver samples from the experimental groups 1-7. Grossly, the livers from the normal control group rats appeared in reddish color had smooth surfaces and did not show any sign of nodules. The histological examination showed normal liver architecture with normal plates of hepatocytes separated by sinusoidal capillaries and central vein. In cirrhosis control group, the liver appeared congested with numerous micro and macro-nodules, lost its normal architecture by the presence of regenerating nodules that were separated by fibrous septae extending from the central vein to potal triad. In addition, the fibrous septae was accompanied by severe proliferation of bile duct and heavy invasion of inflammatory cells. The cirrhotic nodules showed thick purple colored bundles of collagen fibers. The livers of the high doses of *B. rotunda* extract and *C. longa* extract showed relatively minor micro-nodules, lesser amount of fibrous septae development and expansion and an increase in the extension of normal hepatic parenchyma compared to the silymarin-treated group (reference control),. In contrast, the livers of the low dose *B. rotunda* and *C. longa* groups were occupied by lesser macro-nodules and lesser fibrotic nodules than those of the reference group, but the improvements were not as much as those seen in high dose groups of both plant extracts. These results based on the visual evaluations provided further independent confirmation that the applied *B. rotunda* and *C. longa* extracts were effectively protecting the liver against the progression of cirrhosis, but in a dose-dependent manner.

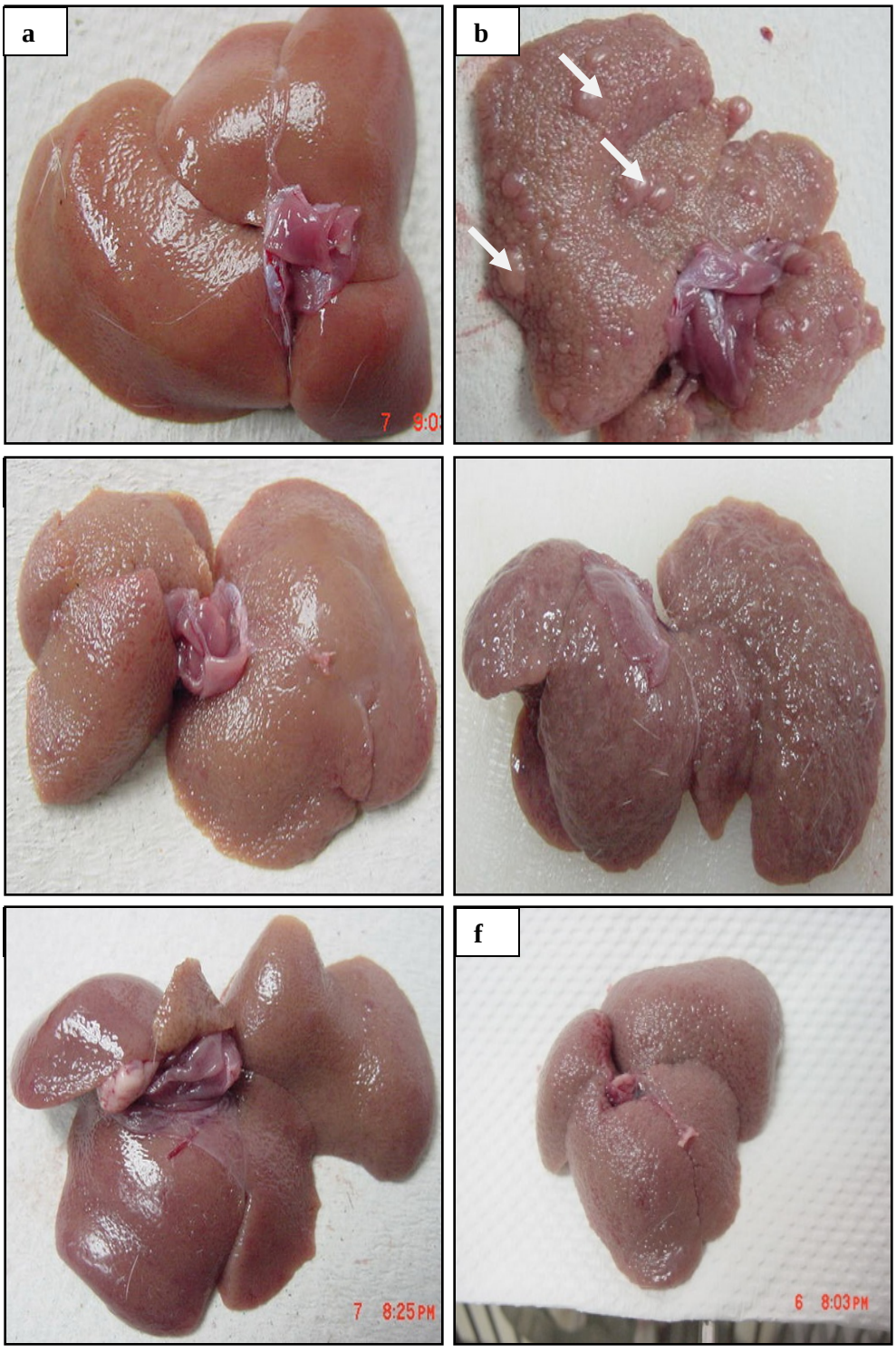
a
b
f
8:25 PM
6 8:03 PM

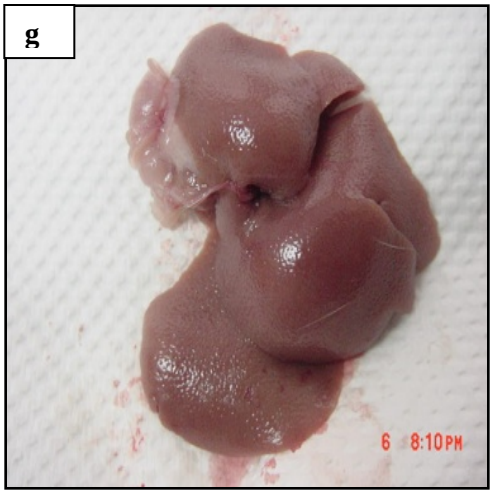

Figure 4.5: Gross images showing macroscopic appearances of the livers sampled from rats in different experimental groups. **(a)** The liver of a normal control rat exhibited regular smooth surface. **(b)** The liver of a hepatotoxic rat depicted numerous irregular whitish micro- and macronodules on its surface and a large area of ductular cholangiocellular proliferation (white arrow) embedded within fibrosis. **(c)** The liver of a hepatoprotective rat treated with silymarin showed relatively smooth surface**. (d, f)** Livers of rats treated with 250 mg/kg of the *B. rotunda* (BR) and *C. longa* (CL) extracts respectively illustrated nearly smooth surface with fewer granules (black arrow). **(e, g)** Livers of rats treated with 500 mg/kg of the *B. rotunda* and *C. longa* extracts respectively had normal smooth surface.

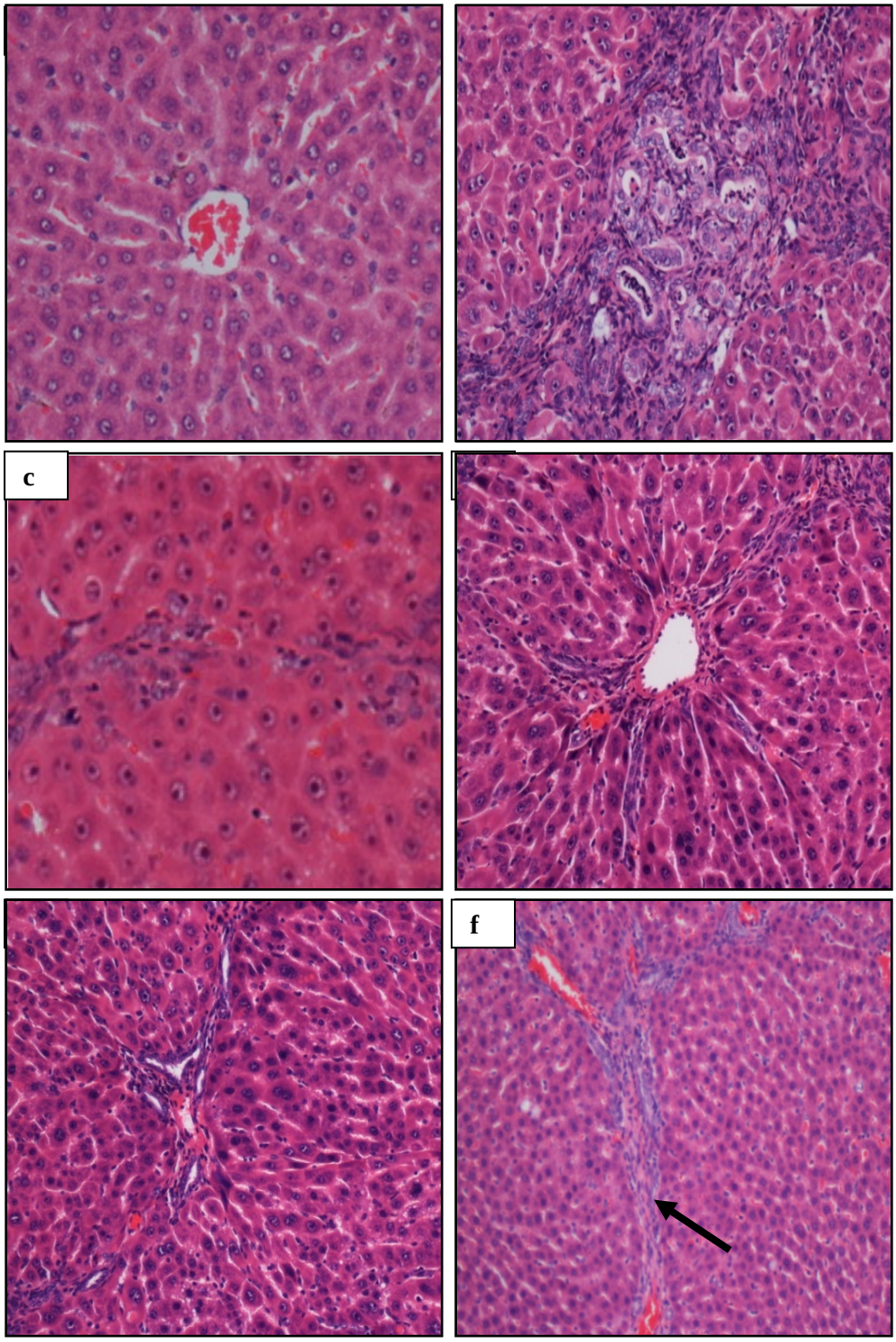
c
f

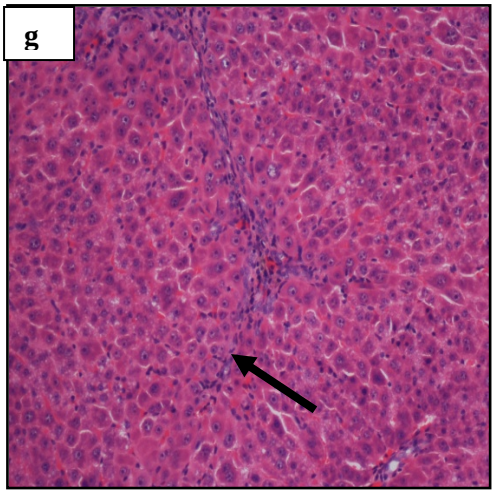

Figure 4.6: Histopathological sections (H&E) of livers sampled from rats in different experimental groups. **(a)** Normal histological structure and architecture were seen in livers of a normal control rat. **(b)** Severe structural damage, formation of pseudolobules with thick fibrotic septa and proliferation of bile duct (white arrow) were present in the liver of a cirrhotic rat. **(c)** Minor inflammation but no fibrotic septa was depicted in the liver of a hepatoprotected rat treated with silymarin. **(d, f)** Partially preserved hepatocytes and architecture with mild area of necrosis and fibrotic septae (black arrow) existed in the liver of the rats treated with 250 mg/kg of the *B. rotunda* (BR)and *C. longa* (CL) extracts respectively. **(e, g)** Highly preserved hepatocytes and architecture with very small areas of minor fibrosis were observed in the liver of the rats treated with 500 mg/kg of the *B. rotunda* and *C. longa* extracts respectively. (Original magnification of H&E stain 20x).

4.3.3. Cell loss and survival

The results concerning the normality of the hepatocytes were illustrated in Figure **4.7** for rats of all the groups According to the data, the administration of TAA was seen to significantly decrease the number of normal liver cells from about 94% measured from the livers of the normal rats to about 11% measured from the livers of the cirrhotic rats of the cirrhosis control group. In the low dose *B. rotunda* and *C. longa* (250 mg/kg) treatment, the population of the normal cells was higher, about 65% and 71% respectively. But, the treatment with the high dose *B. rotunda* and *C. longa* (500 mg/kg) maintained much higher number of normal cells, about 90% and 91% respectively, which was nearly equal to those

obtained from the silymarin-treated rats (93%) and comparable in the same manner to the normal rats. Figure **4.8** shows the difference between normal and dead hepatocytes.

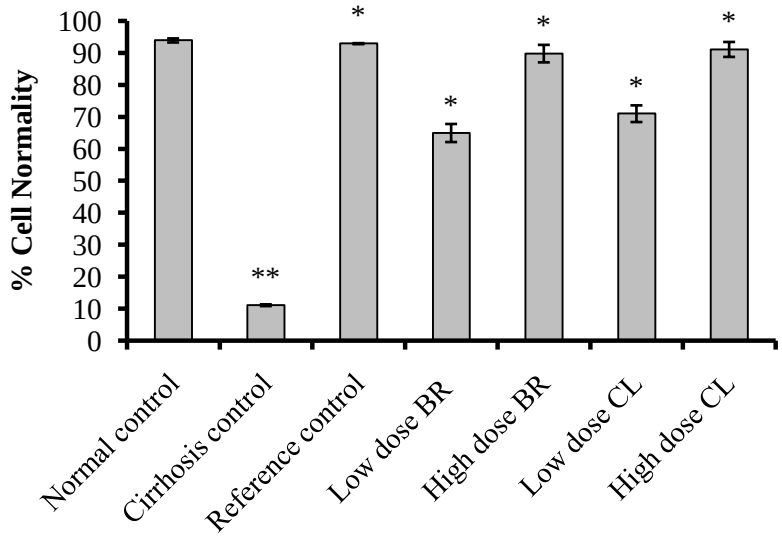

Figure 4.7: Effect of *B. rotunda* (BR) and *C. longa* (CL) crude extracts on % cell normality. Data are expressed as mean ± SEM. Means among groups (n = 6 rats/group) show significant difference, ***P*< 0.001 compared to normal control group, **P*< 0.001 compared to cirrhosis control group. Normal control (distilled water. Cirrhosis control (TAA 200 mg/kg). Reference control (Silymarin 50 mg/kg). Low dose BR and CL (250 mg/kg). High dose BR and CL (500 mg/kg).

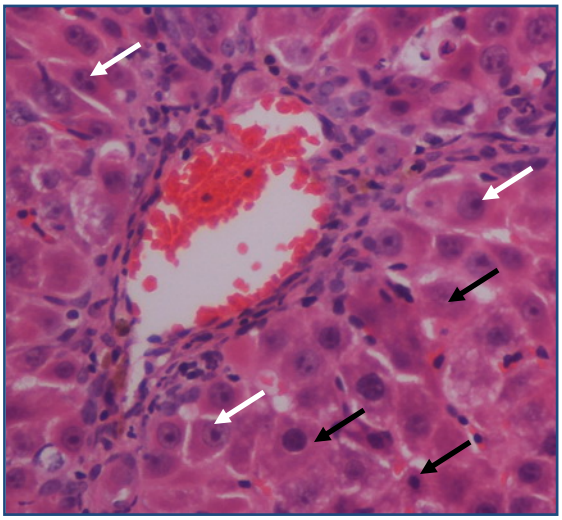

Figure 4.8: Liver section showing the difference between normal hepatocytes (white arrows) and dead hepatocytes (black arrows). (H&E stain Original magnification 40x).

4.3.4. Masson's Trichrome Staining

To measure the degree of fibrosis in the liver of experimental animals, the stain of Masson's Trichrome was used to measure the degree of deposition of collagen fibers as shown in Figure **4.9**. Liver sections of normal control group rats were normal with no signs for collagen deposition. Sections of cirrhosis control group rats showed increased collagen fibers deposition and congestion was observed clearly around the central vein showing high degree of fibrosis. Liver tissues from the group treated with Silymarin revealed minor collagen deposition indicating minor fibrosis. The central vein showed moderate congestion in the livers of the rats treated with low dose *B. rotunda* and *C. longa* extracts as indicated by moderate deposition of collagen fibers. The central vein was surrounded by mild collagen deposition in the liver samples of the high dose *B. rotunda* and *C. longa* extracts-treated. This evaluation of the degree of fibrosis confirms the previous findings that treatment with *B. rotunda* or *C. longa* extracts might suppress liver fibrosis in the animals.

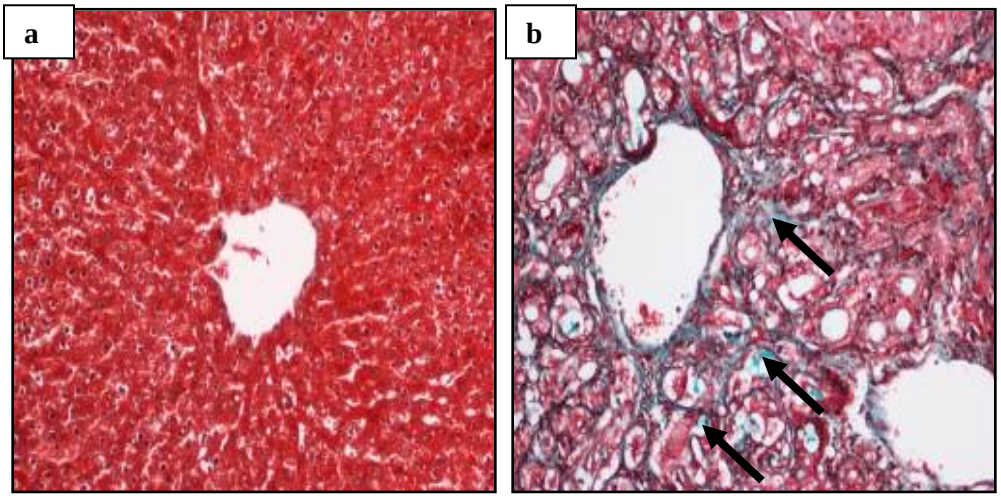

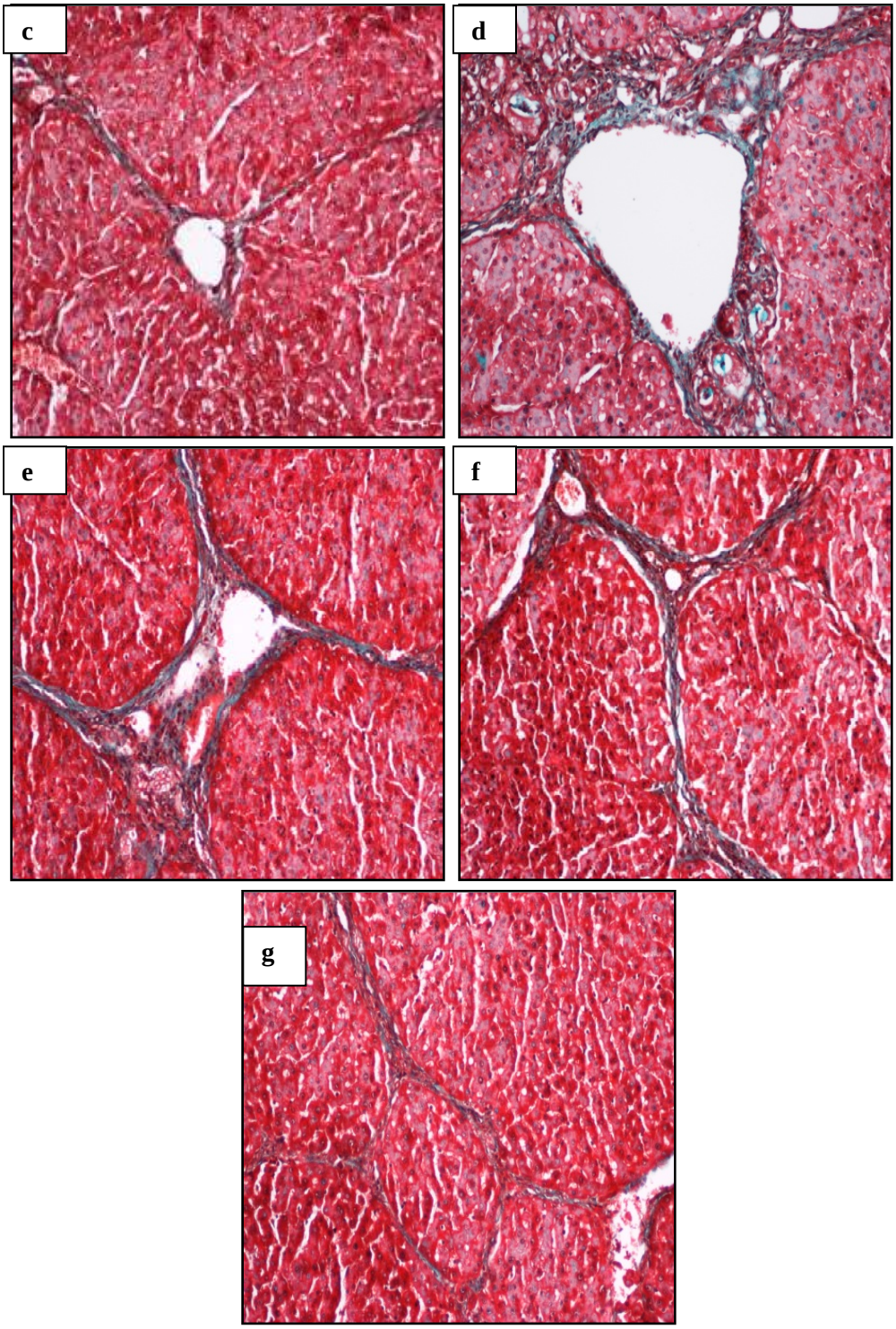

Figure 4.9: The staining of Masson's Trichrome of representative liver samples of all the experimental groups. **(a)** The liver of normal rats showed absence of of collagen deposition

in livers from a normal control rat. **(b)** High degree of fibrosis with intensive collagen deposition (arrow) was noticed in the livers from a cirrhosis rat. **(c)** Minor deposition of collagen fibers in the liver of Silymarin-treated group. **(d, f)** The central vein of the liver of rats treated with low dose *B. rotunda* (BR) and *C. longa* (CL) extracts respectively showed moderate congestion with moderate collagen deposition. **(e, g)** Minor collagen deposition was seen in the livers of rats treated with high dose *B. rotunda* and *C. longa* extracts respectively (Original magnification ×20).

4.3.5. Liver markers and lipid profile

Liver function of each rat was measured by determining the plasma levels of specific liver enzymes and lipid profile, and the results were presented in Tables **4.5**, **4.6** and **4.7**. According to the data shown in Table **4.5** and **4.6,** the liver damage due to TAA significantly elevated the levels of specific liver enzymes AP, ALT, AST, GGT, LDH, bilirubin and Prothrombin time ($P< 0.001$) and significantly declined the protein and albumin levels in the cirrhotic rats of cirrhosis control group as compared with those measured from all the other groups. Similarly, the lipid profiles in the cirrhotic rats altered significantly such that the cholesterol, LDL and triglycerides levels were higher and the HDL level was lower (Table **4.7**). The high dose *B. rotunda* and *C. longa* (500 mg/kg) treatment resulted in the readings on the biochemical markers that were comparable to those of the normal control and the silymarin-treated (50 mg/kg) groups and better than the readings obtained from the treatment with the low dose *B. rotunda* and *C. longa* (250 mg/kg) treatment groups. These data further supported the qualitative gross, anatomical histopathological findings, the quantitative cell counts, presented above, and demonstrated that the effects of the toxicity induced by TAA on the liver function can effectively be counterbalanced by the positive effects of the *B. rotunda* and *C. longa* extracts treatment, but in a dose dependent manner.

Table 4.5: Effect of *B. rotunda* and *C. longa* crude extracts on the plasma levels of specific liver enzymes measured from the rats at the end of the 8 week study.

Group	AP (IU/L)	ALT (IU/L)	AST (IU/L)	GGT (IU/L)	LDH (IU/L)
Normal control (10% Tween 20, 5ml/kg)	79.28 ± 0.58	30.57 ± 1.51	70.35 ± 0.21	3.08 ± 0.08	490.97 ± 3.9
Cirrhosis control (TAA i.p, 200mg/kg)	270.50 ± 4.88**	150.42 ± 2.60**	25.88 ± 2.99**	12.37 ± 0.26**	991.72 ± 5.00**
Reference control (Silymarin 50 mg/kg)	83.85 ± 1.06*	31.62 ± 0.63*	70.35 ± 0.43*	2.95 ± 0.08*	546.33 ± 10.46*
Low dose *B. rotunda* (250 mg/kg)	110.22 ± 0.49*	91.02 ± 1.61*	106.00 ± 2.59*	5.80 ± 0.17*	792.00 ± 3.51*
High dose *B. rotunda* (500 mg/kg)	86.13 ± 0.56*	33.42 ± 0.56*	71.10 ± 0.78*	3.22 ± 0.07*	574.00 ± 5.34*
Low dose *C. longa* (250 mg/kg)	98.98 ± 4.57*	85.62 ± 6.15*	84.48 ± 14.63*	8.08 ± 0.46*	564.17 ± 8.63*
High dose *C. longa* (500 mg/kg)	90.10 ± 8.38*	62.48 ± 9.97*	84.30 ± 15.44*	3.93 ± 0.13*	688.73 ± 4.38*

AP alkaline phosphatase; ALT alanine transferase; AST aspartate transferase; GGT gamma-glutamyl transferase; LDH lactate dehydrogenase. Data are expressed as mean ± SEM. Means among groups (n = 6 rats/group) show significant difference.. *P<0.001 compared with cirrhosis control group. **P<0.001 compared with normal control group.

Table 4.6: Effect of *B. rotunda* and *C. longa* crude extracts on the plasma protein, albumin and globulin levels and serum Prothrombin time measured from the rats at the end of the 8 week study

Group	Protein (g/L)	Albumin (g/L)	Bilirubin (umol/L)	PT
Normal control (10% Tween 20, 5ml/kg)	76.58 ± 0.70	31.93 ± 0.64	1.20 ± 0.06	1.02 ± 0.01
Cirrhosis control (TAA i.p, 200mg/kg)	59.92 ± 1.14$^{\#\#}$	11.22 ± 0.33**	4.98 ± 0.12**	1.38 ± 0.02**
Reference control (Silymarin 50 mg/kg)	75.82 ± 0.70$^{\#}$	32.38 ± 0.88*	1.28 ± 0.07*	1.02 ± 0.00*
Low dose *B. rotunda* (250 mg/kg)	63.37 ± 1.20	20.20 ± 0.20$^{\#}$	2.85 ± 0.10*	1.28 ± 0.01#
High dose *B. rotunda* (500 mg/kg)	75.10 ± 1.07$^{\#}$	29.38 ± 0.28*	1.68 ± 0.05*	1.03 ± 0.00*
Low dose *C. longa* (250 mg/kg)	53.50 ± 6.64	12.73 ± 1.66	2.57 ± 0.30*	1.26 ± 0.04*
High dose *C. longa* (500 mg/kg)	75.08 ± 2.35$^{\#}$	25.32 ± 3.36*	1.63 ± 0.25*	1.02 ± 0.01*

PT; prothrombin time. Data are expressed as mean ± SEM. Means among groups (n = 6 rats/group) show significant difference,. *P<0.001 compared to cirrhosis control group. **P<0.001 compared to normal control group. $^{\#}$P<0.01 compared to cirrhosis control group. $^{\#\#}P$<0.01 compared to normal control group.

Table 4.7: Effect of *B. rotunda* and *C. longa* crude extracts on the plasma lipid profiles measured from the rats at the end of the 8 week study.

Group	Cholesterol (mmol/L)	HDL (mmol/L)	LDL (mmol/L)	Triglycerides {mmol/L)
Normal control (10% Tween 20, 5ml/kg)	1.42 ± 0.05	1.13 ± 0.04	0.13 ± 0.02	1.27 ± 0.03
Cirrhosis control (TAA i.p, 200mg/kg)	3.22 ± 0.06**	0.53 ± 0.04**	2.50 ± 0.10**	2.83 ± 0.07**
Reference control (Silymarin 50 mg/kg)	1.80 ± 0.37*	1.32 ± 0.04*	0.33 ± 0.03*	1.45 ± 0.04*
Low dose *B. rotunda* (250 mg/kg)	2.00 ± 0.06*	0.62 ± 0.07	1.22 ± 0.07*	1.78 ± 0.03*
High dose *B. rotunda* (500 mg/kg)	1.57 ± 0.05*	1.17 ± 0.05*	0.23 ± 0.02*	1.42 ± 0.05*
Low dose *C. longa* (250 mg/kg)	2.23 ± 0.11*	0.82 ± 0.04#	1.28 ± 0.09*	1.83 ± 0.03*
High dose *C. longa* (500 mg/kg)	1.78 ± 0.03*	1.30 ± 0.03*	0.33 ± 0.03*	1.47 ± 0.03*

HDL; high density lipoprotein, LDL; low density lipoprotein. Data are expressed as mean ± SEM. Means among groups (n = 6 rats/group) show significant difference. *P<0.001 compared to cirrhosis control group. **P<0.001 compared to normal control group. $^{\#}P$<0.01 compared to cirrhosis control group.

4.3.6. Hepatic CYP2E1 Levels

The results of the effect of *B. rotunda* and *C. longa* extracts on the hepatic cytochrome enzyme CYP2E1 are shown in Figure **4.10**. Animals from cirrhosis control group had significantly (P<0.01) higher levels (2.85 ± 0.12 ng/ml) of CYP2E1 compared with normal group (0.96 ± 0.36 ng/ml) and Silymarin-treated group (1.14 ± 0.05 ng/ml). Low dose and high dose *B. rotunda*-treated rats showed significantly (P<0.01) lower levels (1.37 ± 0.15 and 1.10 ± 0.09 ng/ml respectively) of liver CYP2E1 when compared with the animals of cirrhosis control. On the contrary, no differences were noticed between the animals treated with the low dose *C. longa* and those treated with the high dose *C. longa* which had similar CYP2E1 levels (2.65 ± 0.37 and 2.61 ± 0.27 ng/ml respectively). Also no significant difference was noticed between any of these groups and cirrhosis control group.

4.3.7. Oxidative Stress Markers

The markers of oxidative stress (MDA and nitrotyrosine, and urinary 8-OH-dG) are shown in Table **4.8**. Generally, the cirrhotic livers of cirrhosis control group rats, had significantly higher levels of MDA, nitrotyrosine and 8-OH-dG (P<0.001) than those rats of the normal group and the plant extracts-treated groups. Particularly, the rats-treated with low dose and high dose *B. rotunda* extract, and low dose and high dose *C. longa* extract had significantly lower levels (P< 0.001) of liver MDA and nitrotyrosine and urinary 8-OH-dG compared to cirrhosis control group. Moreover, no significant differences were detected between the plant extract-treated animals and Silymarin-treated animals in the tested biomarkers. These results suggest that treatment with *B. rotunda* and *C. longa* extracts may protect hepatic cells from further damage during liver injury.

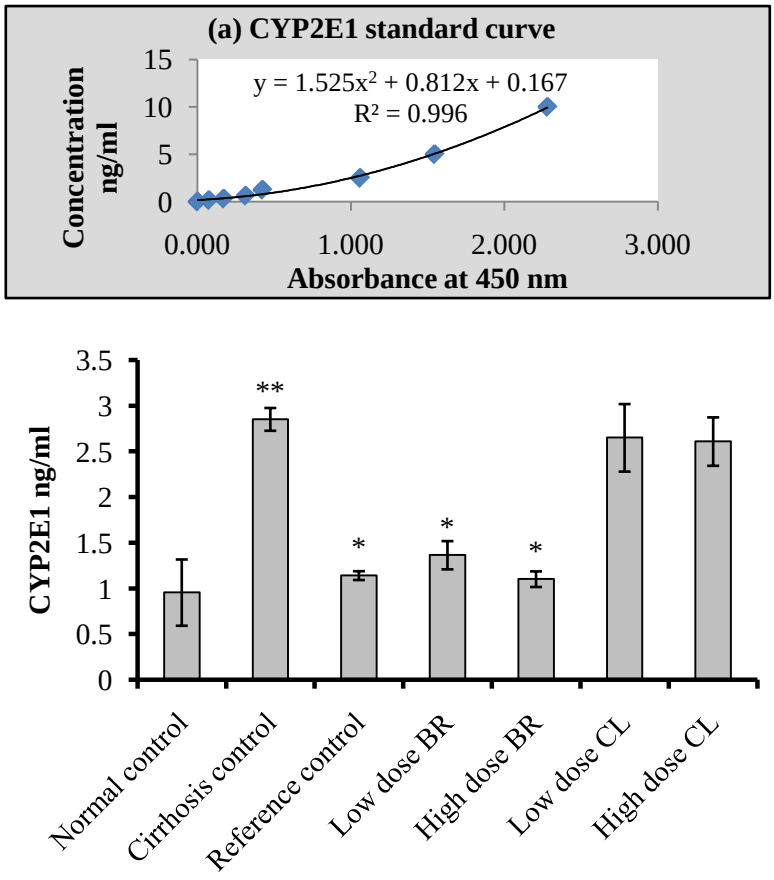

Figure 4.10: (a) CYP2E1 standard curve. **(b)** Effect of *B. rotunda* (BR) and *C. longa* (CL) crude extracts on hepatic levels of CYP2E1 in rats at the end of the experiment. Data were expressed as mean ± SEM. Means among groups (n = 6 rats/group) show significant difference, ***P*<0.01 compared with the normal control group. **P*<0.01 compared with cirrhosis control group. No significant difference was observed between the low dose CL and high dose CL when compared with cirrhosis control group. Normal control (distilled water). Cirrhosis control (TAA 200 mg/kg). Reference control (Silymarin 50 mg/kg). Low dose BR and CL (250 mg/kg). High dose BR and CL (500 mg/kg).

Table 4.8: Effect of *B. rotunda* and *C. longa* crude extracts treatment on urine level of OHdG and liver tissue homogenate level of Nitrotyrosine and MDA from the rats at the end of 8 weeks study.

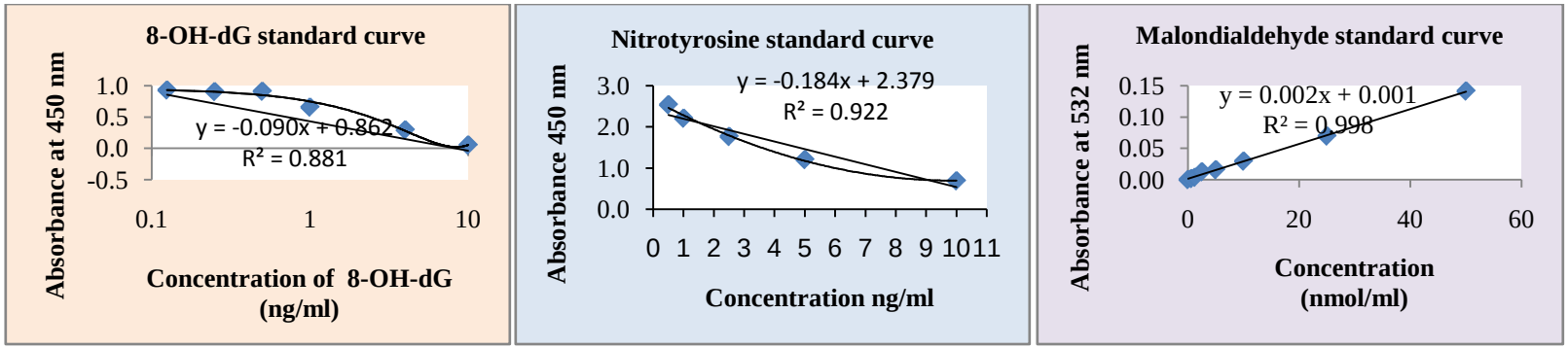

Group	8-OH-dG (ng/ml)	Nitrotyrosine (ng/ml)	MDA (nmol/mg protein)
Normal control (10% Tween 20, 5ml/kg)	2.17 ± 0.33	1.06 ± 0.07	1.22 ± 0.15
Cirrhosis control (TAA i.p, 200mg/kg)	5.40 ± 0.34**	3.87 ± 0.13**	3.94 ± 0.09**
Reference control (Silymarin 50 mg/kg)	2.80 ± 0.15*	1.67 ± 0.07*	1.94 ± 0.21*
Low dose *B. rotunda* (250 mg/kg)	3.13 ± 0.37*	2.33 ± 0.24*	2.08 ± 0.04*
High dose *B. rotunda* (500 mg/kg)	3.07± 0.09*	1.47 ± 0.13*	1.60 ± 0.03*
Low dose *C. longa* (250 mg/kg)	2.83 ± 0.03*	1.40 ± 0.20*	1.67 ± 0.36*
High dose *C. longa* (500 mg/kg)	2.37 ± 0.09*	1.33 ± 0.13*	1.29 ± 0.32*

8-OH-DG; 8-hydroxy deoxy guanosine, MDA; malondialdehyde. Data are expressed as mean ± SEM. Means among groups (n = 6 rats/group) show significant difference. *P<0.001 compared with cirrhosis control group. **P<0.001 compared with the normal rats of the control group.

4.3.8. Liver Antioxidant Enzymes

The endogenous antioxidant enzymes SOD, CAT.and GPx were used to indirectly measure the loss of hepatocytes in the cirrhotic livers of animals and the results are shown in Table. **4.9**. SOD, CAT and GPx results were similar to that of the markers of oxidative but oppositely, where the rats of the cirrhosis control group recorded lower values of SOD, CAT and GPx than in normal rats. The severe damage that happened to the cells of the cirrhotic livers explains these results. The treatment of the cirrhotic animals with low and high dose *B. rotunda* extract or *C. longa* extract significantly ($P<0.05$) increased the levels of SOD, CAT and GPx, and induced the survival of hepatocytes. Collectively, these results encourage the suggestion that treatment with either plant extract could provide a favorable protection of the hepatocytes from further damage.

Table 4.9: Effect of *B. rotunda* and *C. longa* crude extracts treatment on the liver tissue homogenate level of SOD, CAT and GPx from the rats at the end of 8 weeks study.

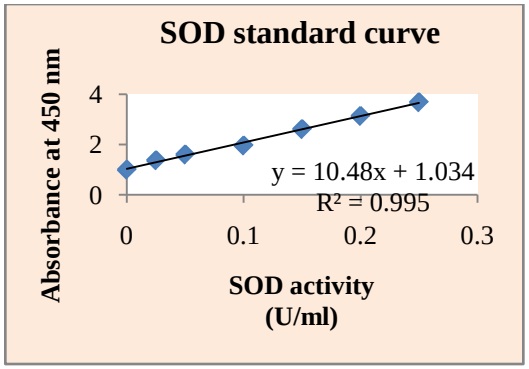

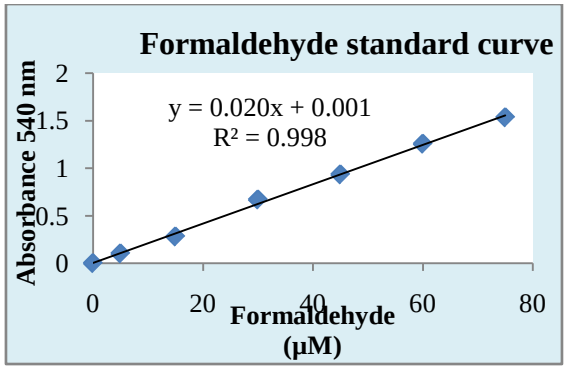

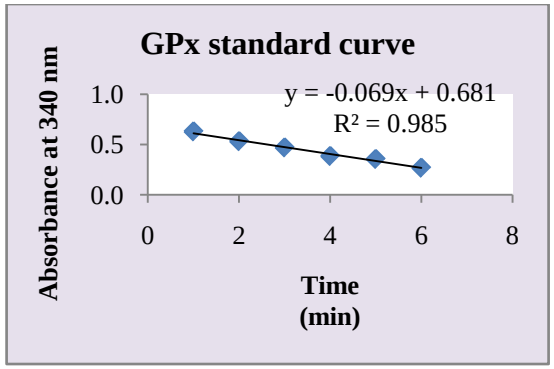

Group	SOD (U/mg protein)	CAT (nmol/min/mg protein)	GPx (nmol/min/mg protein)
Normal control (10% Tween 20, 5ml/kg)	14.89 ± 0.28	54.00 ± 0.36	860.37 ± 19.32
Cirrhosis control (TAA i.p, 200mg/kg)	9.80 ± 0.13**	27.49 ± 1.67**	451.00 ± 89.68$^{\#\#}$
Reference control (Silymarin 50 mg/kg)	14.03 ± 0.18*	52.76 ± 3.29*	926.11 ± 36.42*
Low dose *B. rotunda* (250 mg/kg)	12.03 0.06 (P=0.51)	41.34 ± 2.74$^{\#}$	902.59 ± 69.09$^{\#}$
High dose *B. rotunda* (500 mg/kg)	14.17 ± 0.19*	51.42 ± 1.34*	975.05 ± 54.08*
Low dose *C. longa* (250 mg/kg)	13.70 ± 1.08$^{\#}$	51.06 ± 1.80*	975.47 ± 26.32*
High dose *C. longa* (500 mg/kg)	14.77 ± 0.41*	54.07 ± 2.06*	1011.80 ± 46.84*

SOD: superoxide dismutase, CAT: catalase, GPx: glutathione peroxidase. Data are expressed as mean ± SEM. Means among groups (n = 6 rats/group) show significant difference. *P<0.001 compared with cirrhosis control group. **P<0.001 compared with normal control group. $^{\#}P$<0.01 compared with cirrhosis control group. $^{\#\#}P$<0.01 compared with normal control group.

4.3.9. Cytokines and Chemokines Assessment

The serum level of TGF-β1 and the serum levels of NF-κB and IL-6 from the samples collected from all sacrificed rats are shown in Figure **4.11**. The serum level of TGF-β1 and the levels of hepatic NF-κB and IL-6 were significantly elevated ($P<0.05$) in the samples from cirrhosis control group (100.00 ± 10.00 pg/ml, 2.86 ± 0.06 ng/ml and 288.58 ± 11.15 pg/ml respectively) compared to other experimental groups. Treatment of animals with of *B. rotunda* extract, reduced the serum levels of the fibrogenic factor TGF-β1 to 81.67 ± 1.67 pg/ml and the inflammatory mediators NF-κB and IL-6 to 1.93 ± 0.05 ng/ml and 148.12 ± 15.61 pg/ml respectively in the low dose *B. rotunda*-treated rats and 58.33 ± 4.41 pg/ml, 1.43 ± 0.07 ng/ml and 129.50 ± 3.79 respectively in the high dose *B. rotunda*-treated rats. In addition, the serum levels of TGF-β1, NF-κB and IL-6 decreased to 60.00 ± 5.00 pg/ml, 1.45 ± 0.07 ng/ml and 154.76 ± 19.45 pg/ml respectively in the low dose *C. longa*-treated group and 53.33 ± 1.67 pg/ml, 1.35 ± 0.04 ng/ml and 129.94 ± 18.87 pg/ml in the high dose *C. longa*-treated group. Levels of TGF-β, NF-κB and IL-6 from the high dose of both plant extracts approached the values obtained from the Silymarin-treated group (63.33 ± 1.67 pg/ml, 1.49 ± 0.06 ng/ml and 125.35 ± 5.06 pg/ml, respectively) compared to the higher values in the low dose from each plant extract. Results suggest that both plant extracts have dose-dependent nature in their inhibitory effect to the profibrogenic and proinflammatory cytokines and NF-kB chemokine.

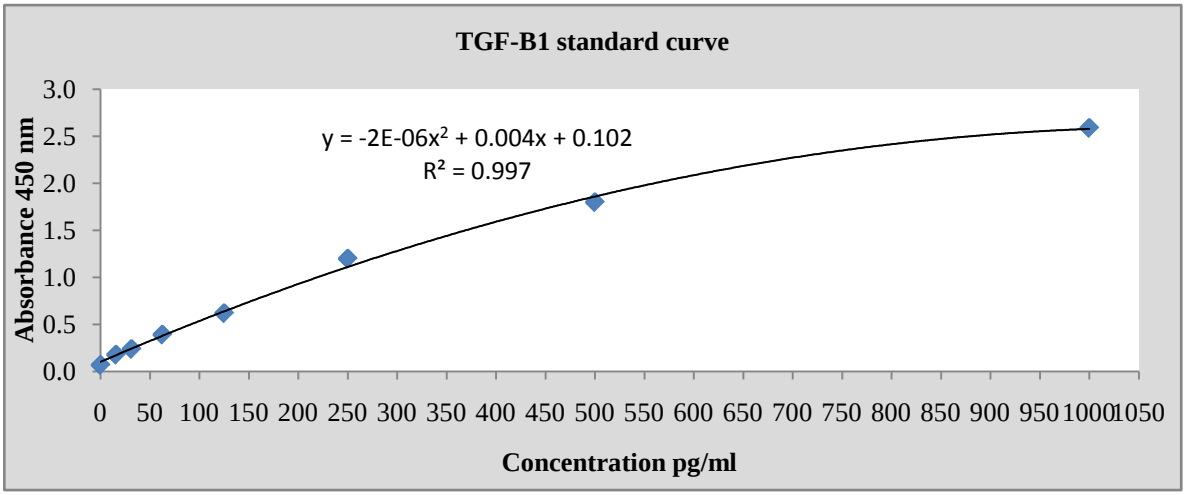
TGF-B1 standard curve
y = -2E-06x² + 0.004x + 0.102
R² = 0.997
Absorbance 450 nm
3.0
2.5
2.0
1.5
1.0
0.5
0.0
0 50 100 150 200 250 300 350 400 450 500 550 600 650 700 750 800 850 900 950 1000 1050
Concentration pg/ml

(b) TGF-β1

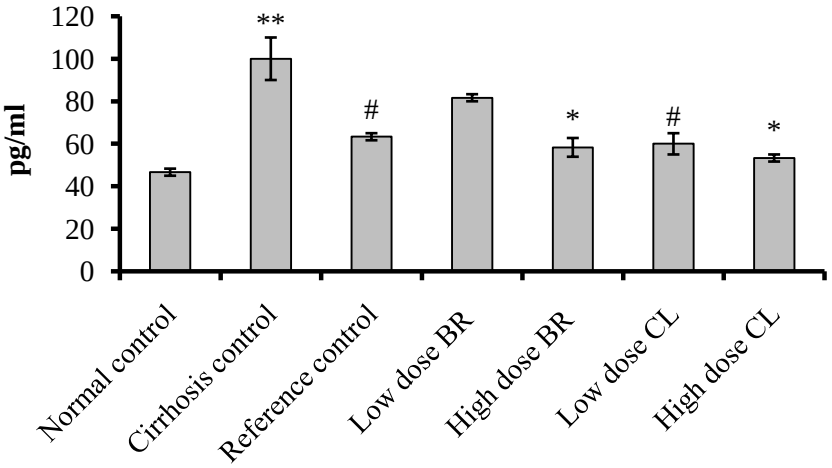
pg/ml
120
100
80
60
40
20
0
**
#
*
#
*
Normal control
Cirrhosis control
Reference control
Low dose BR
High dose BR
Low dose CL
High dose CL

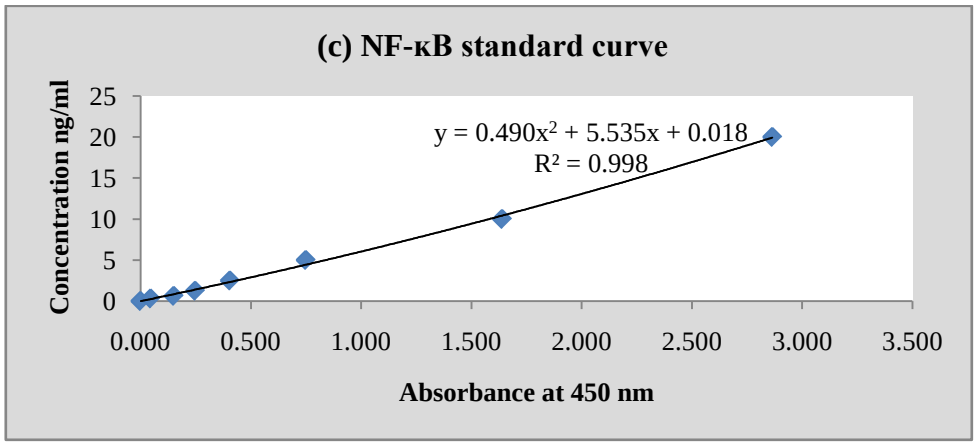
(c) NF-κB standard curve
Concentration ng/ml
25
20
15
10
5
0
y = 0.490x² + 5.535x + 0.018
R² = 0.998
0.000
0.500
1.000
1.500
2.000
2.500
3.000
3.500
Absorbance at 450 nm

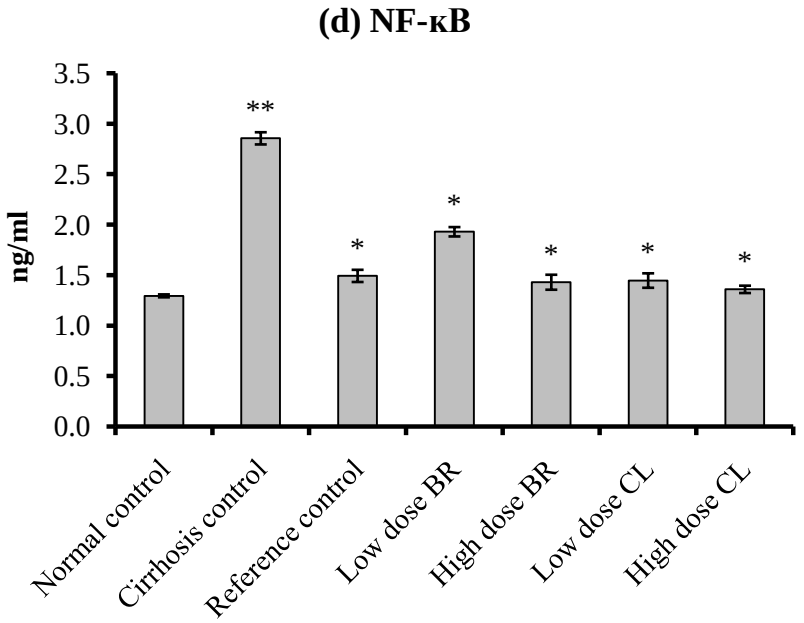
(d) NF-κB
ng/ml
3.5
3.0
2.5
2.0
1.5
1.0
0.5
0.0
**
*
*
*
*
*
Normal control
Cirrhosis control
Reference control
Low dose BR
High dose BR
Low dose CL
High dose CL

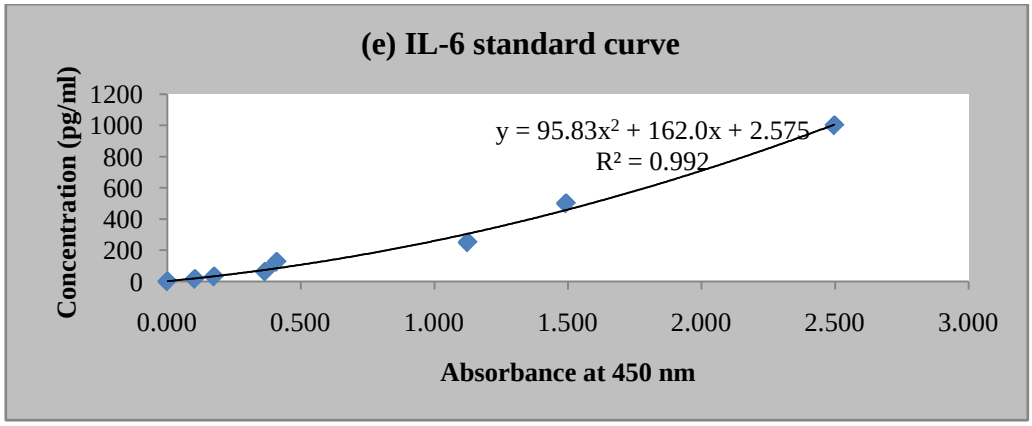

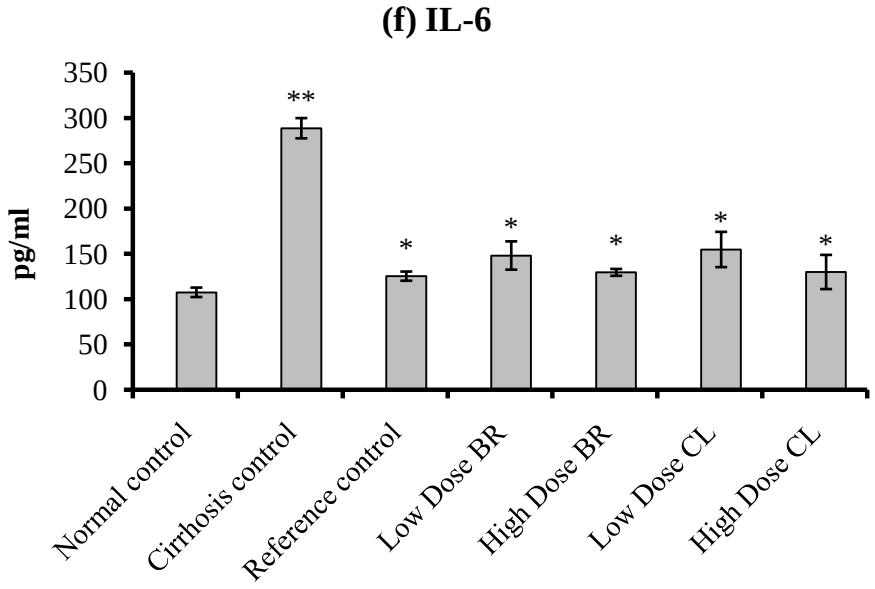

Figure 4.11: Effect of *B. rotunda* (BR) and *C. longa* (CL) crude extracts on the serum level of TGF-B1, NF-kB and IL-6 in rats at the end of 8 weeks study. (**a**) TGF-β1 standard curve **(b)** Effect of BR and CL on TGF-β1 **(c)** NF-κB standard curve **(d)** Effect of BR and CL on NF-κB **(e)** IL-6 standard curve **(f)** Effect of BR and CL on IL-6. The data were analyzed as as Mean ± SEM. Significant difference was noticed between the means of groups (n = 5 rats/group), ***P*<0.001 compared to the normal control group. **P*<0.001 compared to cirrhosis control group $^{\#}P$<0.01 compared to cirrhosis control group. Normal control (distilled water). Cirrhosis control (TAA 200 mg/kg). Reference control (Silymarin 50 mg/kg). Low dose BR and CL (250 mg/kg). High dose BR and CL (500 mg/kg).

4.3.10. Serum Bax, BcL-2 and Caspase-3

The level of the pro-apoptotic protein Bax and the anti-apoptotic protein Bcl-2 in the rat sera are shown in Figure **4.12c** and the ratio of Bax/Bcl-2 is shown in Figure **4.12d**. Bax results showed no significance between cirrhosis and normal control group rats (1.61 ± 0.15 and 1.07 ± 0.04 ng/ml respectively). On the other hand, there was significant increase (P<0.05) in the level of Bax from silymarin-treated, high dose *B. rotunda*-treated low dose and high dose *C. longa*-treated groups (4.95 ± 0.11, 4.68 ± 0.19, 4.47 ± 0.15 and 5.43 ± 0.12 ng/ml respectively) compared to cirrhosis control group. On the contrary, the level of anti-apoptotic protein Bcl-2 showed significant increase (P<0.05) in the cirrhosis control group compared to normal group (2.57 ± 0.23 and 0.89 ± 0.09 ng/ml respectively), whereas no significance observed between any of the treated groups when compared with cirrhosis control group indicating enhanced apoptosis in silymarin, *B. rotunda* and *C. longa* treated groups as confirmed by the ratio Bax/Bcl-2 in Figure **4.12b**. Furthermore, the serum level of caspase-3 in the cirrhosis control group was not significantly higher (2.11 ± 0.48 ng/ml) compared to normal group (1.43 ± 0.33 ng/ml) as illustrated in Figure **4.13**. Treating the cirrhotic livers with silymarin, high dose *B. rotunda*, low and high dose *C. longa* elevated the caspase-3 value to reach 5.54 ± 0.27, 5.83 ± 0.19, 5.08 ± 0.08 and 6.58 ± 0.35 ng/ml respectively. The similarity observed in the results of Bax and caspase-3 confirms the enhancement of apoptosis by both plant extracts in the same manner as the reference drug, silymarin.

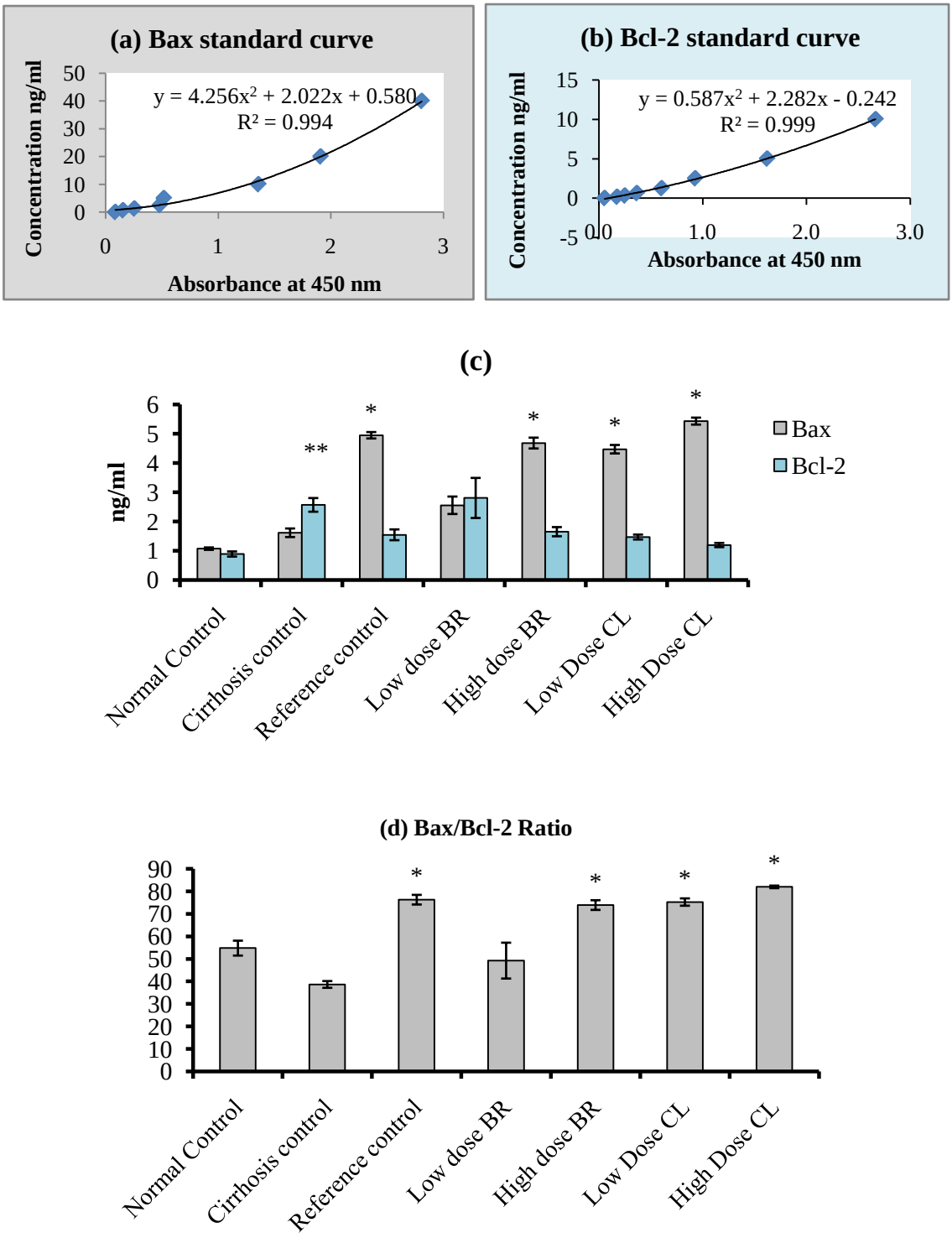

Figure 4.12: (a) Bax standard curve **(b)** Bcl-2 standard curve **(c)** Effect of BR and CL crude extracts on serum level of the pro-apoptotic protein Bax and the anti-apoptotic protein Bcl-2 at the end of 8 weeks study **(d)** Bax/Bcl-2 Ratio. Data were expressed as mean ± SEM. **P*<0.05 significance compared to the group of cirrhosis control. ***P*<0.05 significance compared to the group of normal rats. Normal control (distilled water). Cirrhosis control (Thioacetamide 200 mg/kg), Reference control

(Silymarin 50 mg/kg), Low dose BR and CL (250 mg/kg), High dose BR and CL (500 mg/kg).

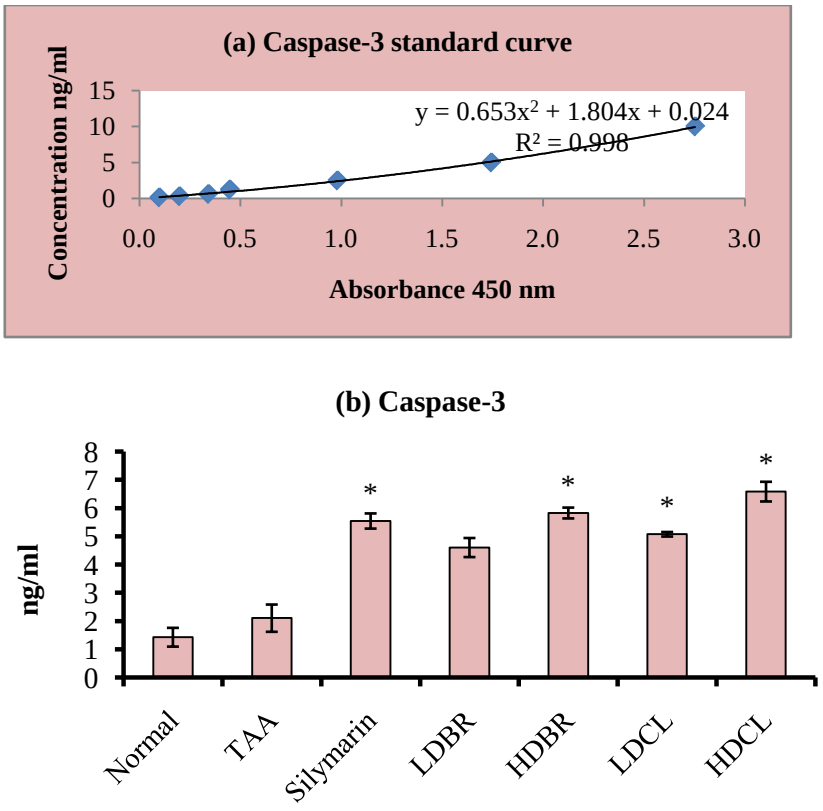

Figure 4.13: (a) Caspase-3 standard curve **(b)** Effect of *B. rotunda* and *C. longa* crude extracts on the serum caspase-3 level at the end of 8 weeks period of experiment. Data were expressed as mean ± SEM. **P*<0.05 significance compared to the group of cirrhosis control. Normal control (distilled water). Cirrhosis control (TAA 200 mg/kg), Reference control (Silymarin 50 mg/kg), Low dose BR and CL (250 mg/kg), High dose BR and CL (500 mg/kg).

4.3.11. Hepatic MMP-2, MMP-9 and TIMP-1

The results of the effect of *B. rotunda* and *C. longa* extracts treatment on the liver tissue homogenate level of MMP-2, MMP-9 and TIMP-1collected from all experimental animals are illustrated in Table **4.10**. From the results, the level of the tested enzymes were significantly high (*P*<0.05) in the cirrhosis control group rats compared to all other groups.

On the other hand, administration of *B. rotunda* extract to the animals significantly ($P<0.05$) attenuated the enzymatic level of MMP-2, MMP-9 and TIMP-1 to approach the values of the reference control group with the exception of the low dose *B. rotunda* group which didn't show significance to cirrhosis control group in MMP-2 indicating the efficacy of the plant extract treatment in a dose-dependent manner. Furthermore, Oral administration of low and high doses of *C. longa*-treated animals reduced the level of MMP-9 in their liver homogenates, to approach the values of silymarin-treated group, but didn't show significant effect on the level of MMP-2 and TIMP-1. These results recommend *B. rotunda* more than *C. longa* treatment in inhibiting extracellular matrix deposition in the rat livers via down-regulation of MMP-2, MMP-9 and TIMP-1.

Table 4.10: Effect of *B. rotunda* and *C. longa* extracts treatment on the liver tissue homogenate level of MMP-2, MMP-9 and TIMP-1 from the rats at the end of 8 weeks study.

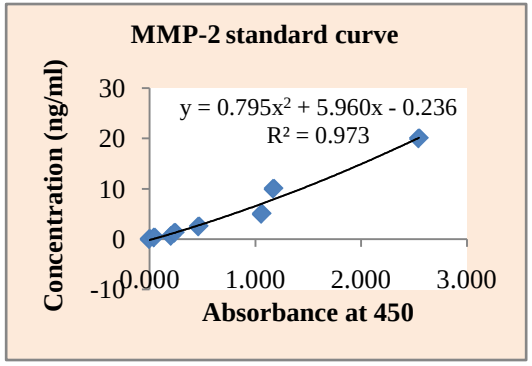

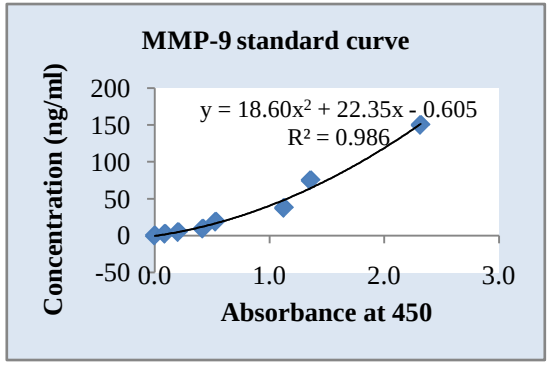

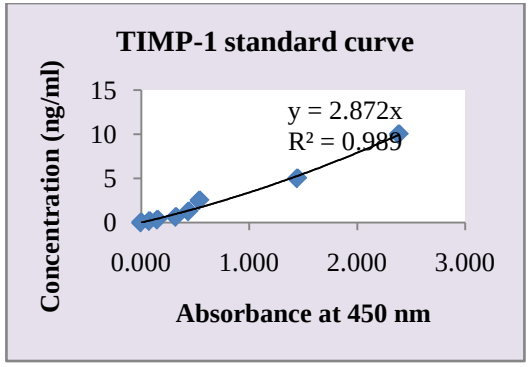

Group	MMP-2 (ng/ml)	MMP-9 (ng/ml)	TIMP-1 (ng/ml)
Normal control (10% Tween 20, 5ml/kg)	2.65 ± 1.07	9.01 ± 2.34	1.42 ± 0.55
Cirrhosis control (TAA i.p, 200mg/kg)	8.43 ± 0.86**	45.61 ± 1.88**	6.09 ± 1.35**
Reference control (Silymarin 50 mg/kg)	3.34 ± 0.13*	16.72 ± 2.43*	1.77 ± 0.06*
Low dose *B. rotunda* (250 mg/kg)	5.86 ± 0.26	30.21 ± 4.43*	2.06 ± 0.19*
High dose *B. rotunda* (500 mg/kg)	3.86 ± 0.69*	14.80 ± 2.30*	1.82 ± 0.05*
Low dose *C. longa* (250 mg/kg)	6.40 ± 0.66	21.14 ± 4.29*	3.98 ± 0.16
High dose *C. longa* (500 mg/kg)	6.92 ± 0.16	13.46 ± 3.16*	3.89 ± 0.67

MMP-2; matrix metalloproteinase-2, MMP-9; matrix metalloproteinase-9, TIMP-1; metalloproteinase inhibitor-1. Data are expressed as mean ± SEM. Means among groups (n = 6 rats/group) show significant difference. *P<0.05 compared to cirrhosis control group. **P<0.05 compared with normal control group.

4.3.12. Immunohistochemistry of Bax, Bcl2 and PCNA

Bax, Bcl2 and PCNA staining of hepatic cells of all rats are shown in Figures. (**4.14a** and **b,** and **4.15**). Hepatocytes of liver tissues from cirrhosis control group rats showed down-regulation of Bax staining with up-regulation of Bcl2-positive hepatocytes and more PCNA staining indicating severe necrosis with high cell proliferation to repair the damaged hepatocytes. Hepatocytes from Silymarin-treated rats showed up-regulated Bax expression, down-regulated Bcl2 expression and few PCNA staining indicating lower levels of proliferation to regenerate the necrotized hepatocytes and more apoptosis than necrosis. Liver tissues treated with low dose and high dose *B. rotunda* and *C. longa* extracts induced hepatocyte apoptosis and shifted necrosis to apoptosis as indicated by up-regulated Bax expression, down-regulated Bcl2 and down-regulated cell proliferation as indicated by reduced PCNA staining. These findings support the idea of *B. rotunda* and *C. longa* extract-induced hepatoprotective activities against progressive liver damage by increasing apoptosis and ameliorating cell proliferation.

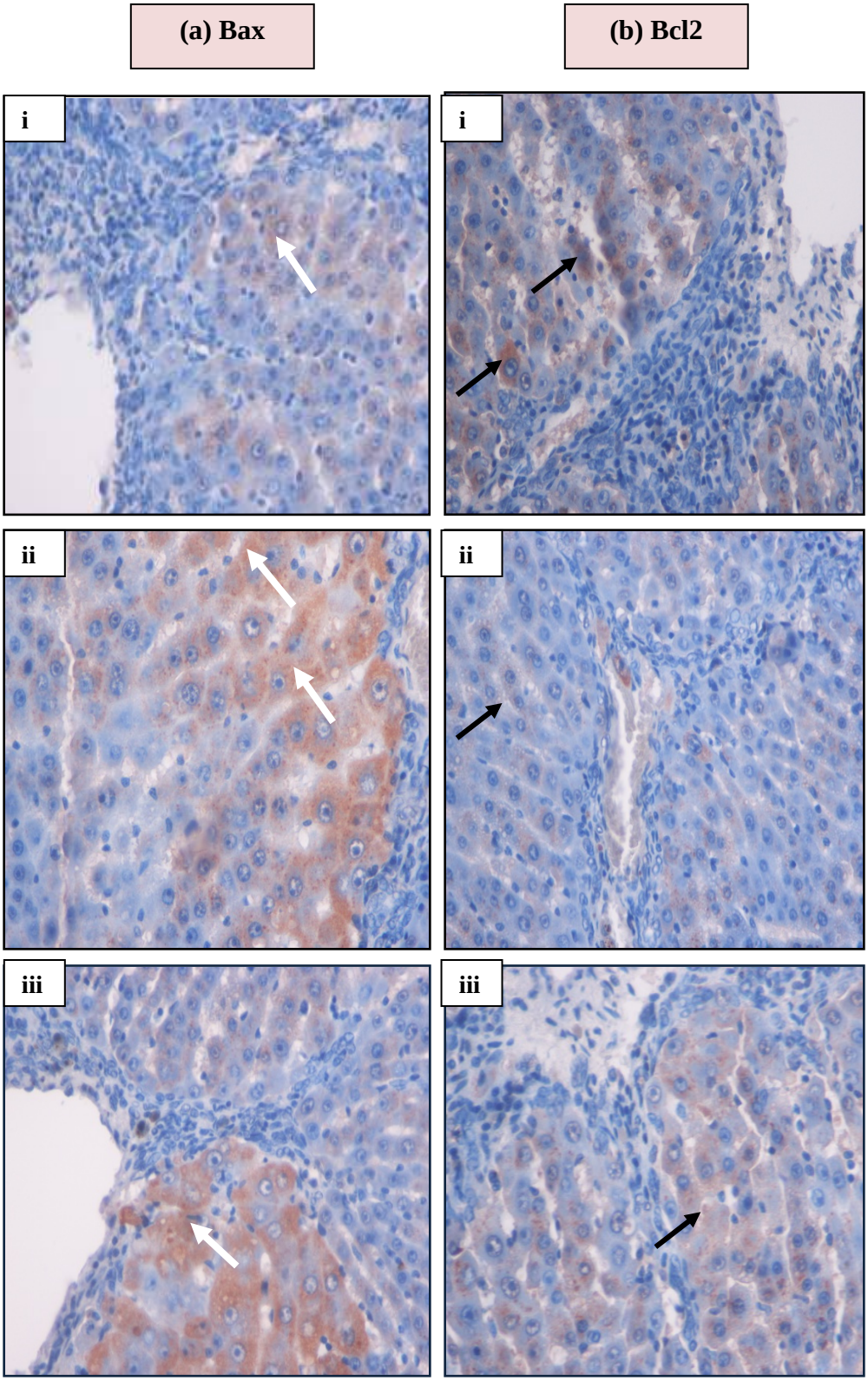
(a) Bax
(b) Bcl2
i
i
ii
ii
iii
iii

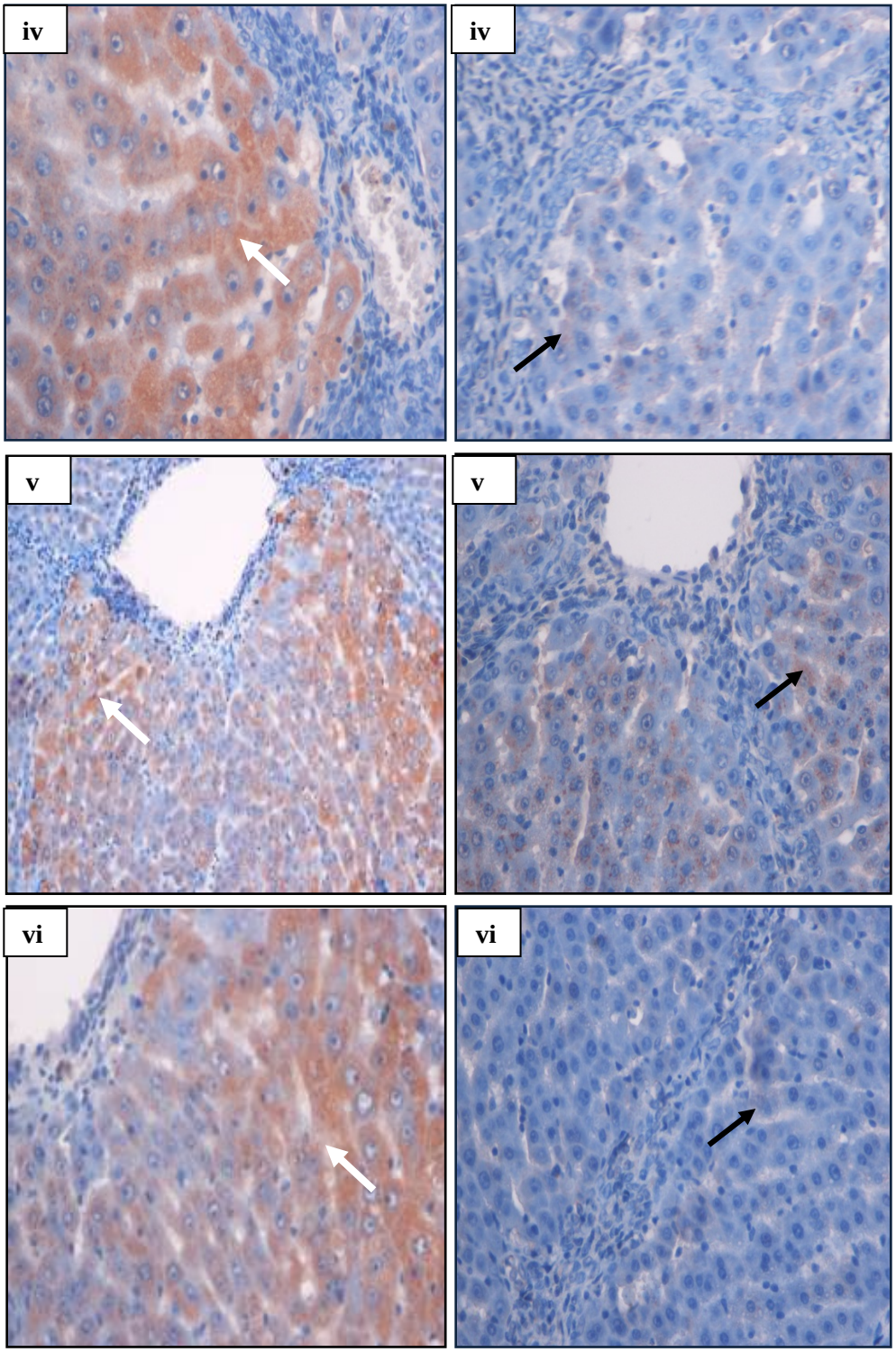

Figure 4.14: Immunohistochemistry staining of Bax and Bcl2 of representative livers sampled from rats in different experimental groups. **(ia)** Less apoptosis indicated by few Bax-positive hepatocytes (white arrow) and **(ib)** more Bcl2-positive hepatocytes (black arrow) in liver tissues from a cirrhosis control rat. **(iia)** High numbers of Bax-positive

hepatocytes (White arrow) and **(iib)** very less Bcl2-positive hepatocytes (black arrow) noticed in the liver from a hepatoprotected rat treated with Silymarin. **(iiia, va)** Moderate Bax staining (white arrow) indicating moderate apoptosis and **(iiib, vb)** moderate Bcl2 staining (black arrow) indicating moderate apoptosis in the liver from the rats treated with low dose *B. rotunda* (BR) and *C. longa* (CL) extracts respectively. **(iva, via)** High numbers of Bax-positive cells (white arrow) with severe apoptosis and **(ivb, vib)** very less Bcl2-positive hepatocytes (black arrow) were observed in the liver of the rats treated with high dose *B. rotunda* (BR) and *C. longa* (CL) extracts respectively (Original magnification ×40).

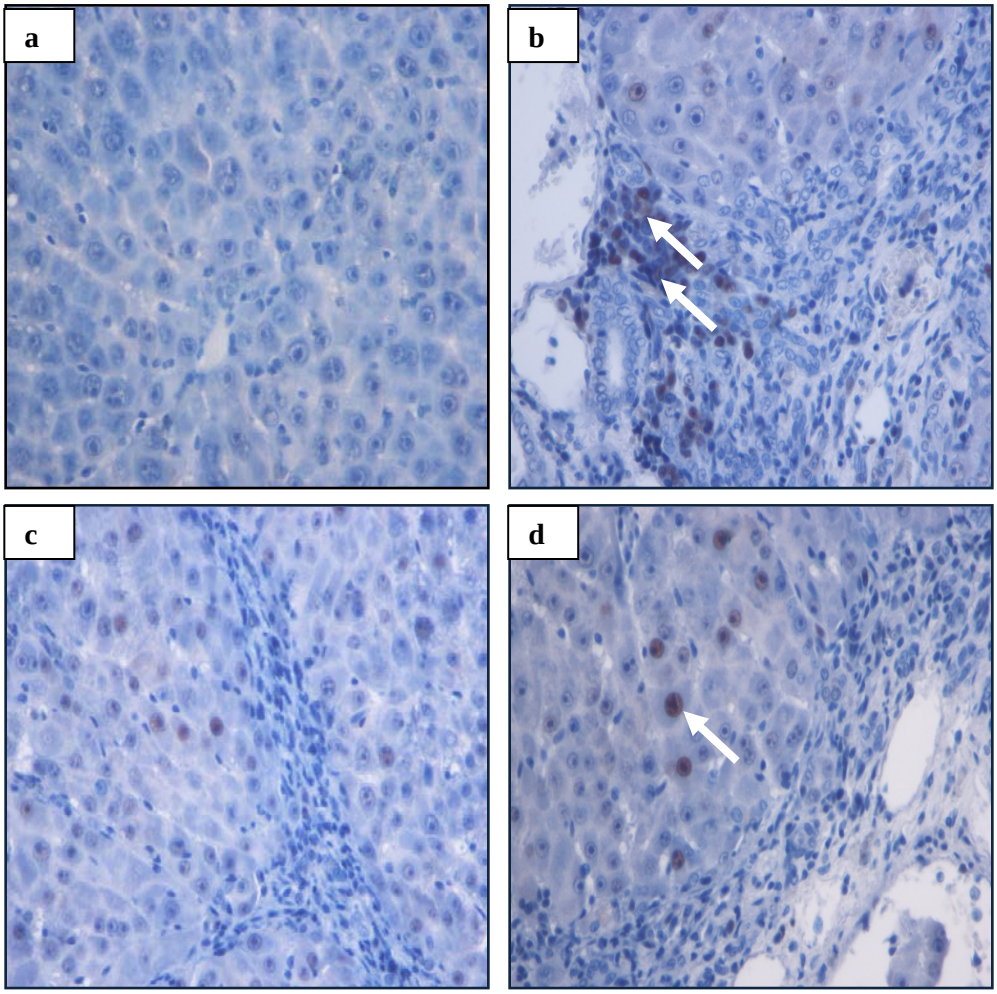

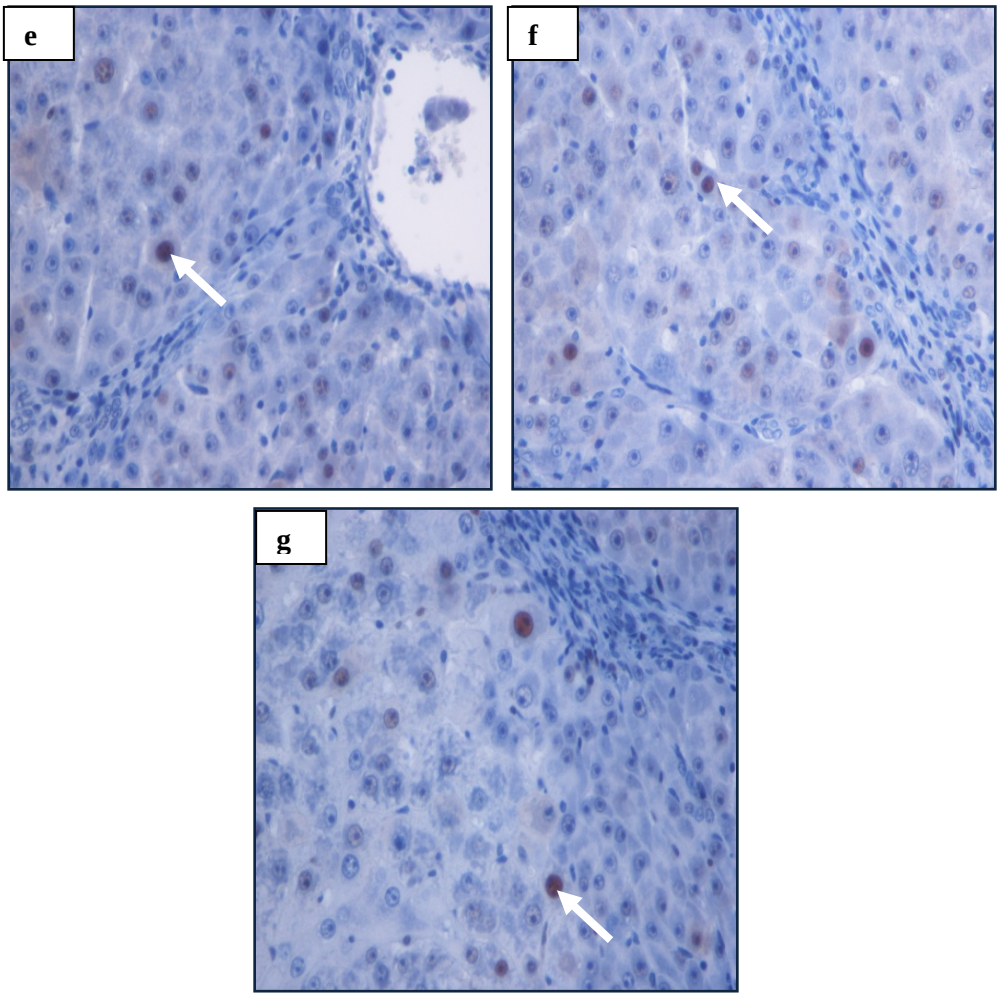

Figure 4.15: Immunohistochemistry staning of PCNA of liver tissue samples of rats in the different groups of the experiment. **(a)** Normal livers showed absence of PCNA expression in hepatocytes of the normal control group. **(b)** Cirrhosis control liver showed high degree of fibrosis associated with high PCNA expression in the necrotized hepatocytes. **(c)** Silymarin-treated liver showed less PCNA-stained hepatocytes (arrow) indicating less hepatocyte proliferation. **(d, f)** The low dose BR and low dose CL-treated liver respectively showed moderate hepatocyte proliferation as indicated by moderate PCNA staining (arrow) in the hepatocytes. **(e, g)** High dose BR and High dose CL-treated livers respectively showed minor PCNA expression (arrow) with few proliferated hepatocytes was observed in the liver. (Original magnification ×40).

4.4. Isolation of Panduratin A and Germacrone Compounds from their Ethanolic Crude Extracts

4.4.1 Isolation of Panduratin A from *B. rotunda* extract

Dry pack column chromatography of *B. rotunda* crude extract resulted in 11 fractions as shown in (Table **4.11**). The results of TLC of all fractions versus Panduratin A compound showed that fraction BR-3 contained panduratin A (Figure **4.16a** and **b)** recording a retardation factor similar to that of Panduratin A standard (R_f = 0.29). These results were also confirmed by High performance liquid chromatography (Figure **4.17a** and **b**). LCMS chromatogram of the isolated Panduratin A is illustrated in Figure **18a** and **c** showing that the compound was detected at m/z 407.2211.

4.4.2 Isolation of Germacrone from *C. longa* extract

Dry-pack column chromatography of *C. longa* crude extract resulted in 18 fractions as illustrated in (Figure **3.2**). TLC screening of all the resulting fractions showed that fractions CL-1-4 might contain germacrone compound when compared to TLC from the Germacrone standard (R_f = 0.41). Column chromatography for the combined fractions CL-1-4 resulted in 21 fractions (Table **4.12**) TLC screening for the resulting fractions versus germacrone standard showed that fraction CL-1-4-7 and CL-1-4-13 might contain germacrone (Figure **4.19**). HPLC profiling of both fractions versus germacrone standard confirmed that fraction CL-1-4-13 contained the target compound (Figure **4.20**). LCMS of the isolated germacrone showed that the compound was detected at m/z 219.1740 (Figure **4.21**).

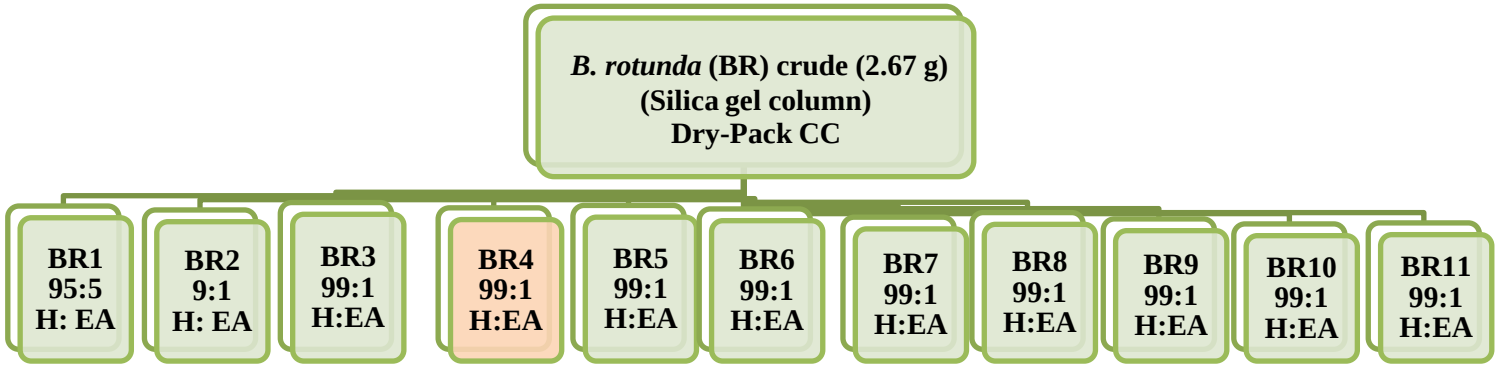

Table 4.11: The % yield of the fractions obtained from dry pack column chromatography.

Fraction	Solvent system (%)	Volume of solvent (ml) (Approx. value)	Weight of tube (g)	Weight of tube+ sample (g)	Weight of sample (mg)	Yield %
BR-(1)	95 Hex: 5 Ea	125 x3	5.3340	5.5070	173	6.48
BR-(2)	90 Hex: 10 Ea	125	5.2983	5.3269	28	1.05
BR-(3)	85 Hex: 15 Ea	125	5.3866	6.1537	767.1	28.73
BR-(4)	80 Hex: 20 Ea	125	5.2738	6.0316	757.8	28.38
BR-(5)	75 Hex: 25 Ea	125	5.1593	5.4257	266.4	9.98
BR-(6)	70 Hex: 30 Ea	125	5.2910	5.3991	108.1	4.04
BR-(7)	65 Hex: 35 Ea	125	5.2428	5.3898	147	5.5
BR-(8)	60 Hex: 40 Ea	125	5.2033	5.3147	114	4.27
BR-(9)	55 Hex: 45 Ea	125	5.2586	5.3831	124.5	4.66
BR-(10)	50 Hex: 50 Ea	125	5.2013	5.2909	89.6	3.36
BR-(11)	100 Ea	125 x2	5.2434	5.4131	169.7	6.30

Total weight= 2.74 g. % yield = 2.74/ 2.67 = 102.6 %.

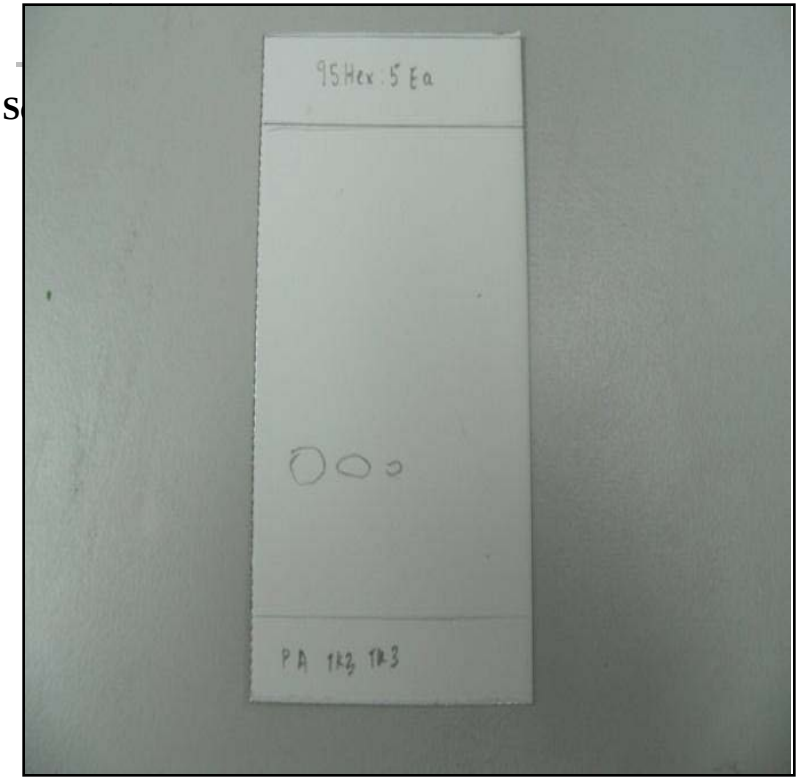

b

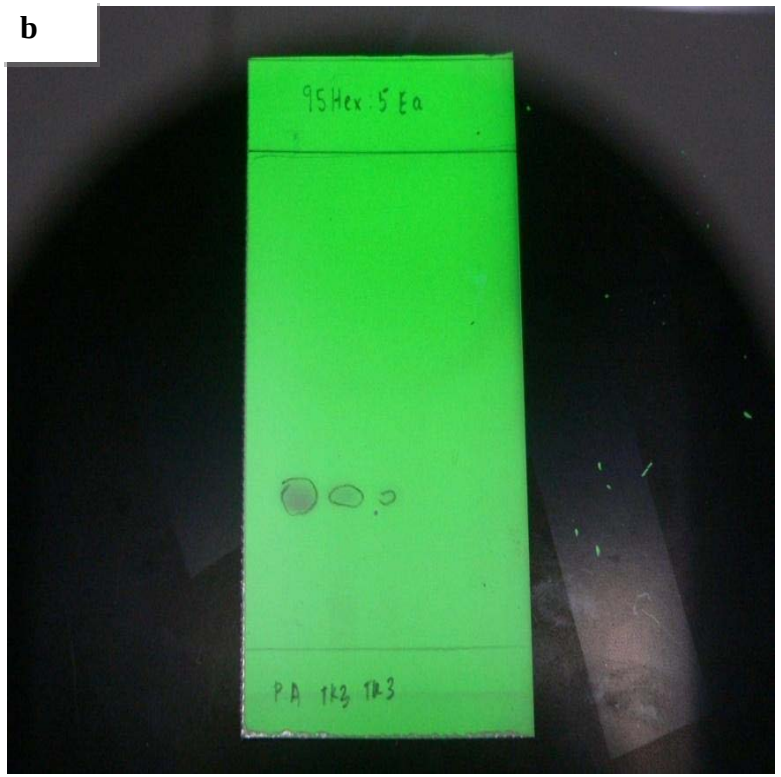

c

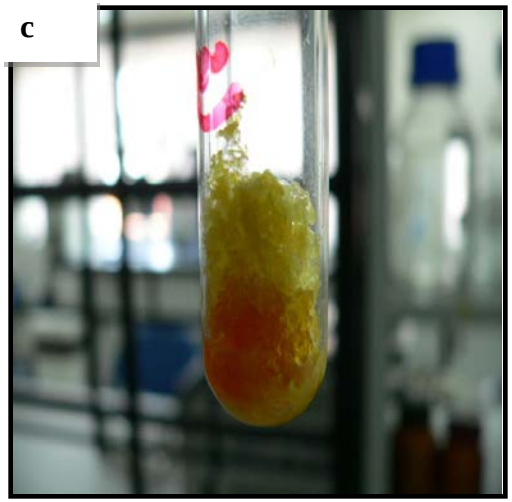

Figure 4.16: TLC of fraction BR-3 versus Panduratin A standard. **(a)** TLC before UV. **(b)** TLC after UV**. (c)** Pure crystals (96.6%) of isolated Panduratin A.

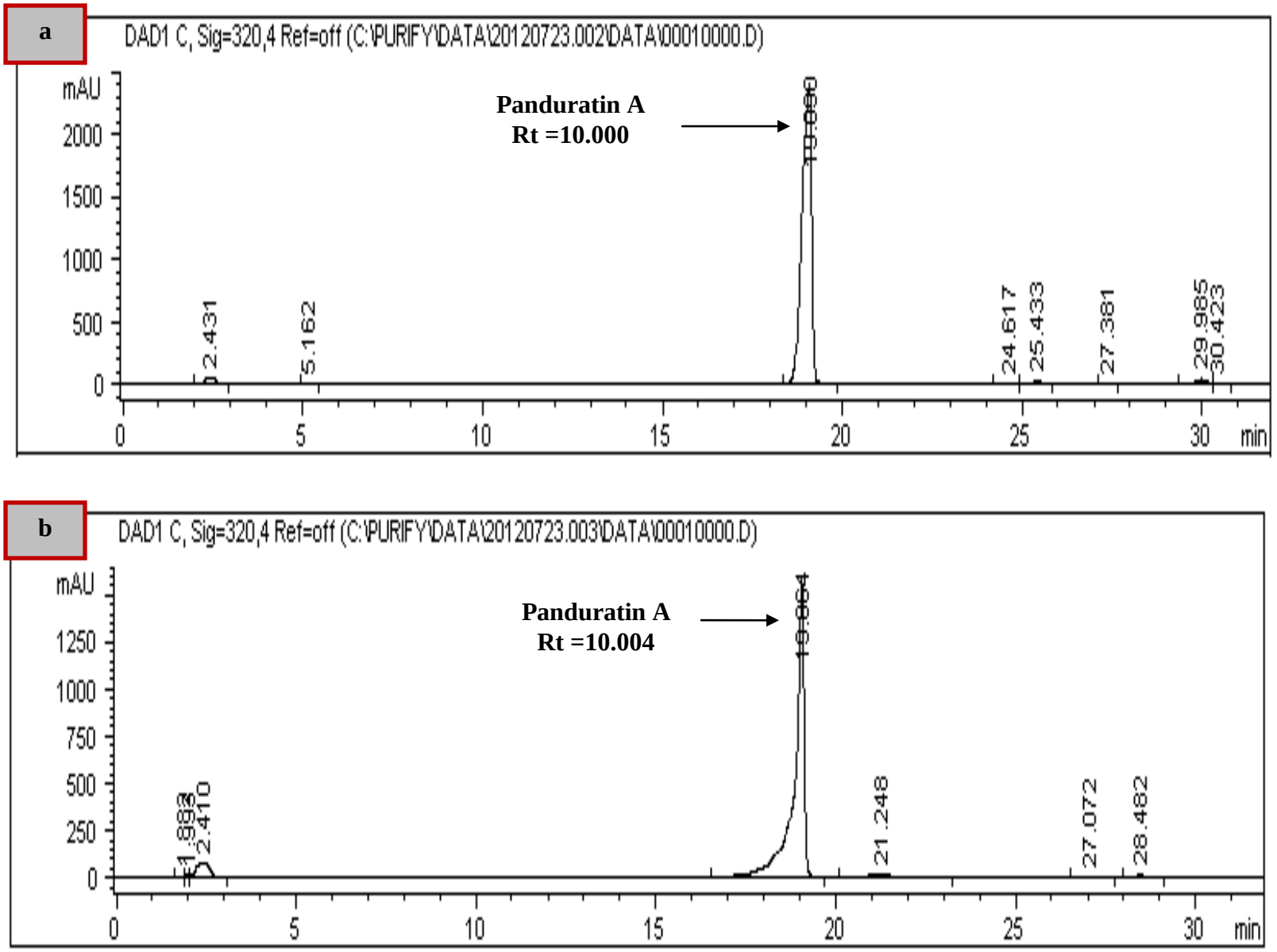

Figure 4.17: HPLC profile of **(a)** BR-3 (20 mg/ml) showing Panduratin A compound, **(b)** Panduratin A standard (10 mg/ml).

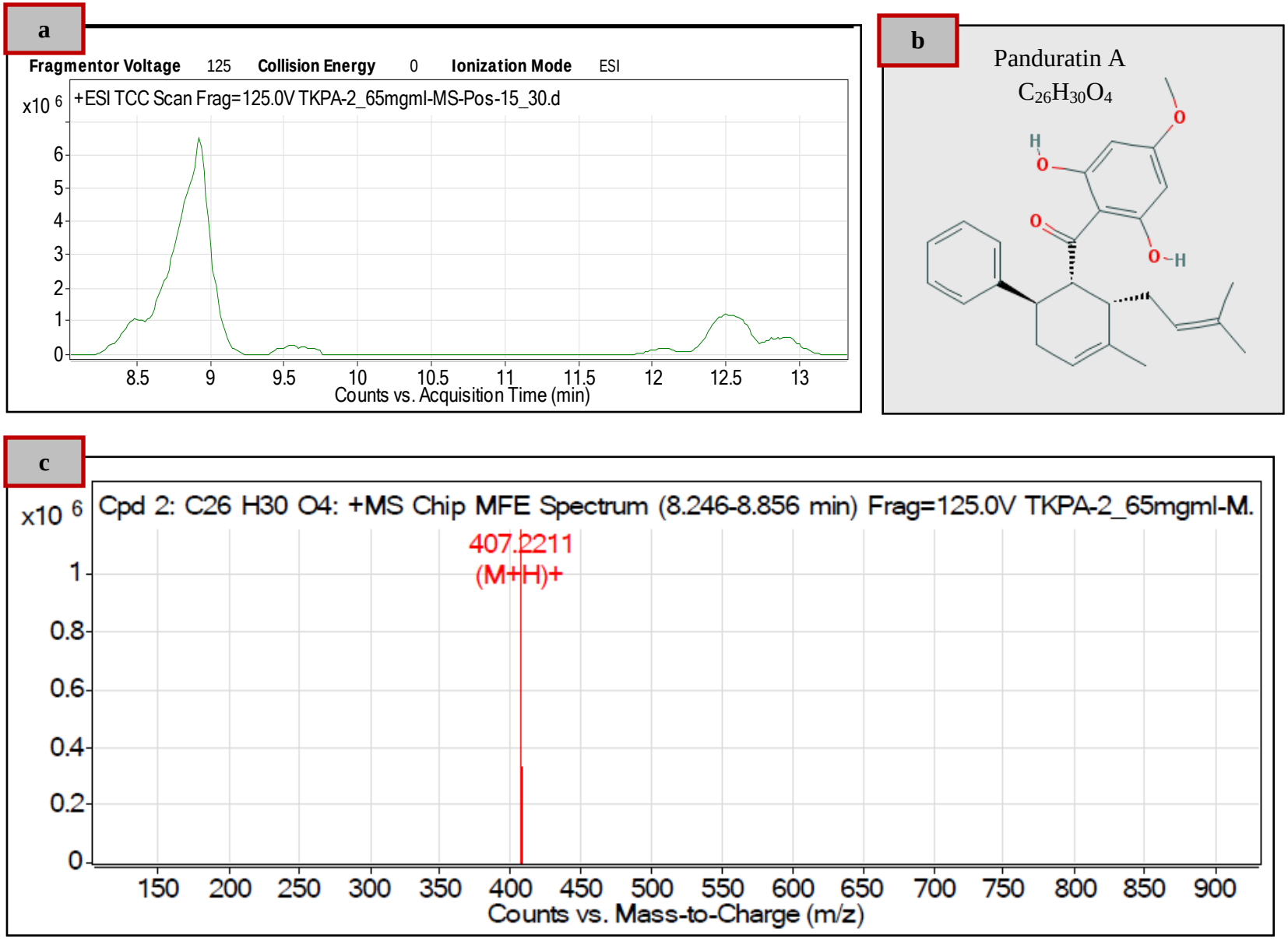

Figure 4.18: (a) LCMS of fraction BR-3. **(b)** Panduratin A structure according to PubChem library. **(c)** Mass spectrum of Panduratin A.

Table 4.12: The % yield of the sub-fractions obtained from dry pack column chromatography of the combined fraction CL-1-4

Fraction	Solvent system (%)	Volume of solvent (ml) (Approx. value)	Weight of tube (g)	Weight of tube+ sample (g)	Weight of sample (mg)	Yield %
CL1-4-(1)	100 Hex	200	5.1430	5.2235	80.5	0.84
CL1-4-(2)	100 Hex	10	5.1370	5.1407	3.7	0.04
CL1-4-(3)	100 Hex	10	5.1673	5.2273	60.0	0.63
CL1-4-(4)	100 Hex	10	5.1894	5.2620	72.6	0.76
CL1-4-(5)	100 Hex	10	5.1185	5.1205	2.0	0.02
CL1-4-(6)	95 Hex : 5 Ea	10	5.1141	5.1942	80.1	0.84
CL1-4-(7)	95 Hex : 5 Ea	10	5.2967	5.3559	59.2	0.62
CL1-4-(8)	95 Hex : 5 Ea	10	5.1613	5.2089	47.6	0.50
CL1-4-(9)	95 Hex : 5 Ea	10	5.2877	5.3424	54.7	0.58
CL1-4-(10)	95 Hex : 5 Ea	10	5.3103	5.4989	188.6	1.99
CL1-4-(11)	95 Hex : 5 Ea	10	5.1465	5.4311	284.6	3.00
CL1-4-(12)	95 Hex : 5 Ea	10	5.2431	5.3053	62.2	0.65
CL1-4-(13)	95 Hex : 5 Ea	10	5.2010	5.6434	442.4	4.70
CL1-4-(14)	95 Hex : 5 Ea	10	5.1465	5.5906	444.1	4.70
CL1-4-(15)	95 Hex : 5 Ea	10	5.1611	5.2305	69.4	0.73
CL1-4-(16)	95 Hex : 5 Ea	10	5.2039	5.2347	30.8	0.03
CL1-4-(17)	95 Hex : 5 Ea	10	5.2111	5.2367	25.6	0.27
CL1-4-(18)	95 Hex : 5 Ea	10	5.1342	5.1691	34.9	0.37
CL1-4-(19)	95 Hex : 5 Ea	10	5.1897	5.1915	1.8	0.02
CL1-4-(20)	95 Hex : 5 Ea	100	5.1767	5.1930	16.3	0.17
CL1-4-(21)	80 Hex : 20 Ea	100	5.1699	5.4554	285.5	3.00

Total weight of sample = 2.3466 g % yield= 2.3/ 9.5 x 100%= 24.7%

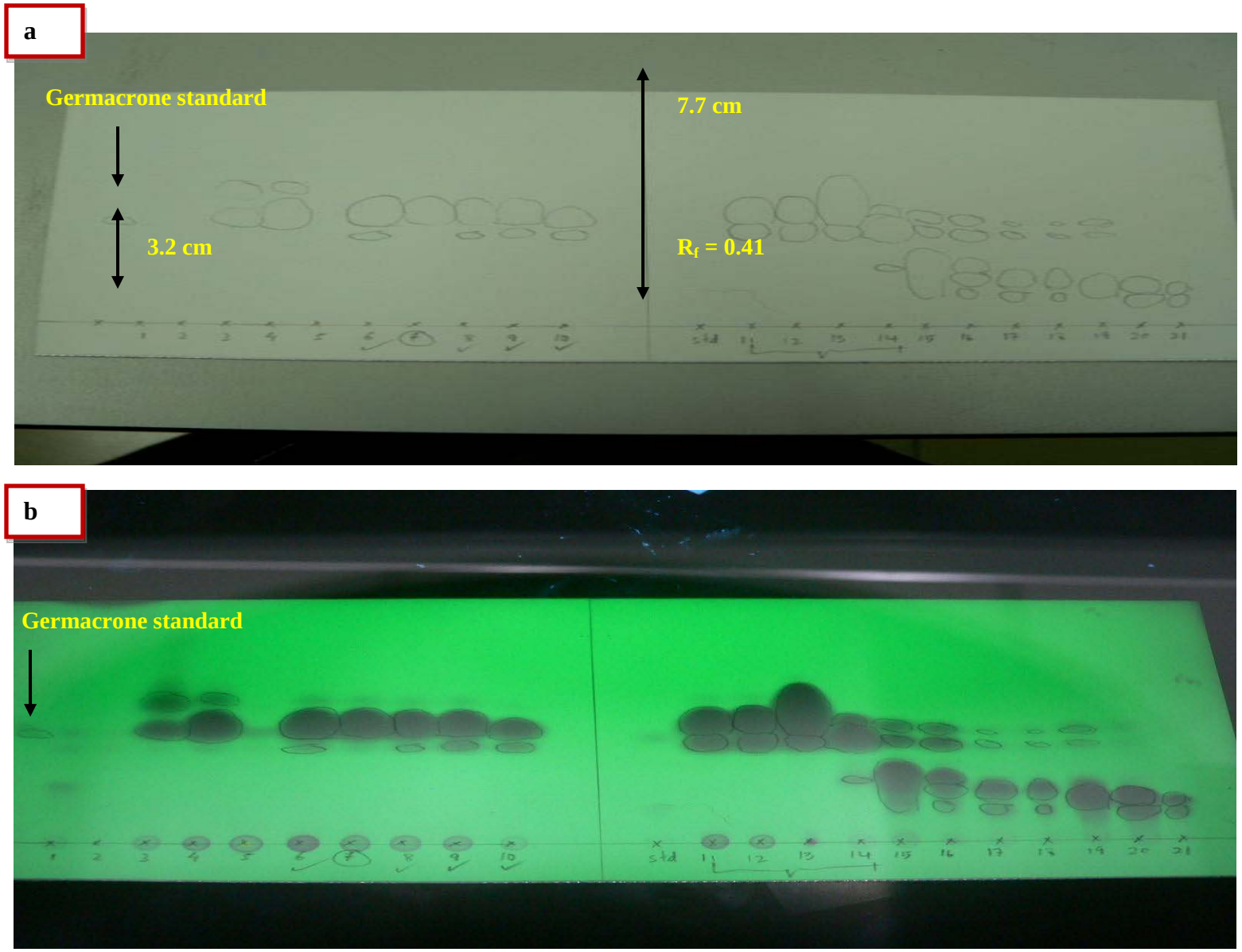

Figure 4.19: TLC of fraction CL-1-4 -7 and CL-1-4-13 versus Germacrone standard. **(a)** TLC before UV**. (b)** TLC after UV.

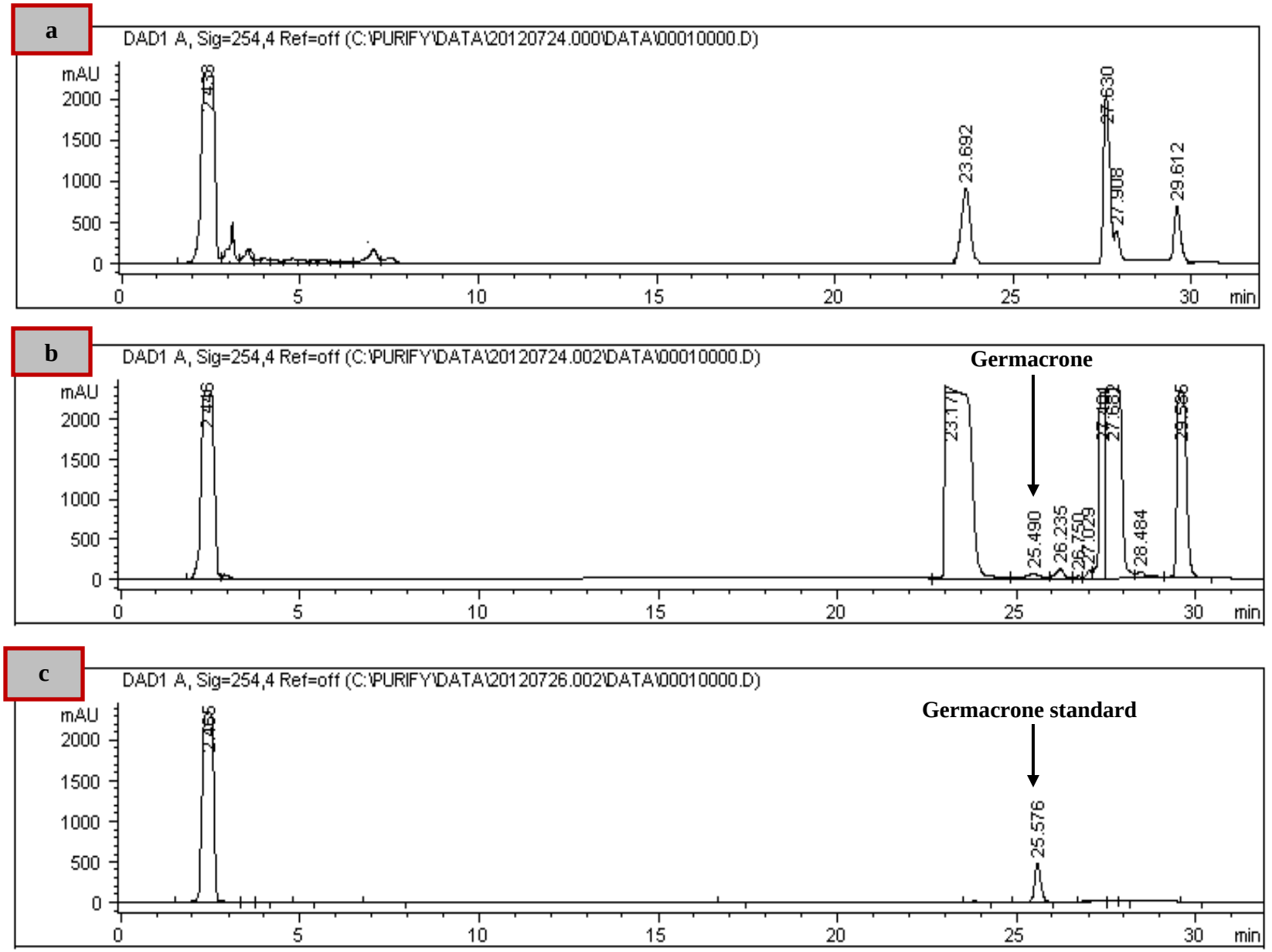

Figure 4.20: HPLC profile of **(a)** Fraction CL-1-7 (20 mg/ml) **(b)** Fraction CL-1-13 (20 mg/ml) **(c)** Germacrone standard (1mg/ml).

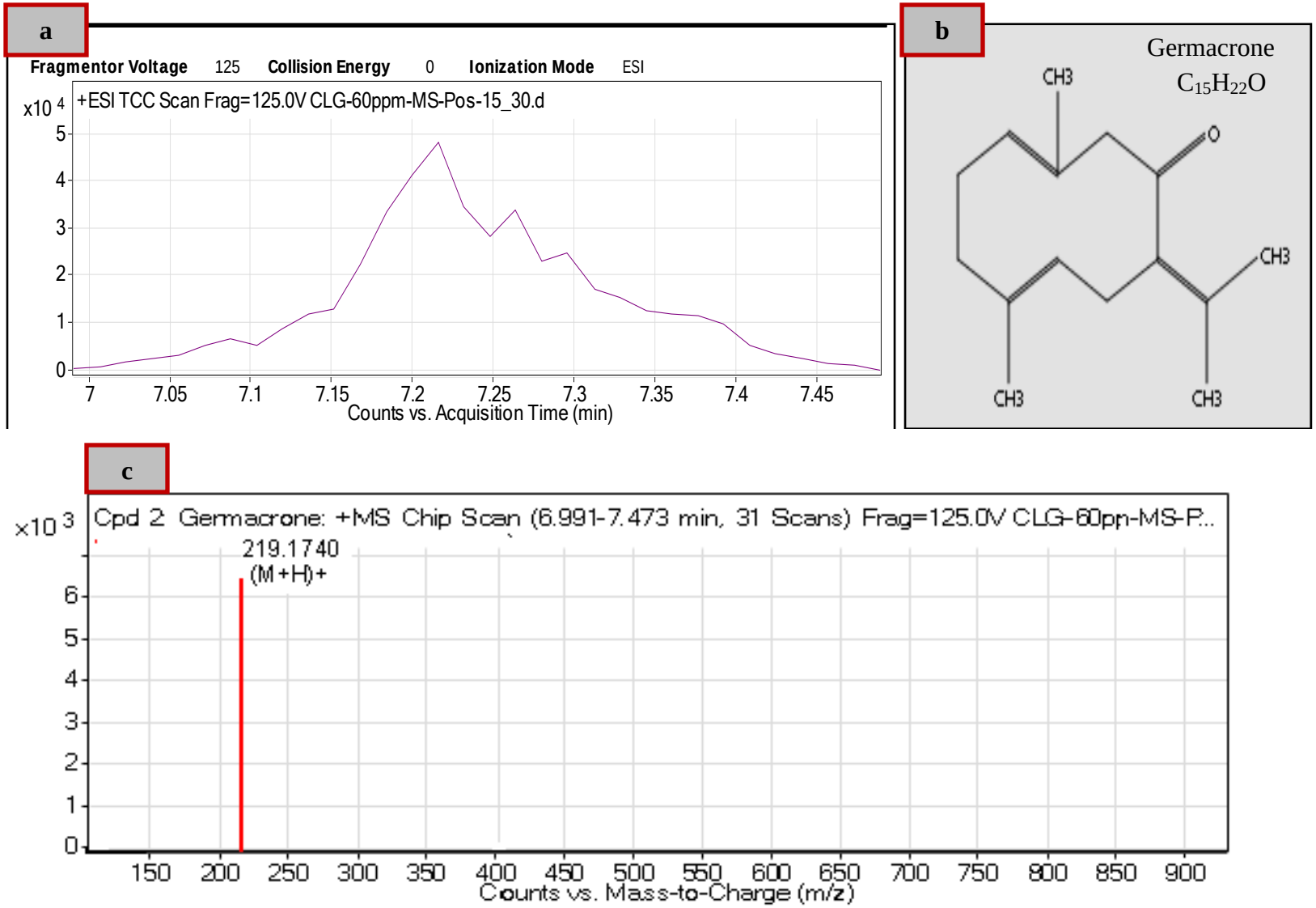

Figure 4.21: (a) LCMS of fraction CL-1-13 after 3 times collection from its HPLC. **(b)** Germacrone structure according to PubChem library.**(c)** Mass spectrum of Germacrone.

4.5. DPPH Scavenging Activity of Panduratin A

Panduratin A compound exhibited comparable free radical scavenging activity for DPPH compared to that of Ascorbic acid (AC) as shown in Figure **4.22**. At the highest tested concentrations 100 μg/ml, the DPPH inhibition % of PA was significantly (P<0.001) lower than that of the standard AC and the reference drug SI. On the other hand, at the lowest tested concentration 1 μg/ml, there was no significance between PA and the standards AC or between PA and the standard drug SI. The medium concentration 10 μg/ml revealed low significance (P<0.001) between PA and the standards AC, while the significance detected between PA and SI was P = 0.52. These results indicated that PA had less potent radical scavenging effect and antioxidant activity than AC, but similar to that of the reference drug SI at the low and medium concentrations 1 and 10 μg/ml, but no significance at the high concentration 100 μg/ml.

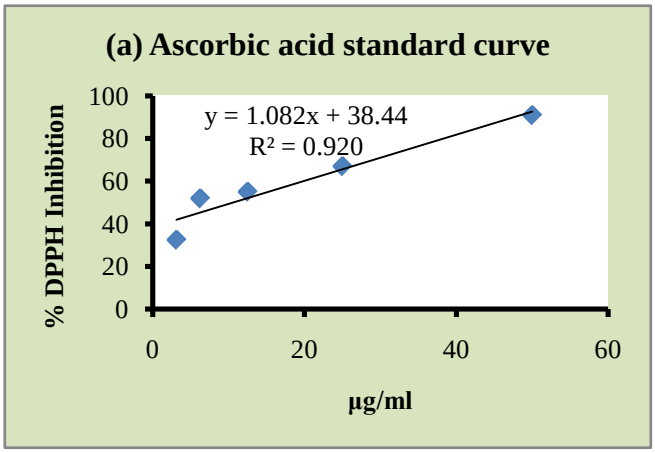

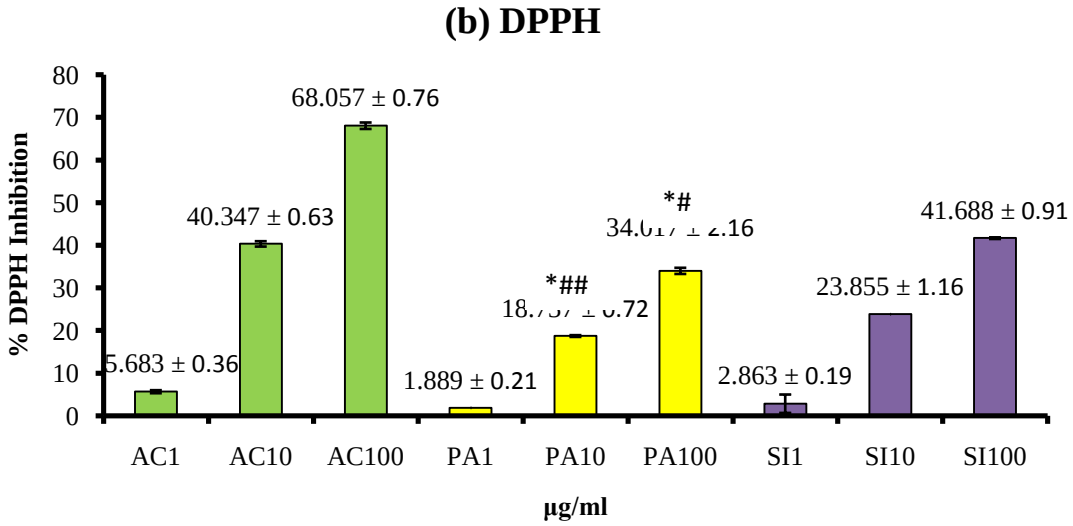

Figure 4.22: (a) Ascorbic acid standard curve. **(b)** % inhibition of DPPH scavenging activity of Panduratin A compound (PA) compared with the standard Ascorbic acid (AC) and the reference drug Silymarin (SI). **P*<0.001compared to AC10/AC100. #*P*<0.001compared to SI100. ##*P*=0.52compared to SI10.

4.6. *In Vitro* Protective Activity of Panduratin A and Germacrone compounds against TAA-cytotoxicity

4.6.1. IC_{50} of TAA

The percentage cell viability of WRL-68 cells after being incubated with different concentrations of TAA (0.03, 0.04 and 0.05 g/ml) for 30, 60, 90 and 120 min, are illustrated on Figure **4.23.** Results showed that incubating the cells with the mentioned

TAA concentrations decreased the cell viability gradually with time from 86.10 ± 0.36, 81.67 ± 1.26 and 83.74 ± 3.60 % respectively after 30 minutes of incubation reaching 42.94 ± 1.35, 44.77 ± 1.93 and 37.33 ± 2.19% respectively after 120 minutes of incubation. Furthermore, the % cell viability recorded 51.17 ± 1.49 % after 60 minutes of incubation with TAA 0.04 g/ml compared with 61.33 ± 1.86 % for the lower tested dose of TAA (0.03 g/ml) and 44.14 ± 2.13 % for the higher tested dose of TAA (0.05 g/ml) indicating that the IC_{50} of TAA is 0.04 g/ml.

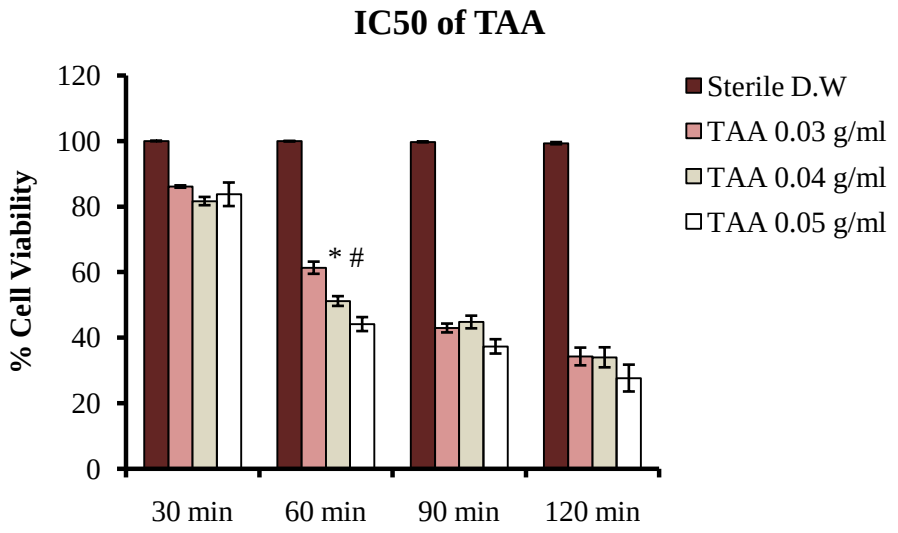

Figure 4.23: IC_{50} of TAA, data were presentd in the form of Mean ± SEM. *P<0.05 compared to TAA-treated cells (0.03 g/ml) and $^{\#}P$<0.001 compared with TAA-treated cell (0.04 g/ml). D.W: distilled water; TAA: thioacetamide.

4.6.2. Cytotoxicity Effect of Panduratin A and Germacrone compounds in WRL-68

Cytotoxicity screening of the tested concentrations of Panduratin A (PA) and Germacrone (GE) compounds in WRL-68 showed that both compounds were not cytotoxic even at the highest tested concentration 100 µg/ml. In addition, results showed that no significance between the various groups as shown in Figure **4.24**.

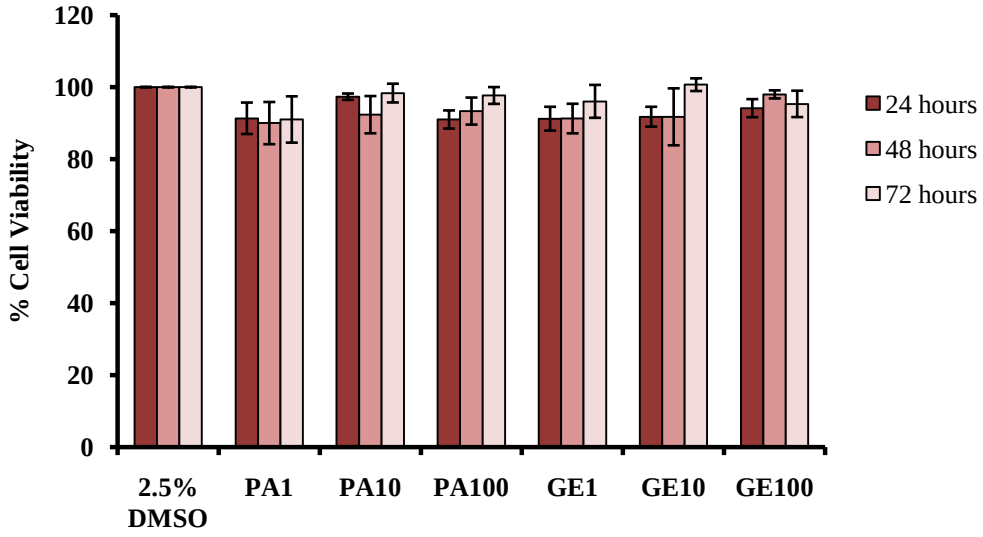

Figure 4.24: Cytotoxicity test of different concentrations of Panduratin A (PA) and Germacrone (GE) compounds on WRL-68 cell line. Data were presented in the form of Mean ± SEM. No significance between the treated and the control group 2.5% dimethyl sulphoxide (DMSO). SI1: 1 µg/ml, SI10: 10 µg/ml, SI100: 100 µg/ml, PA1: Panduratin A 1µg/ml, PA10: 10 µg/ml, PA100: 100 µg/ml.

4.6.3. Protective Effect of Panduratin A and Germacrone Treatment on Cell Viability

The results of treating WRL-68 cells with different concentrations of Panduratin A and Germacrone compounds after inducing TAA-cytotoxicty are shown in Figure **4.25**. Results revealed that cell viability decreased dramatically in the toxin control cells from 24.67 ± 1.20 % after 24 hours of incubation to reach 5.33 ± 2.03 % after 72 hours of incubation. Treatment of the injured cells with PA10 (10 µg/ml) significantly improved ($P<0.05$) the cell viability from 55.00 ± 2.65% after 24 hours of incubation to 75.67 ±1.45 % after 72 hours of incubation approaching the values of SI10 treatment (10 µg/ml) 52.67 ± 3.38 % after 24 hours of incubation and 78.00 ± 1.15 after 72 hours of incubation. Moreover, treatment of the cells with PA100 and GE100 (100 µg/ml) improved the cell viability from 61.00 ± 1.15 and 56.67 ± 1.86% respectively after 24 hours of incubation to 83.63 ± 1.16 % and 77.97 ± 2.65 % respectively after 72 hours of incubation approaching

the values recorded from the reference compound SI100-treated cells 64.00 ± 3.21 % after 24 hours of incubation and 82.18 ± 1.41 % after 72 hours of incubation. Besides, PA1, GE1 and GE10-treated cells did not show significant improvement in the cell viability suggesting that the protective effect of Panduratin A and Germacrone compounds is dose-dependent.

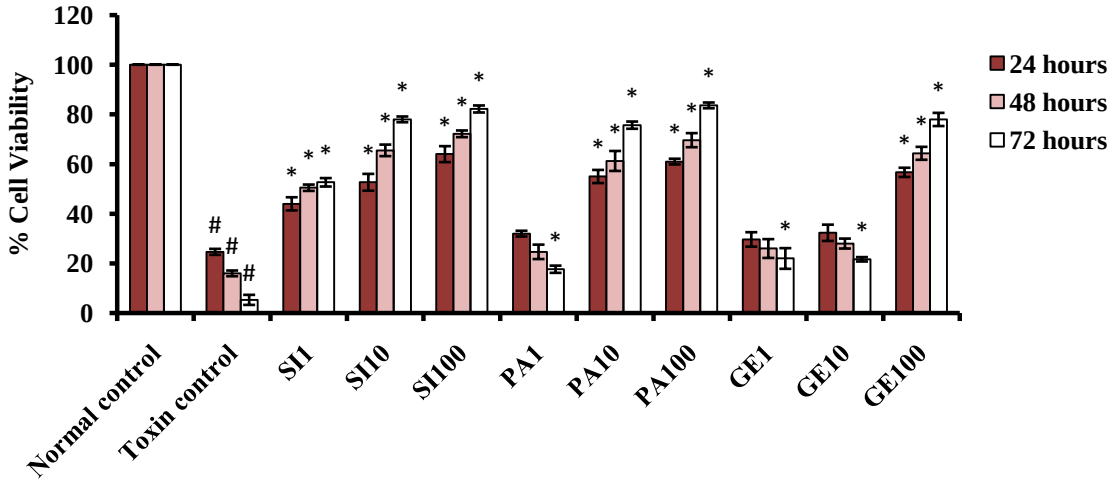

Figure 4.25: Effect of Panduratin A (PA) and Germacrone (GE) compounds on the cell viability after 24, 48 and 72 hours of incubation with different concentrations of the compounds compared to the reference drug silymarin (SI). Data were presented in the form of Mean ± SEM. **P*<0.05 compared to toxin control (0.04 g/ml). $^{\#}$*P*<0.05 compared to normal control (2.5% DMSO). SI1: 1 µg/ml, SI10: 10 µg/ml, SI100: 100 µg/ml, PA1: Panduratin A 1µg/ml, PA10: 10 µg/ml, PA100: 100 µg/ml.

4.6.4. MDA and SOD Assessments

Following the oxidative damage caused by incubating the cells with 0.04 g/ml TAA, MDA significantly increased (*P*<0.05) in the cell lysates collected from the cells of the toxin control group to (18.11 ± 2.21 nmol/ml) compared to normal control group cells (3.70 ± 0.70 nmol/ml) as shown in Figure **4.26**. Treatment of cells with the medium dose (SI10) and the high dose (SI100) of silymarin reduced significantly (*P*<0.05) the level of MDA in

the cell lysates collected from their cells to 9.00 ± 0.58 and 5.67 ± 1.45 nmol/ml respectively compared to the toxin control group cells. In the same manner, the high dose PA100 and GE100 (100 μg/ml) significantly reduced the level of MDA to 7.33 ± 1.45 and 7.00 ± 1.15 nmol/ml respectively. Treatment of the cells with the medium dose (10 μg/ml) showed significant decrease in MDA level in PA10 group cells (9.11 ± 2.31 nmol/ml) compared to toxin control cells, but not in GE10 group cells. Conversely, the high dose of SI, PA and GE (100 μg/ml) increased the level of SOD to 2.52 ± 0.46, 2.12 ± 0.14 and 1.87 ± 0.15 nmol/ml respectively compared to the low level of the toxin control group (0.49 ± 0.22 nmol/ml). The results suggest that Panduratin A and Germacrone compounds may protect the liver cells from TAA-induced oxidative damage.

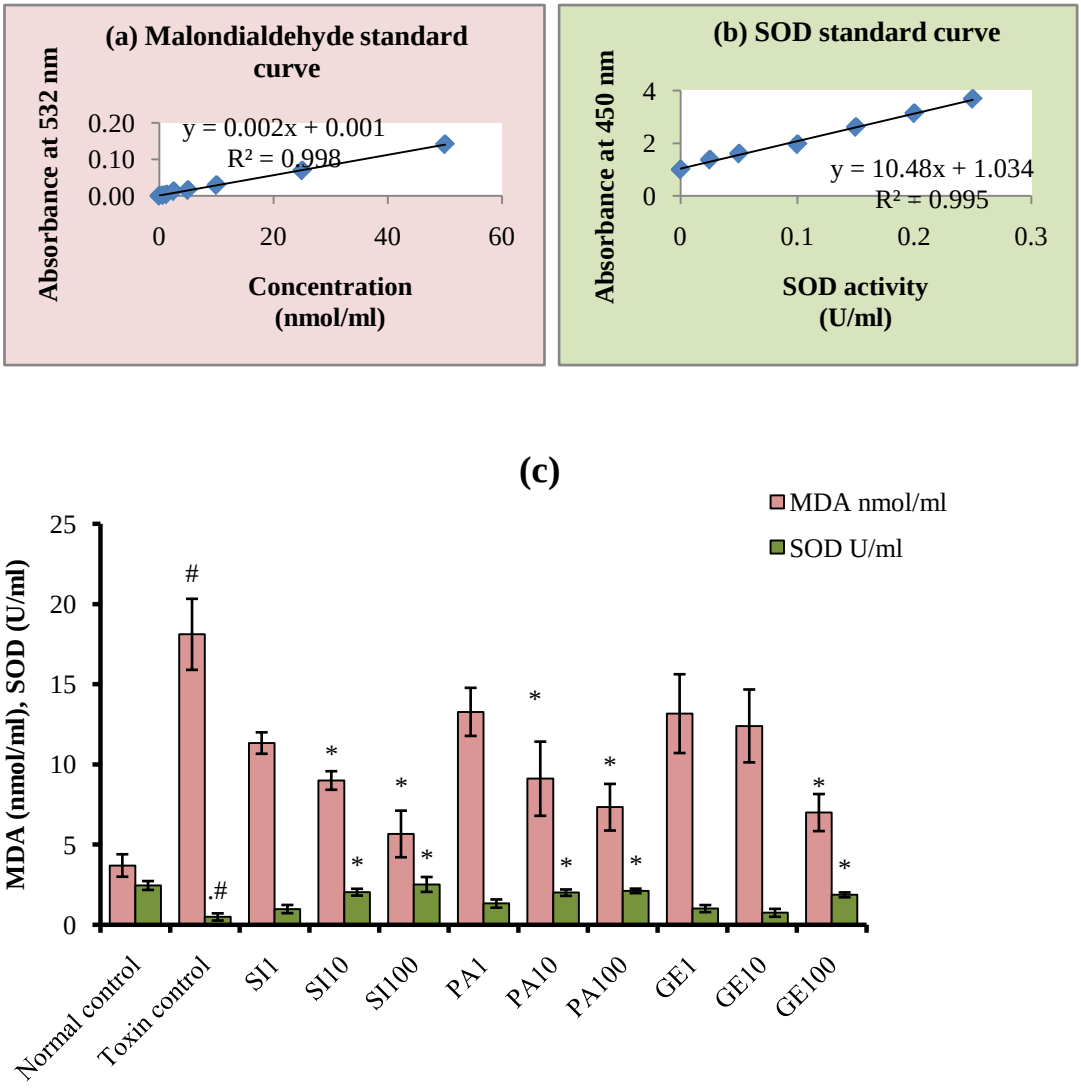

Figure 4.26: (a) Malondialdehyde standard curve. **(b)** SOD standard curve. **(c)** Effect of Panduratin A (PA) and Germacrone (GE) compounds on the level of MDA and SOD in the cell lysates collected from all cell groups after 72 hours of incubation with TAA and different concentrations of the compounds (1,10 and 100 µg/ml) in parallel with the reference drug silymarin (SI). Data were presented in the form of Mean ± SEM. **P*<0.05 compared with to toxin control (0.04 g/ml). $^{\#}P$<0.05 compared to normal control (2.5% DMSO). SI1: 1 µg/ml, SI10: 10 µg/ml, SI100: 100 µg/ml, PA1: Panduratin A 1µg/ml, PA10: 10 µg/ml, PA100: 100 µg/ml.

4.7. *In Vivo* Hepatoprotective activity of The isolated Panduratin A (PA) agianst TAA-Induced Liver Damage in Rats

4.7.1. Acute toxicity

All the rats in the acute toxicity experiment stayed in existence and did not expose death rate or any noticeable toxicity symptoms throughout the 14 days study at the high dose of 500 mg/kg. The physical results indicated no symptoms and no changes observed in their furs, eyes and mucous walls, habits, shaking, salivations, diarrhea situations and snoozes. The body weight of the treated male and female rats increased progressively but were not significantly different as compared to those of the control group rats (Table **4.13**) Serum biochemical parameters recorded the metabolism of normal kidney and liver, and the histopathological assessments of the renal and the liver tissues showed no significant variations between the control and experimental groups, as shown by the quantitative information in Tables **4.14** and **4.15**, and Figure **4.27**.

Table 4.13: Effect of Panduratin A on the initial and the final body weights of rats measured from the acute toxicity test.

Dose	Body weight on day 0 (g)	Body weight on day 15 (g)
Vehicle (10% Tween 20)	204 ± 10.1	245 ± 10.61
Low Dose (50 mg/kg)	205 ± 9.93	246 ± 13.07
High Dose (500 mg/kg)	199 ± 5.02	239 ± 8.12

The values were expressed as mean ± SEM. There were no significant differences between the groups. Significant value was at $P<0.05$.

Table 4.14: Effect of Panduratin A (PA) on the renal function measured from the acute toxicity test on rats.

Dose	Sodium (mmol/L)	Pottasium (mmol/L)	Chloride (mmol/L)	Urea (mmol/L)	Creatinine (µmol/L)
Vehicle (10% Tween 20)	139.33 ± 0.24	5.96 ± 0.05	103.98 ± 0.05	6.07 ± 0.03	47.13 ± 0.02
Low Dose PA (50 mg/kg)	140.02 ± 0.26	6.00 ± 0.03	103.98 ± 0.08	6.14 ± 0.02	47.11 ± 0.03
High Dose PA (500 mg/kg)	139.76 ± 0.31	5.95 ± 0.03	103.94 ± 0.10	6.11 ± 0.02	47.15 ± 0.02

Values were expressed as mean ± SEM. There were no significant differences between PA-treated groups and the vehicle group. Significant value was at $P<0.05$.

Table 4.15: Effect of Panduratin A (PA) on the liver function measured from the acute toxicity test on rats.

Dose	Total protein (g/L)	Albumin (g/L)	Globulin (g/L)	AP (IU/L)	ALT (IU/L)	AST (IU/L)	GGT (IU/L)
Vehicle (10% Tween 20)	70.98 ± 0.08	10.85 ± 0.05	60.13 ± 0.08	133.345 ± 0.14	48.78 ± 0.15	154.01 ± 0.05	4.10 ± 0.01
Low Dose PA (50 mg/kg)	71.25 ± 0.20	10.85 ± 0.05	60.40 ± 0.23	133.23 ± 0.17	48.99 ± 0.19	154.02 ± 0.11	4.12 ± 0.01
High Dose PA (500 mg/kg)	70.81 ± 0.10	10.73 ± 0.05	60.08 ± 0.05	133.08 ± 0.20	48.98 ± 0.05	153.96 ± 0.06	4.10 ± 0.01

Values were expressed as mean ± SEM. There were no significant differences between PA-treated groups and the vehicle group. Significant value was at $P<0.05$.

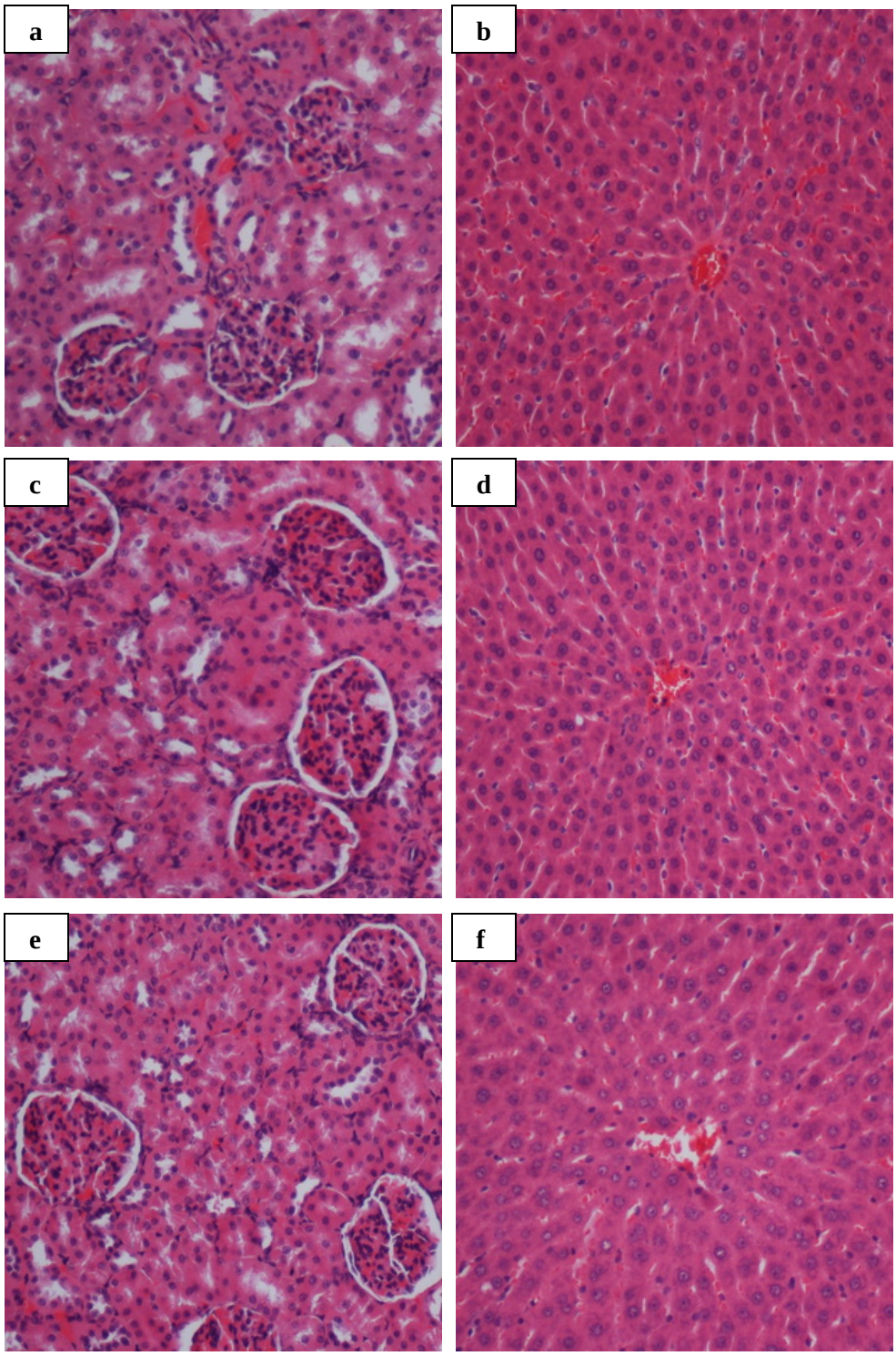

Figure 4.27: Histological sections (H&E) of livers (right column) and kidneys (left column) obtained from the rats in the acute toxicity test. Rat with the kidney and liver shown in **(a)** and **(b)** was treated with 5 ml/kg vehicle (10% Tween 20). Rat with the kidney and liver shown in **(c)** and **(d)** was treated with 5 mg/kg (5 ml/kg) dose of the isolated Panduratin A (PA) compound. Rat with the kidney and liver shown in **(e)** and **(f)**

was treated with 500 mg/kg (5 ml/kg) dose of the PA compound. There was no significant difference in the structures of the liver and kidney between the treatment and control groups. (Original magnification x20)

4.7.2. *In Vivo* Hepatoprotective Activity of PA against TAA-Induced Liver Damage in Rats

4.7.2.1. Body Weight and Liver Index

The total body weight of each rat was measured prior to the sacrifice. Similarly, the liver weighted after being excised (Table **4.16**). The normal control rats followed normal growth pattern and attained normal weight gains from about 210.17 ± 11.39 g to 330.00 ± 10.43 g in 4 weeks. The injection of TAA made the rats hepatotoxic and suffered growth retardation as they weighted significantly less than those measured from the other groups. When the body weights were factored in, the cirrhotic rats in cirrhosis control group had the highest liver index. The rats of silymarin-treated and HDPA-treated groups attained body weights as equivalent as the normal rats (Table **4.16**). Figure **4.28** showed that the weight gain in HDPA (50 mg/kg) and silymarin-treated rats (46.79 ± 1.76 and 46.25 ± 2.51 % respectively) was significantly high compared to cirrhosis control group (33.75 ± 4.64 %). The rats of LDPA (5 mg/kg) and MDPA (10 mg/kg) treated animals had better weight gain (35.31 ± 2.38 and 45.14 ± 1.55 % respectively) than those of cirrhosis control group, but not as much as those attained in the silymarin and the HDPA-treated animals. These findings implied that the outcome of the treatment was susceptible to the administered dose amount, but the PA at this high dose appeared to be optimal since it was as effective as silymarin in counteracting the progression of liver damage.

Table 4.16: Effect of Panduratin A (PA) on the measurements results of liver index of the rats after the 8 week study against TAA toxicity.

Treatment	Initial body weight (g)	Final Body weight (g)	Liver weight (g)	Liver index (%)
Normal control	210.17 ± 11.39	330.00 ± 10.43	8.74 ± 0.25	2.67 ± 0.14
Cirrhosis control	185.00 ± 13.99	244.33 ± 12.56**	9.93 ± 0.36**	4.09 ± 0.14**
Reference control (Silymarin 50 mg/kg)	219.00 ± 12.32	318.83 ± 13.04*	8.93 ± 0.35	2.80 ± 0.04*
LDPA (5 mg/kg)	212.00 ± 9.28	258.83 ± 7.93	8.92 ± 0.27	3.32 ± 0.13*
MDPA (10 mg/kg)	200.83 ± 4.92	291.33 ± 6.59	8.45 ± 0.13*	2.90 ± 0.05*
HDPA (50 mg/kg)	211.00 ± 12.44	308.83 ± 15.11*	8.28 ± 0.20*	2.70 ± 0.07*

The data were analyzed as as Mean ± SEM. Significant difference was noticed between the means of groups (n = 5 rats/group), silymarin-treated group, low dose, medium dose and high dose PA-treated groups. *P<0.05 compared to cirrhosis control group. **P<0.05 compared to the normal control group.

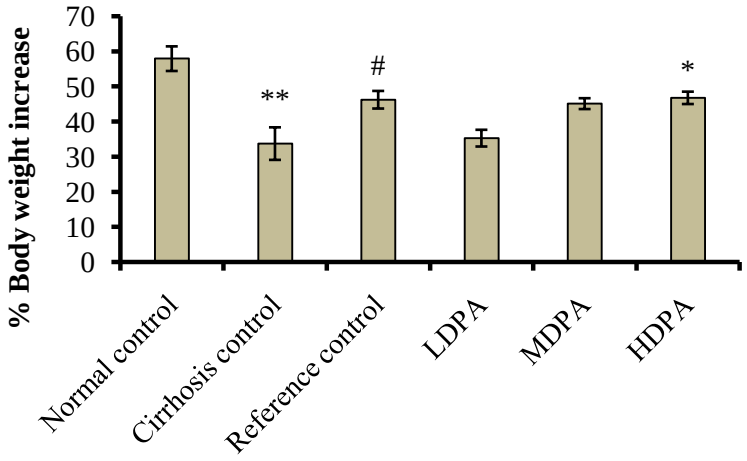

Figure 4.28: Effect of Panduratin A (PA) on % body weight increase measured from the rats at the end of the 8 week study against TAA toxicity.Data were expressed as Mean ± SEM. Means among groups (n = 5 rats/group) show significant difference, *P<0.05 compared to cirrhosis control group. **P<0.05 compared with the normal control group. $^{\#}P$=0.52 compared to the group of cirrhosis control. Normal control (distilled water). Cirrhosis

control: (Thioacetamide 200 mg/kg). Reference control (Silymarin 50 mg/kg). LDPA (Low Dose Panduratin A 5 mg/kg). MDPA (Medium Dose Panduratin A 10 mg/kg). HDPA (High Dose Panduratin A 50 mg/kg).

4.7.3. Biochemical Analysis

Liver function of all rats was determined by measuring the plasma levels of specific liver enzymes, and the results are illustrated in Table **4.17**. Data revealed that TAA-induced liver damage significantly brought up the levels of specific liver enzymes AP, ALT, AST and GGT ($P< 0.001$) compared to the normal control group. The high dose of PA (50 mg/kg) given to the animals of HDPA group has led to lower enzymatic levels that were much like those of normal control group and the silymarin-treated (50 mg/kg) group, and better than the levels obtained from the low dose (LDPA) (5 mg/kg) group and the medium dose (MDPA). These results verified that the repercussions of the toxicity induced by TAA on the liver function may be efficiently be counterbalanced by the explicit results of the PA treatment, but in a dose-dependent way.

Table 4.17: Effect of Panduratin A (PA) on the liver enzymes of the rats' plasma after the four weeks period of study against TAA toxicity

Treatment	AP (IU/L)	ALT (IU/L)	AST (IU/L)	GGT (IU/L)
Normal control	95.70 ± 2.97	76.33 ± 2.69	137.33 ± 5.25	2.65 ± 0.31
Cirrhosis control	307.77± 17.82**	195.27 ± 26.41**	320.67 ± 35.50**	10.72 ± 0.80**
Reference control (Silymarin 50 mg/kg)	92.12 ± 4.92*	74.67 ± 6.30*	117.50 ± 7.56*	3.46 ± 0.32*
LDPA (5 mg/kg)	131.59 ± 18.27*	110.83 ± 7.64*	238.33 ± 25.51*	7.31 ± 0.54*
MDPA (10 mg/kg)	106.72 ± 8.09*	97.12 ± 13.21*	188.00 ± 11.85*	5.18 ± 0.55*
HDPA (50 mg/kg)	100.46 ± 6.97*	92.67 ± 7.25*	199.29 ± 15.70*	2.50 ± 0.32*

AP alkaline phosphatase; ALT alanine transaminase; AST aspartate transaminase; GGT gamma-glutamyl transferase. Data are expressed as mean ± SEM. Means among groups (n = 5 rats/group) show significant difference. *P<0.001 compared to cirrhosis control group. **P<0.001 compared to normal control group.

4.7.4. Parameters of Oxidative Damage

Oxidative stress parameters measured from all rats (urine 8-OH-dG and liver tissues homogenate MDA and nitrotyrosine NT) levels are shown in Figures **4.29** and **4.30**. Generally, cirrhosis animals intoxicated with TAA only, had significantly (P<0.001) increased oxidative damage as indicated by the markers OH-dG, NT and MDA (5.87 ± 0.30 ng/ml, 3.87 ± 0.13 ng/ml and 22.78 ± 5.05 nmol/mg protein respectively) than normal control group (1.83 ± 0.07 ng/ml, 0.67 ± 0.07 ng/ml and 7.31 ± 1.79 nmol/mg protein respectively) and the other experimental animals. Administration of HDPA had significantly reduced (P< 0.01) the level of OH-dG, NT and MDA (2.73 ± 0.03 ng/ml, 1.07 ± 0.27 ng/ml and 10.08 ± 2.83 nmol/mg protein respectively) compared to cirrhosis control

group. In addition, there were no significant modifications in the analyzed markers between HDPA-treated and Silymarin-treated rats (2.73 ± 0.18 ng/ml, 1.47 ± 0.13 ng/ml and 7.83 ± 2.62 nmol/mg protein respectively). These results suggested that treatment with PA may protect hepatic tissues from further damage during liver injury.

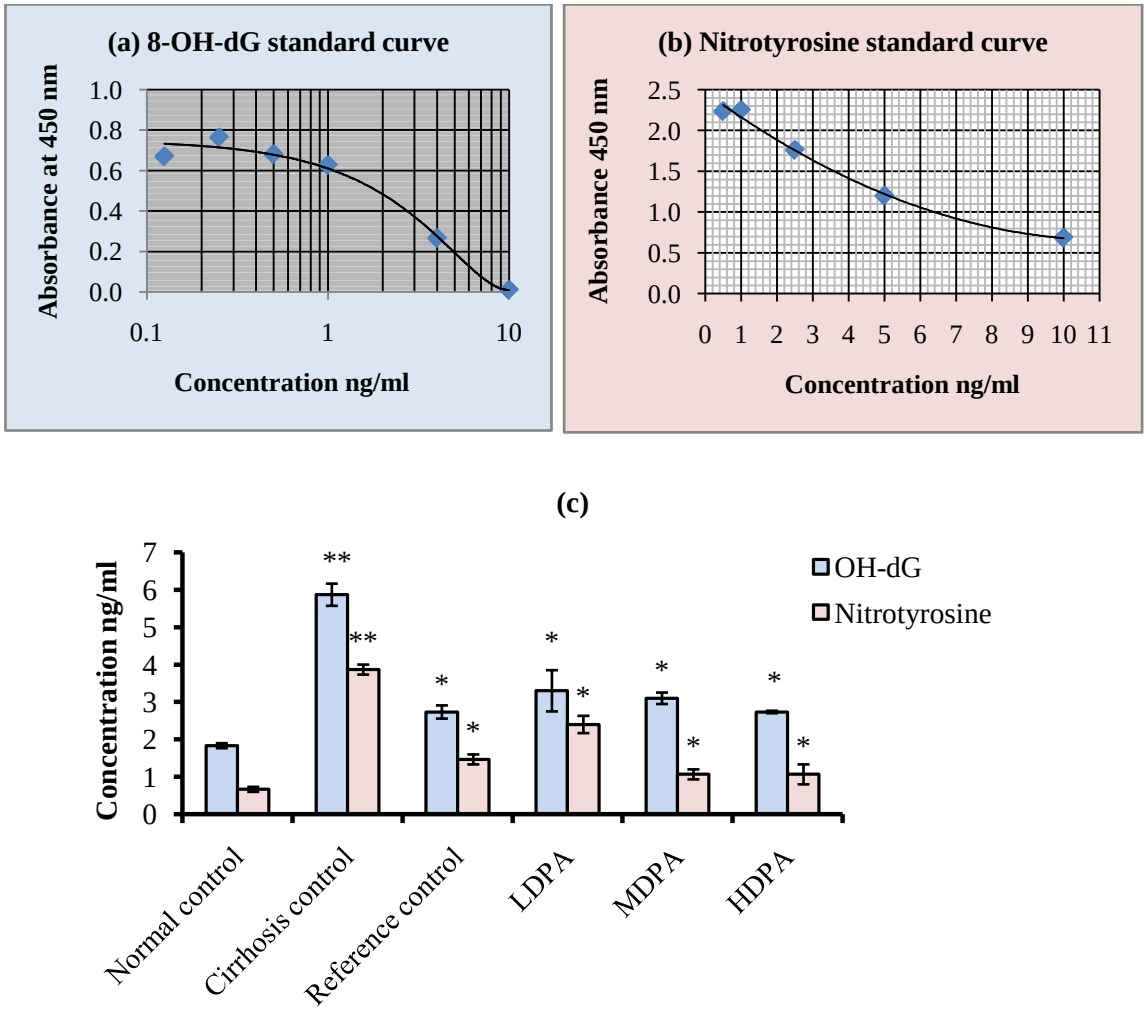

Figure 4.29: (a) 8-OH-dG standard curve **(b)** Nitrotyrosine standard curve **(c)** Effect of Panduratin A (PA) on the urine level of 8-Hydroxy Deoxy Guanosine (8-OH-dG) and liver tissue homogenate level of Nitrotyrosine. Data are expressed as mean ± SEM. ***P*<0.001 compared to the normal control group. **P*<0.01 compared to cirrhosis control group. Normal control (distilled water). Cirrhosis control (TAA 200 mg/kg). Reference control

(Silymarin 50 mg/kg). LDPA (Low Dose Panduratin A 5 mg/kg). MDPA (Medium Dose Panduratin A 10 mg/kg). HDPA (High Dose Panduratin A 50 mg/kg).

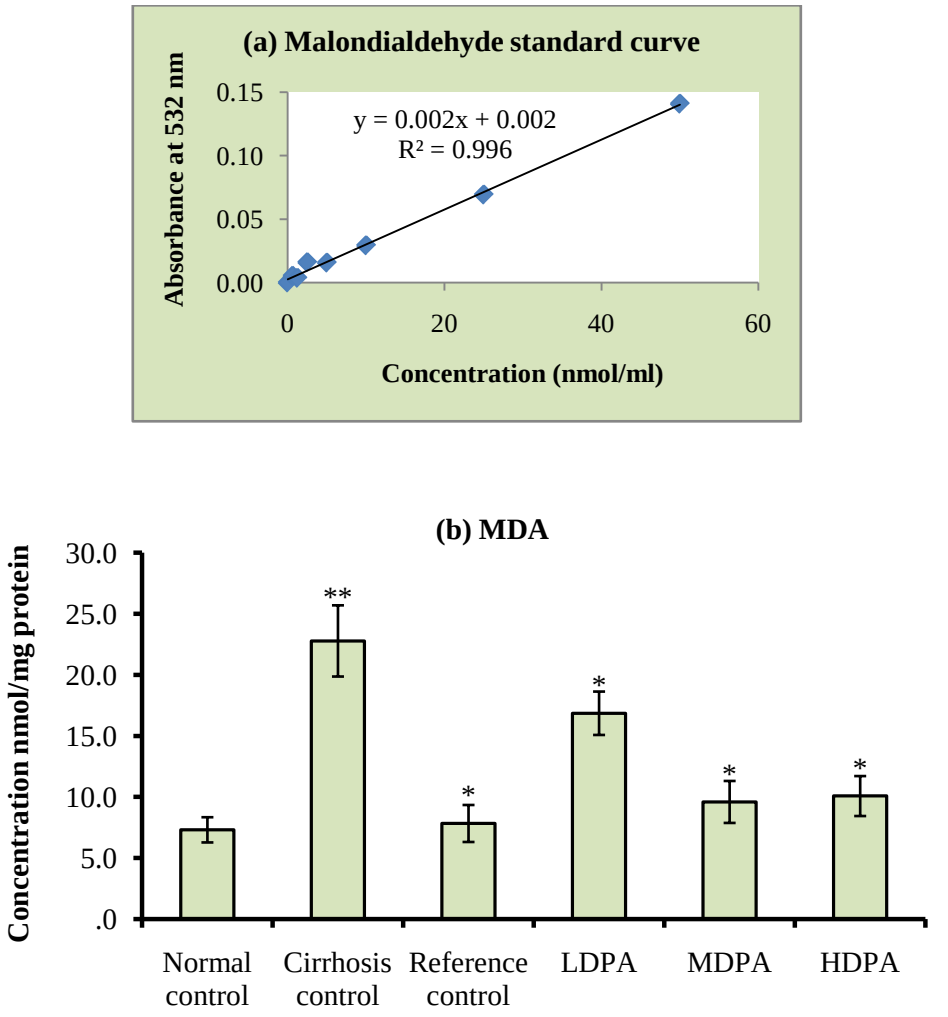

Figure 4.30: (a) Malondialdehyde standard curve **(b)** Effect of Panduratin A (PA) on the liver tissue homogenate level of Malondialdehyde (MDA). Data are expressed as mean ± SEM. ***P*<0.01 compared to the normal control group. **P*<0.01 compared to cirrhosis control group. Normal control (distilled water). Cirrhosis control: (TAA 200 mg/kg). Reference control (Silymarin 50 mg/kg). LDPA (Low Dose Panduratin A 5 mg/kg). MDPA (Medium Dose Panduratin A 10 mg/kg). HDPA (High Dose Panduratin A 50 mg/kg).

4.7.5. Hepatocellular Antioxidant Enzymes

Hepatocellular loss in the livers of cirrhosis rats was ultimately examined by the activity of the endogenous enzymes SOD, CAT and GPx. The outcomes are proven in

Figure **4.31**. SOD, CAT and GPx in cirrhotic rats (9.46 ± 1.90 U/mg protein, 5.24 ± 1.74 U/min/mg protein and 73.79 ± 11.95 nmol/min/mg protein respectively) were reduced than in normal rats indicating the incident of serious harm in the tissues of cirrhotic livers. Treating the cirrhotic livers with the high dose of PA (50 mg/kg) significantly ($P<0.01$) improved the levels of SOD, CAT and GPx (46.26 ± 3.89 U/mg protein, 15.06 ± 1.53 U/min/mg protein and 744.82 ± 13.42 nmol/min/ mg protein respectively) and promoted the hepatocellular survival. Moreover, SOD, CAT and GPx levels in the HDPA-treated rats approached that of silymarin-treated animals (41.32 ± 3.90 U/mg protein, 14.55 ± 0.50 U/min/mg protein and 473.26 ± 47.13 nmol/min/mg protein respectively). On the other hand, The LDPA and MDPA-treated rats didn't show significant increase in these endogenous enzymes compared to cirrhosis control group. These outcomes jointly reinforced the recommendation that therapy with PA could offer a protective environment for hepatocytes from further loss, but in a dose dependent way.

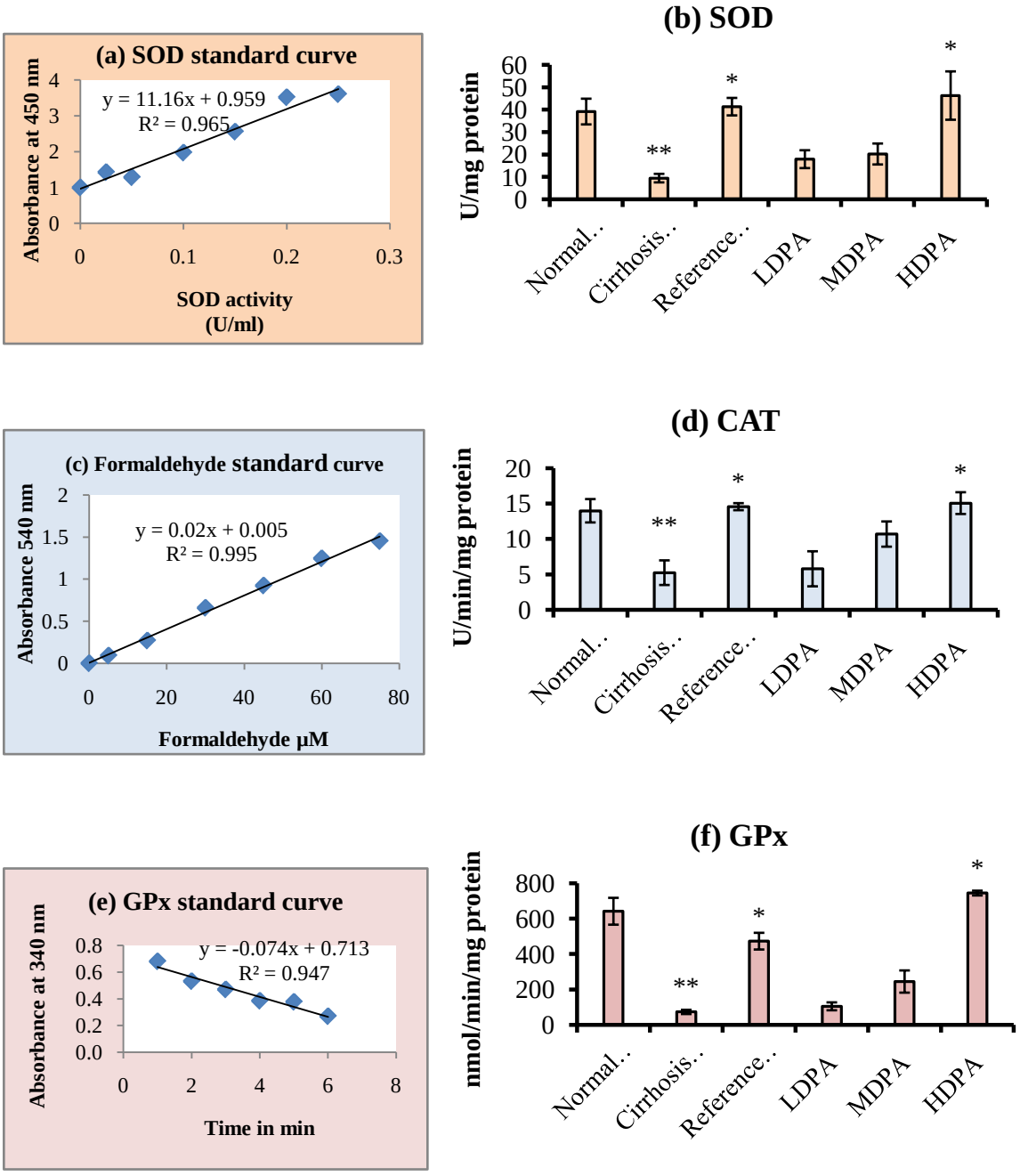

Figure 4.31: (a) Superoxide dismutase (SOD) standard curve **(b)** Effect of Panduratin A (PA) on the hepatic SOD **(c)** Catalase (CAT) standard curve **(d)** Effect of PA on the hepatic CAT **(e)** GPx standard curve **(f)** Effect of PA on the hepatic GPx. Data are expressed as mean ± SEM. ***P*<0.05 significance compared to the group of normal control. **P*<0.05 significance compared to the group of cirrhosis control. Normal control (distilled water). Cirrhosis control: (Thioacetamide 200 mg/kg). Reference control (Silymarin 50 mg/kg). LDPA (Low Dose Panduratin A 5 mg/kg). MDPA (Medium Dose Panduratin A 10 mg/kg). HDPA (High Dose Panduratin A 50 mg/kg).

4.7.6. Liver Gross and Histopathology

Liver gross and H&E histology sections obtained from all animal groups are shown in Figures.**4.32** and **4.33** respectively. Normal group rats showed smooth surfaces and absence of nodules confirmed histologically by normal liver architecture. Liver gross from the untreated cirrhosis rats showed congested livers combined with numerous micro-nodules and their histology revealed fibrous septae accompanied by proliferated bile ducts and inflammatory cells. Very few micro-nodules with less septae and more normal hepatocytes were observed on the livers from silymarin-treated and those of the high dose PA-treated rats, HDPA On the other hand, MDPA showed improvement in the micro-nodules which appeared less than LDPA but not as efficient as HDPA or silymarin-treated rats. These visual tests afforded further confirmation that PA can be efficient in protecting the liver from further damage in a dose-dependent way.

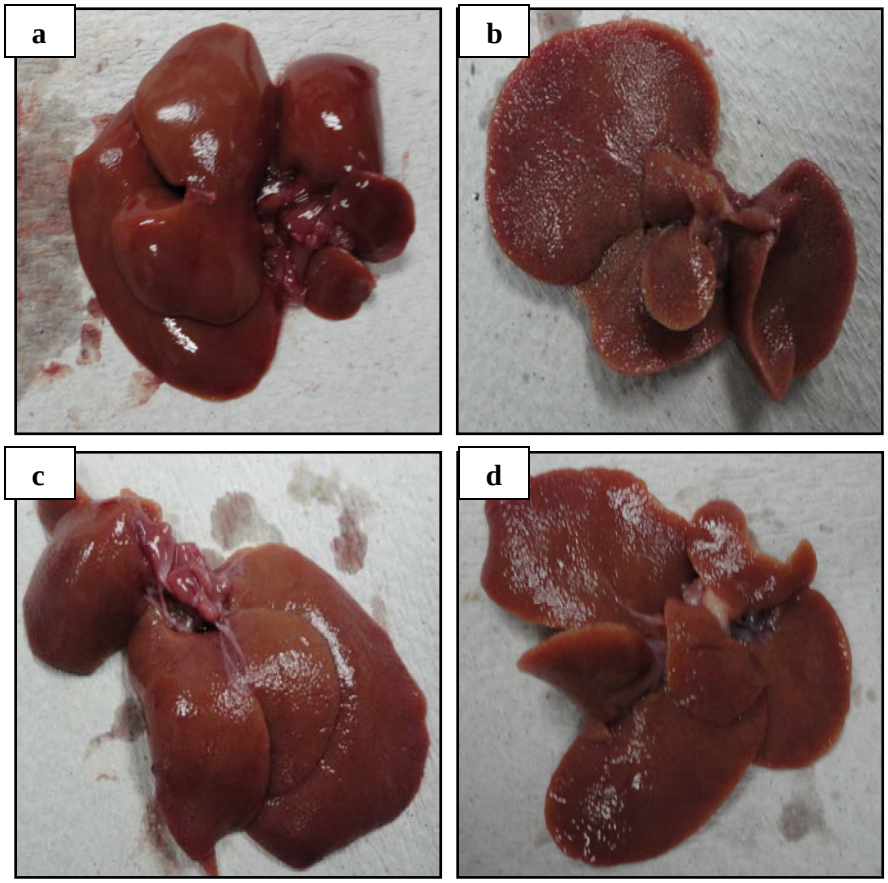

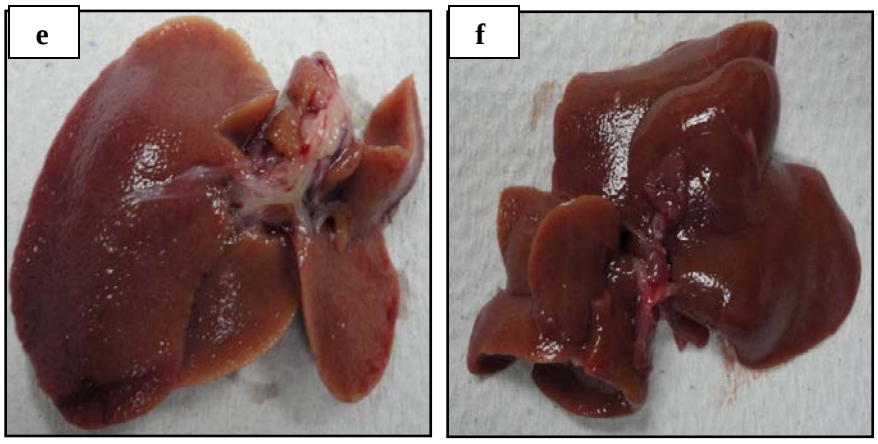

Figure 4.32: Macroscopic appearances of liver samples collected from all experimental rats. **(a)** Normal liver had smooth surface**. (b)** Cirrhotic liver showed several micro-nodules on its surface place. **(c)** Liver from a silymarin-treated rat showed smooth surface with very few micro-nodules. **(d)** Liver from a rat treated with LDPA showed surface with slightly more micro-nodules. **(e)** Liver from a rat treated with MDPA showed very minor micro-nodules on its surface. **(f)** Liver from a rat treated with HDPA showed smooth normal surface.

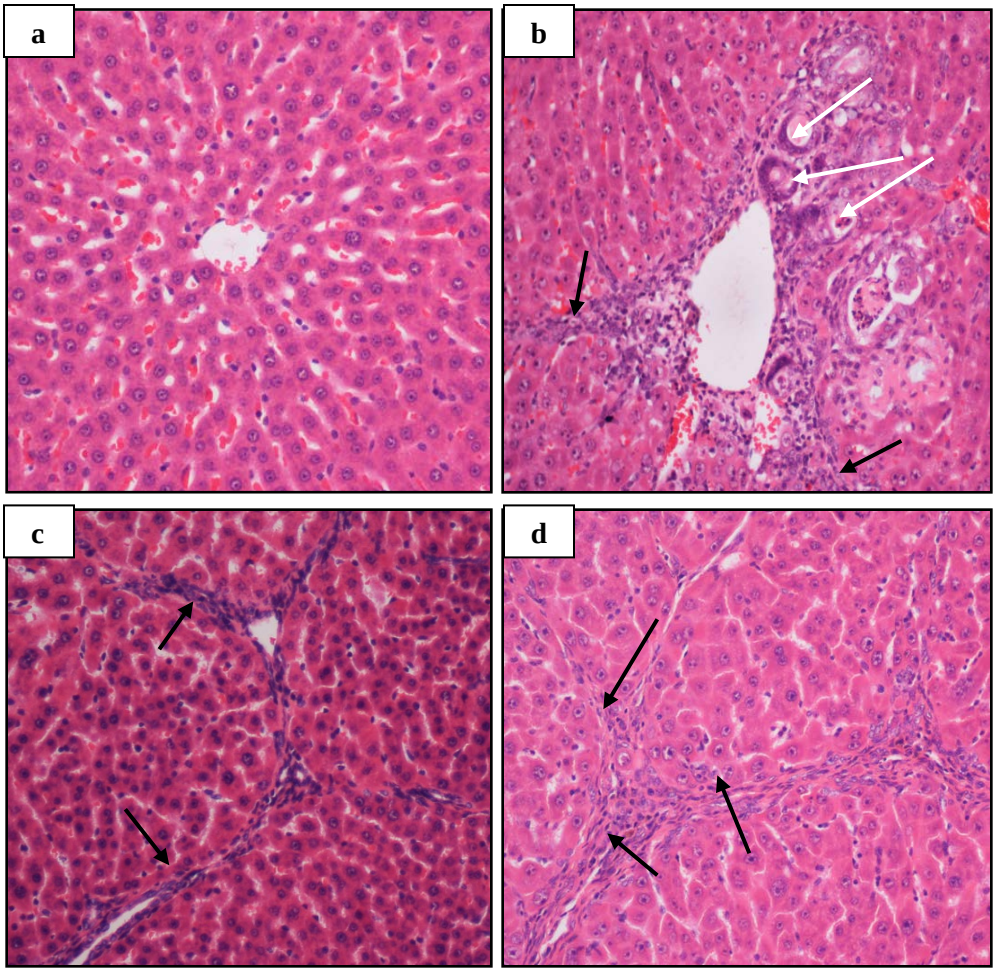

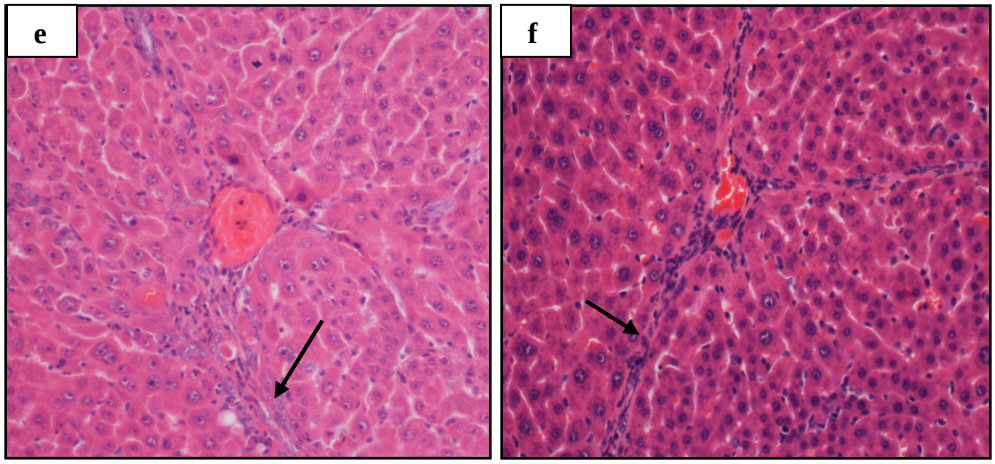

Figure 4.33: Histopathological sections of liver samples from rats of all experimental groups. **(a)** Normal liver architecture from a normal control rat. **(b)** Structural damage with fibrotic septae (black arrow) and necrotic proliferated bile ducts (white arrows) in the liver of a cirrhotic rat. **(c)** Mild inflammation with very less fibrotic septae (black arrow) in the liver of a silymarin-treated rat. **(d)** Slightly preserved hepatocytes with small necrotic area and fibrotic septa in the livers of rats treated with LDPA. **(e, f)** Improved hepatocytes and architecture with small necrotic areas in the liver of rats treated with MDPA and HDPA respectively.

4.7.7. Massson's Trichrome Staining

Fibrosis level of liver samples collected from all experimental animals and evaluated by Masson's Trichrome staining, are illustrated in Figure **4.34**. No signs of collagen deposition in the liver sample of normal control group. Cirrhotic liver of cirrhosis control group rats showed congested central vein surrounded by highly deposited collagen fibers indicating high level of fibrosis. Silymarin-treated liver showed very low level of fibrosis indicated by very less collagen fibers deposit. Gradual decrease in the level of fibrosis indicated by the gradual decrease in collagen fibers deposition was observed in the liver sections obtained from the PA-treated groups rats. Treating the cirrhotic rats with MDPA or HDPA reduced effectively collagen deposition around the central vein more than

LDPA group rats. This assessment of the level of fibrosis verifies the previous results that PA-treatment protected the livers of animals from progressive fibrosis.

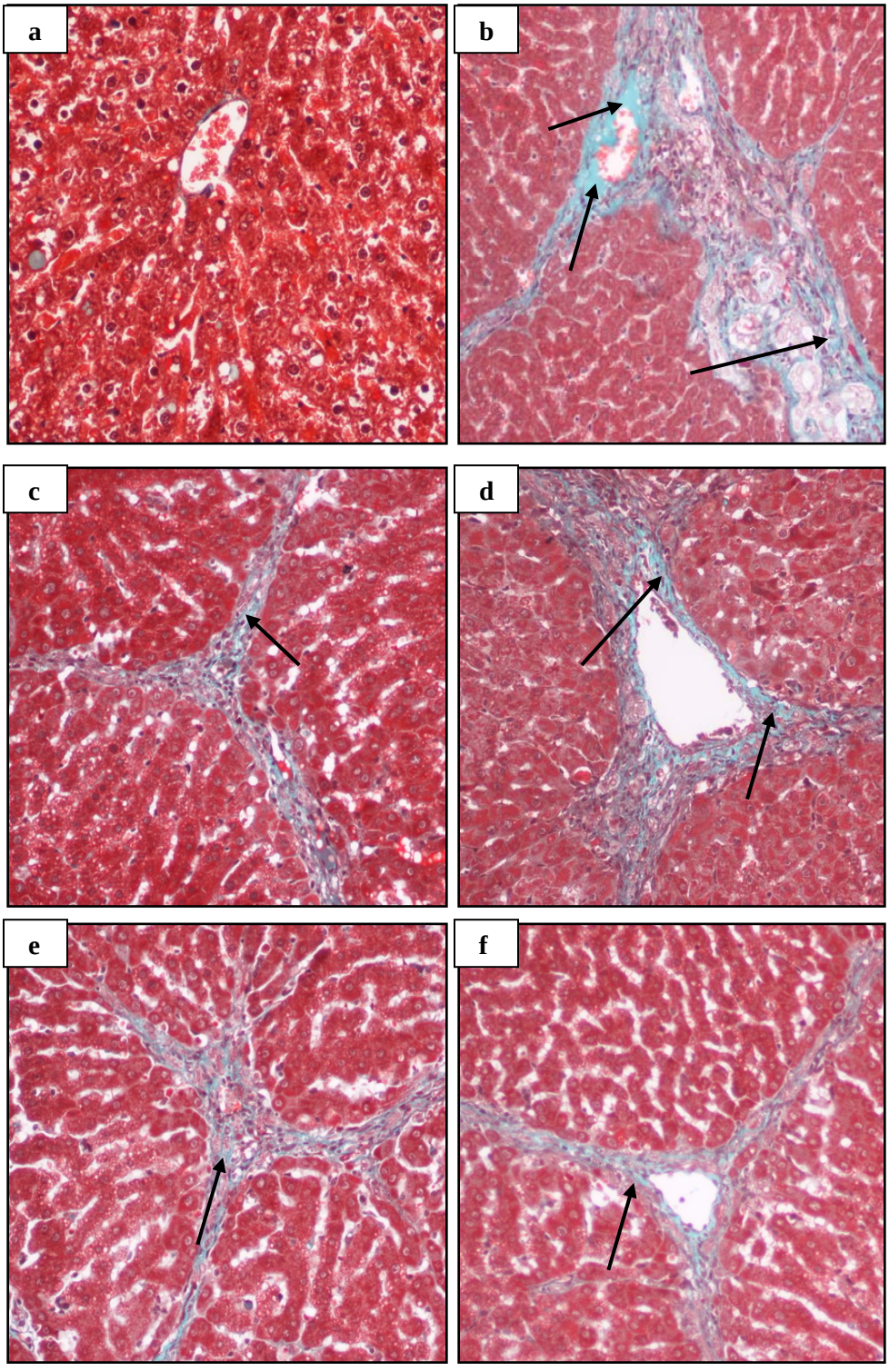

Figure 4.34: Masson's trichrome staining of the liver sections collected from all experimental groups and stained with Masson's Trichrome. **(a)** No signs of collagen deposition or fibrosis in the liver sample from normal rats. **(b)** Increased deposition of collagen fibers stained green (black arrow) around congested central vein showing high grade of fibrosis in the liver from a cirrhotic rat. **(c)** Very less deposited collagen and minor fibrosis in the liver of a silymarin-treated rat. **(d)** Moderate grade of deposited collagen around the central vein and moderate level of fibrosis in the liver sample from a rat treated with LDPA. **(e)** Less collagen fibers in the liver of a rat treated with MDPA. **(f)** Very less collagen deposition in the liver a rat treated with HDPA. (Original magnification ×20).

4.7.8. Alpha Smooth Muscle Actin (α-SMA) staining

Alpha smooth muscle staining of liver sections prepared from the rats of all experimental groups demonstrating activated hepatic stellate cells is shown in Figure **4.35**. The α-SMA was missing from the liver from normal group rats. Highly activated hepatic stellate cells indicated by the deep staining of α-SMA in the liver from cirrhosis rats of cirrhosis control group. The intensity of α-SMA staining was almost absent in the liver of silymarin-treated group livers compared to liver sections from the cirrhosis control group. Gradual decrease in the intensity of α-SMA staining in the liver sections from the experimental rats treated with different doses of PA with very low staining in the medium dose PA-treated rats (MDPA) and the high dose PA-treated rats (HDPA) compared to the low dose PA-treated rats (LDPA) demonstrating marked decrease in the number of activated hepatic stellate cells in the liver of MDPA group and HDPA rats compared to those of group LDPA rats.

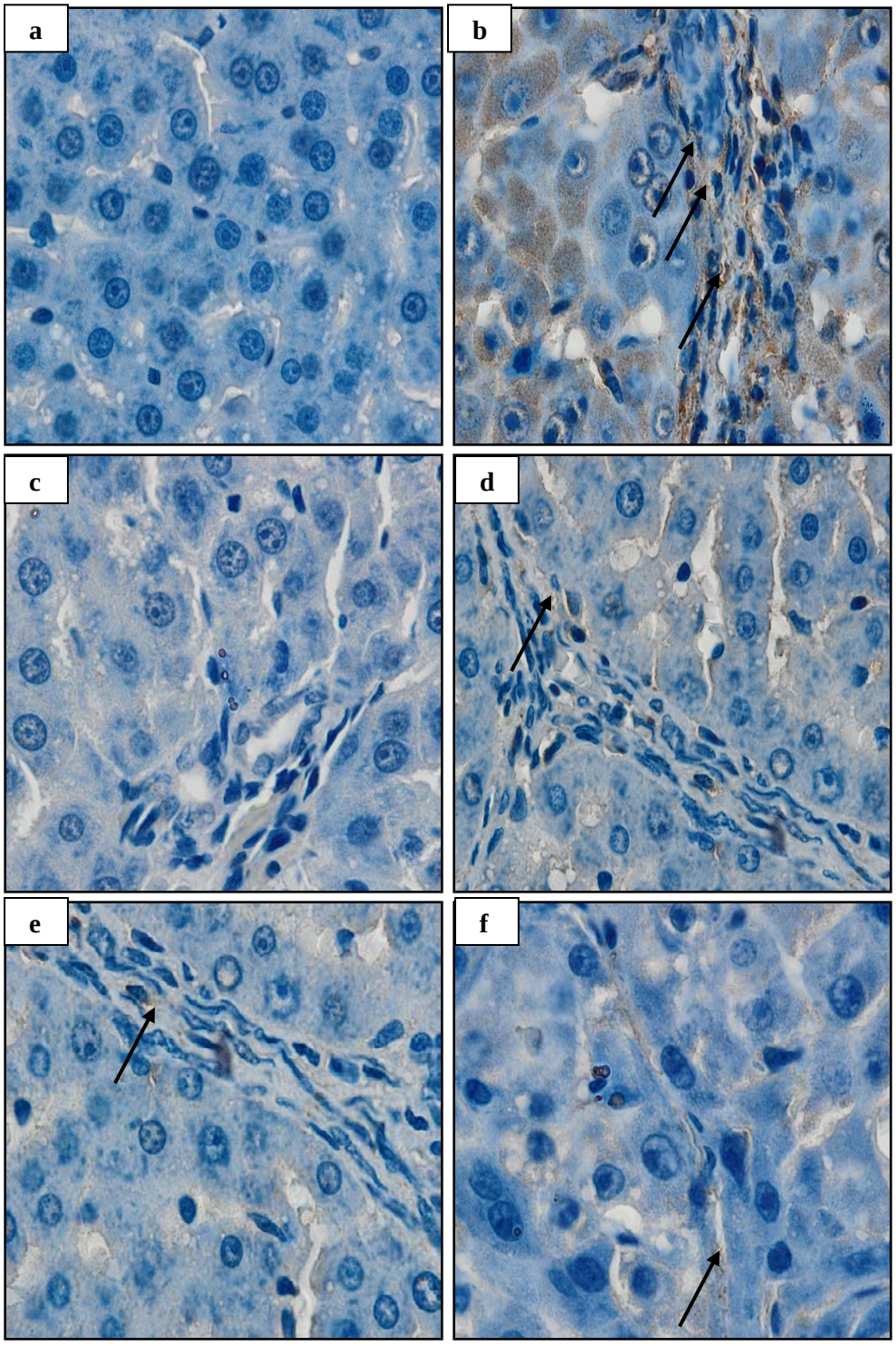

Figure 4.35: Immunohistochemistry staining of alpha smooth muscle actin (α-SMA) of liver sections sampled from all experimental groups. **(a)** Normal liver did not show signs of positive α-SMA staining. **(b)** Dense brown stain with highly expressed α-SMA (black arrow) demonstrating highly activated hepatic stellate cells in the liver of a cirrhotic rat. **(c)** Very few positive α-SMA staining in the silymarin-treated liver. **(d)** Moderate positive

staining of α-SMA in the liver from LDPA group. **(e)** Few positive α-SMA staining in the liver from MDPA group. **(f)** Very few positive α-SMA staining reflecting very few activated hepatic stellate cells in the liver from HDPA group. (Original magnification x100).

CHAPTER V

DISCUSSION AND CONCLUSIONS

5.1. Discussion

Clinical and toxicological research has been performed for therapeutic to ensure the safety of these plants. During the experimental period on *B. rotunda* and *C. longa* plant extracts, all animals did not show any abnormal behavioural expression and toxicological signs. Histology of liver and kidneys, and serum biochemistry revealed no significant differences between groups (Tables **4.2** and **4.3**). These results conclude that the extracts are safe enough even at the higher doses and have no acute toxicity.

(Jing *et al*., 2010) reported on *B.rotunda* and its antioxidants properties which may be due to its high contents of flavanoids, Quercetin and Kaempferol. (Kumar *et al*., 2006) reported that *C. longa* extract contains potent antioxidants. In the present study, *C. longa* extract exhibited higher DPPH scavenging power and ferric reducing power more than *B. rotunda* extract, where both plant extracts showed higher total phenolic content. The antioxidant activity of *C. longa* rhizomes could be attributed to its content of the potent phenol compounds curcumin and curcuminoids (Kumar, *et al*., 2006).

Furthermore, in this study silymarin was used as control to compare the ferric reducing power and the total phenol content of the selected plant extracts. Previous studies, explained the silymarin efficacy in hepatoprotective with correlation to curcumin the main constituent of *C. longa* extract (Girish *et al*., 2009). Similarly, the hepatoprotective activity of Quercetin, the active flavonoid in *B. rotunda* extract having the same efficacy of Silymarin (Chouhan *et al*., 2011).

Thioacetamide (TAA) is a potent hepatotoxic chemical, that induces in animal, cirrhosis etiology i.e anatomically, structurally, and functionally similar to liver cirrhosis in humans and with similar values for common biochemical markers (Plonné *et al*., 2001). The liver is an important organ that performs many metabolic activities and any damage occurs in the liver is reflected as disturbance in these functions such as leakage of hepatic enzymes (Rees *et al*., 2005). TAA intoxication is accompanied by elevation in the specific liver enzymes due to oxidative stress (Roy *et al*., 2006). In addition, the damage due to TAA causes elevation in Prothrombin time and serum albumin (Lin *et al*., 2010). Recent studies recommended the protective effect of antioxidants to the liver status and its functions against drug-induced hepatotoxicity (Oz *et al*., 2005). Our study investigated the hepatoprotective effects of *B. rotunda* and *C. longa* ethanolic extracts on the development of liver cirrhosis induced by the sustained exposure of the rats to intraperitoneal injection of 200 mg/kg TAA thrice weekly for 8 weeks. The plasma level of total protein was significantly reduced in the cirrhosis control group animals compared to normal group animals as described in other TAA intoxication models (Alshawsh *et al*., 2011). Hepatic AP, ALT, AST, GGT and LDH were significantly increased in cirrhosis control rats, as previously described (Wong *et al*., 2012). In addition, cirrhosis control group suffered of high level of triglycerides, cholesterol and low-density lipoprotein due to TAA toxicity as previously reported by Al-Attar, (2012). Further, results showed that daily oral administration of *B. rotunda* and *C. longa* extracts resulted in significant recovery of liver function parameters. Both plant extracts revealed high efficacy in protecting the liver from progressive damage as indicated by the protective effect of both extracts on liver markers. This improvement of the liver function parameters in *B. rotunda* and *C. longa* treated

groups compared to cirrhosis control may be attributed to their antioxidant constituents as previously reported (Chen, 2010; Shapiro *et al*., 2005).

Due to the crucial role played by HSCs in liver fibrosis via their resistance to apoptosis, recent treatment strategies of liver diseases is to inhibit their proliferation or induce their apoptosis. The biochemical findings of the present study were supported by the gross and histopathology results of rat liver tissues (Figures **4.5** and **4.6**) showing that livers from *B. rotunda* and *C. longa*-treated rats had liver architecture very close to normal. In addition, Masson's Trichrome slides revealed minor collagen synthesis upon administration of *B. rotunda* and *C. longa* extracts to rats treated with TAA. That was probably due to the inhibitory effect of the plant extracts to hepatic stellate cell activation. Inhibition of HSC activation and down-regulation of collagen-I in the livers treated with *B. rotunda* and *C. longa* extracts may be due to the activity of polyphenol constituents which have been proved to attenuate HSC activity (Wang *et al*., 2012).

Thioacetamide is metabolized by cytochrome enzymes (CYP2E1) inside the liver microsomes and convert it to a toxic reactive intermediate known as thioacetamide sulphur dioxide through oxidation (Kim *et al*., 2000), inducing hepatotoxicity in experimental animals and producing various levels of liver damage (Sadasivan *et al*., 2006). All experimental animals in the present study were tested for CYP2E1 enzyme level in liver homogenate tissues (Figure **4.10**) and it was found that the efficacy of both plant extracts were variable. *B. rotunda* extract in comparison with Silymarin control was able to inhibit metabolism whereas, *C. longa* had no affect on CYP2E1 enzyme. Previous studies showed that, curcumin the active ingredient of *C. longa* which constitutes 2.5-6% of the plant

rhizome constituents has no effect on CYP2E1 (Bruck *et al.*, 2007; Guangwei *et al*., 2010). On the other hand, the inhibitory effect of *B. rotunda* extract against CYP2E1 may be one of the significant factors in hepatoprotective activity by inhibiting the metabolism of TAA and blocking the release of ROS that were responsible for inducing damage of hepatocytes as explained in recent studies (Karamanakos *et al*., 2009).

Free radical like reactive oxygen species (ROS) are produced by the normal cell's metabolism. These free radicals which increase during liver injury by transformation of xenobiotics such as CCl4, ethanol and acetaminophen in the liver, play a crucial role in the death of hepatocytes (Muriel, 2009). Liver cirrhosis development by TAA was reported to be accompanied by multiple mechanisms (Ahmad *et al*., 2002). For instance, TAA induces hepatocyte damage via its metabolite, $TASO_2$, which covalently binds to the bio-molecules of liver cells causing lipid peroxidation, protein oxidation and damage of DNA molecule (Chilakapati *et al*., 2007; Djordjević, 2004). This study evaluated the oxidative stress markers and observed the degree of liver cells damage. The level of urine 8-OH-dG, nitrotyrosine and MDA (Table **4.8**) were high in cirrhosis control compared to treated groups. This supported the crude extracts' antioxidants mechanism in down regulating ROS, inhibiting DNA damage, and attenuating protein and lipid oxidation (Elaziz *et al*., 2010). The ability of both plant extracts to scavenge free radicals suggests their hepatoprotective activity through inhibition of the oxidative stress due to TAA toxicity (Masalkar & Abhang, 2005).

Administration of *B. rotunda* and *C. longa* extracts to rats in this experiment reduced the high levels of cytokines in the rat liver, supporting previous reports on the suppressive

effects of curcumin on the transcription of nuclear factor NF-κB binding activity, (Bruck *et al*., 2007) the inflammatory activity of IL-6 (Fu *et al*., 2008) and the fibrogenic TGF-β1 expression (Gaedeke *et al*., 2004). Further, the suppressive activity of *B. rotunda* to the fibrogenic and inflammatory mediators maybe due to the anti-inflammatory and anti-fibrotic activity of its flavonoid constituents as reported recently (Marcolin *et al*., 2012)

Toxins focus on metabolically effective hepatocytes resulting in hepatocyte malfunction and the discharge of ROS, fibrogenic and inflamation related mediators. Many researchers recommended that part of liver injury induced by TAA and mediated by cytokines (Okuyama *et al*., 2004) (Mehendale, 2005). The free radicals released as the consequences of TAA metabolism in liver cells, activate myofibroblasts that secrete fibrinogen and growth factors (Bassiouny, *et al*., 2011). TGF-β1, a prominent pro-fibrogenic cytokine with anti-proliferative effects that can up-regulate the deposition of ECM via hepatic stellate cells activation. The present study detected high level of TGF-β1 in the cirrhosis control group rats compared to all other groups (Figure **4-11**). In addition, the pro-inflammatory cytokines IL-6 and NF-κB were elevated in cirrhosis group rats due to activation of Kupffer cells by TAA-intoxication indicating a high inflammatory state in the cirrhotic liver as suggested in many studies (Reeves & Friedman, 2002),(Gressner *et al*., 2002), (Wu *et al*., 2010),(Bassiouny, *et al*., 2011).

A number of studies have focused on the molecular regulation of apoptosis. One of the characteristic features of liver diseases is the death of hepatocytes as a response to drug/toxicant-induced liver injury. The mitochondria perform an essential part in the control of cell death (Spierings *et al*., 2005), which generally follows one of two patterns:

necrosis and apoptosis as different results of mitochondrial permeabilization (Malhi *et al*., 2006). In apoptotic cell death, mitochondrial outer wall permealization is said to be the "point of no run" and regulated by panoply of interaction between pro-apoptotic and anti-apoptotic proteins (Kuwana *et al*., 2005). Cytotoxic drugs and cellular stress activate the mitochondrial apoptotic pathway (Kang & Reynolds, 2009) so that the inhibitors of Bcl-2 activate caspase-3 initiating apoptosis, whereas inducers of Bcl-2 induce necrosis of cells (Emi *et al*., 2005). *In vivo*, necrotic death is often associated with extensive damage in the tissue resulting in necro-inflammatory response (Choudhury *et al*., 2012). Following free-radical and cellular stress, the interaction between the pro-apoptotic Bax and the anti-apoptotic Bcl-2 leads to the formation of pores in the mitochondria and the discharge of cytochrome C, which sequentially triggers caspase-3 through caspase cascade causing apoptosis (Kroemer & Martin, 2005). Down-regulation of Bcl-2 and up-regulation of caspase-3 leads to apoptosis (Rana, 2008). In addition, over expression of the pro-apoptotic protein Bax promotes apoptosis (Wu *et al*., 2006). Although in some studies, toxicity induced by TAA was found to be accompanied by over-expression of Bax protein levels and reduction in the anti-apoptotic protein Bcl2 and its translocation into the mitochondria, causing apoptosis (Chen *et al*., 2006) but other studies suggested that the ROS produced from thioacetamide bio-transformation, cause centrolobular necrosis (Sarkar & Sil, 2007). In the current study, we observed significant increase in the sera level of Bax protein and caspase-3 and decrease in Bcl-2 protein in silymarin, *B. rotunda* and *C. longa*- treated animals compared to cirrhosis group animals as shown in Figures **4.12** and **4.13** This was confirmed by the ratio Bax/Bcl-2 (Figures **4.12d**) which was high in the treated groups compared to cirrhosis group. Moreover, immunohistochemistry staining of Bax and Bcl-2

(Figure **4.14)** double confirmed the results as indicated by large number of Bax positive-stained hepatocytes together with few Bcl2 positive-stained hepatocytes in the liver tissues of *B. rotunda* and *C. longa* -treated animals, and in Silymarin-treated animals compared with the cirrhosis control group. Bcl2 over-expression inhibited apoptosis, probably by suppressing the discharge of Cytochrome C from the mitochondria (Choudhury 2012). These results show that those cells are subjected to apoptosis and the role of some antioxidants such as curcumin and curcuminoids (Wang *et al*., 2012) in inducing apoptosis. This explains the enhancing pathway of *C. longa* and *B. rotunda*-treatment to apoptosis. Furthermore, Daily feeding of animals with *B. rotunda* and *C. longa* extracts in parallel with TAA injections three times/week for 8 weeks suppressed the proliferation of hepatocytes and their regeneration as the results showed significant decrease in PCNA staining in the liver sections from the plant extracts-treated groups similar to that in the Silymarin-treated group (Figure **4.15**). Recent studies reported similar results that curcumin the active polyphenol ingredient of *C. longa* extract has inhibitory effect on hepatocyte proliferation (Wang *et al*., 2012). Treating the animals with the plant extracts inhibited the necrotic effect due to thioacetamide administration by modifying necrosis into apoptosis, which may be via cytochrome release from mitochondria and caspase activation (Malhi *et al*., 2006). This modification *in vivo* would scale down the release of inflammatory factors that would suppress further damage in the liver.

In liver fibrosis, there is an imbalance between excess deposition and / or a decrease in the extracellular matrix (ECM) removal with consequent scarring damage (Park *et al*., 2010). ECM is mainly controlled by matrix metalloproteinases (MMPs), which are a group of proteolytic enzymes that are able to degrade the ECM (Abraham *et al*., 2005; Wang *et*

al., 2005). Tissue inhibitors of metalloproteinases (TIMPs) regulate tightly the activity of MMPs (Parsons *et al*., 2004; Shi & Li 2005). MMP-9 and TIMP-1 were verified as the molecular signatures during TAA-induced liver cirrhosis (An *et al*., 2006). Park, (2010) observed that TAA increased MMP-2 expression in the liver tissues of rats and reported that the balance of MMPs and TIMPs determines the degree of liver fibrogenesis. In this research, administered animals with plants extract affected the level of MMP-2, MMP-9 and TIMP-1 in the rat livers intoxicated with TAA. In (Table **4.10**) results revealed that administration of *C. longa* extract didn't show any significant inhibition of MMP-2 and TIMP-1 to compare with cirrhotic control group. In addition, *C. longa* extract treatment significantly down-regulated the level of MMP-9 in the rat liver. Similar study reported on the hepatoprotective effect of curcumin the active antioxidant compound of *C. longa* rhizomes (Bruck *et al*., 2007). On the other hand, the animals treated with *B. rotunda* showed significant down-regulation in the hepatic level of MMP-2, MMP-9 and TIMP-1 similar to silymarin reference group. Although, Cheng *et al*., (2007) reported that curcumin inhibited the proliferation of HSCs isolated from normal *Sprague Dawley* rats via enhancement of MMP-2 and MMP-9 activities, but this study, suggested the efficacy of *B. rotunda* and *C. longa* extracts through the inhibition of kupffer cells activity as indicated by the significant inhibitory effect of both plant extracts on cytokines/chemokine mediators TGF-β1, IL-6 and NF-kB level in rats serum. Consequently, the low level of these mediators might have contributed to HSCs activation and reduced liver injury (Bruck *et al*., 2007). Figure **5.1** illustrates the *in vivo* hepatoprotective results of *B. rotunda* and *c. longa* extracts in TAA-induced liver injury in rats in the present study.

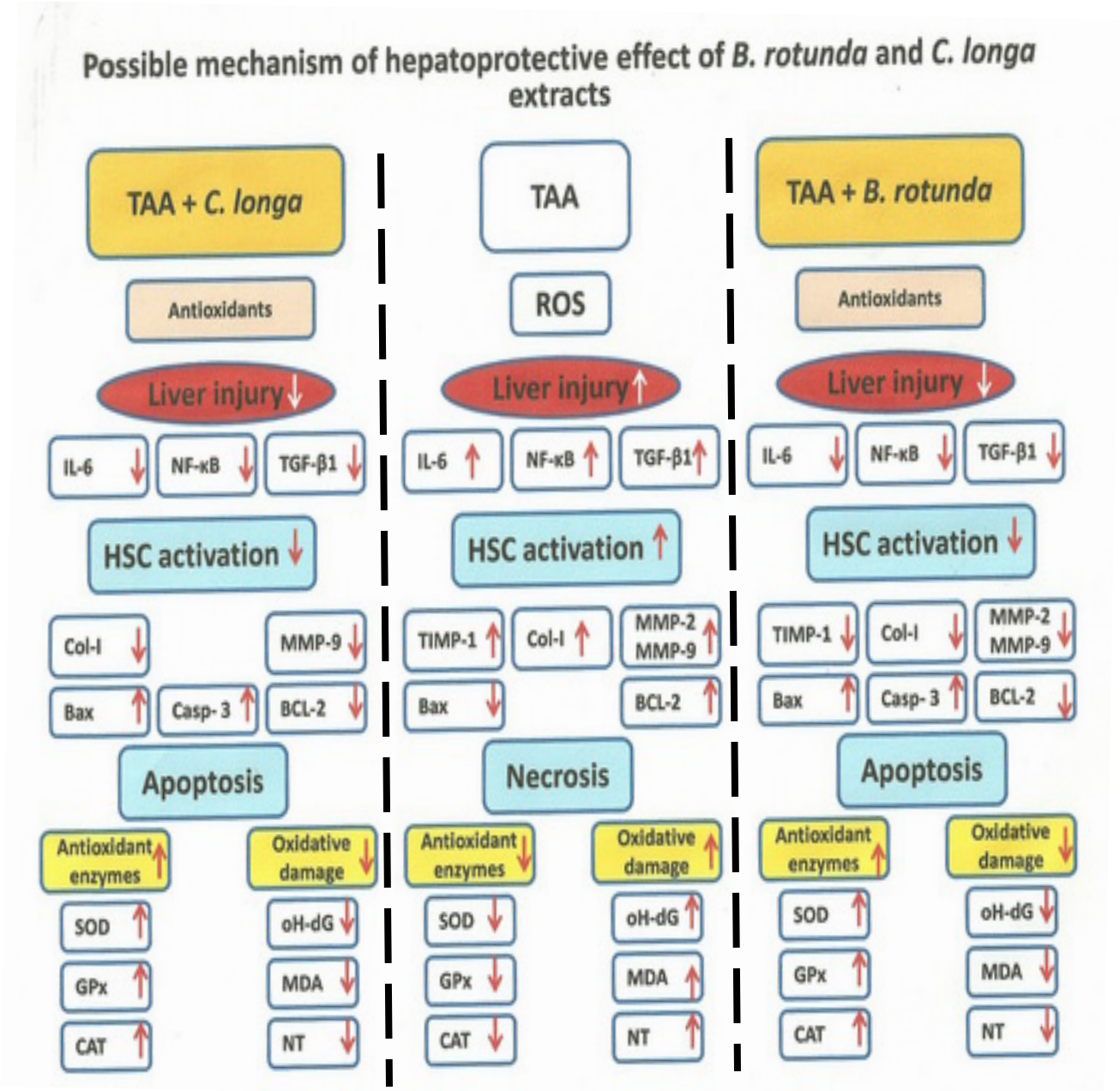
Possible mechanism of hepatoprotective effect of B. rotunda and C. longa extracts
TAA + C. longa
Antioxidants
Liver injury
IL-6
NF-κB
TGF-β1
HSC activation
Col-I
MMP-9
Bax
Casp- 3
BCL-2
Apoptosis
Antioxidant enzymes
Oxidative damage
SOD
GPx
CAT
oH-dG
MDA
NT
TAA
ROS
Liver injury
IL-6
NF-κB
TGF-β1
HSC activation
TIMP-1
Col-I
MMP-2
MMP-9
Bax
BCL-2
Necrosis
Antioxidant enzymes
Oxidative damage
SOD
GPx
CAT
oH-dG
MDA
NT
TAA + B. rotunda
Antioxidants
Liver injury
IL-6
NF-κB
TGF-β1
HSC activation
TIMP-1
Col-I
MMP-2
MMP-9
Bax
Casp- 3
BCL-2
Apoptosis
Antioxidant enzymes
Oxidative damage
SOD
GPx
CAT
oH-dG
MDA
NT

Thioacetamide is a chemical known for its short half life (Chilakapati *et al*., 2005) and was used in many *in vitro* studies on liver cell line to induce ROS production. ROS release enhances lipid peroxidation in the bio-membranes causing cell death through degeneration Of DNA and the degeneration of many cell enzymes (Chen *et al*., 2006; Sarkar & Sil, 2007). Although normal embryonic liver cell line WRL-68 expresses some hepatocyte-like functional characteristics such as liver function enzymes (AP, ALT and AST) (Gutiérrez-Ruiz *et al*., 1994), but nevertheless it was used in this study to test *in vitro* the hepatoprotective activity of Panduratin A, an active antioxidant constituent from *B. rotunda* rhizome (Lai *et al*., 2012) and Germacrone, an active sesquiterpene constituent from *C. longa* rhizomes (Jayaprakasha *et al*., 2005; You *et al*., 2005). In the current research, cytotoxicity study was conducted in WRL 68 for the active compounds Panduratin A and Germacrone. The increase in viable cell counts after 72 hours of incubation up to the tested dose (100 μg/ml) indicates that both compounds are safe to use (Figure **4.24**). Furthermore, both Panduratin A and Germacrone enhanced the increase in cell viability against TAA-induced cytotoxicity (Figure **4.25**), reduced lipid peroxidation (MDA) and elevated SOD enzyme level in the cells treated with the compounds (Figure **4.21**). The results showed that Panduratin A exhibited more capability to protect against TAA in WRL-68 cells compared to Germacrone which showed significant protection only at the highest tested dose (100 μg/ml). The antioxidative activity of Panduratin A can be attributed to its antioxidant property (Sohn *et al*., 2005). Mau *et al.*, (2003) reported that the essential oil constituents of *Curcuma zedoaria* including Germacrone have high DPPH scavenging activity. In addition,

recent efficient preparations of three anticancer compounds have been derived from Germacrone compound (Barrero *et al*., 2011).

PA was tested for hepatoprotective *in vivo* over 4 weeks and showed promise as potential medicine. One of the sensitive tests in the diagnosis of liver diseases is analysis of serum liver enzymes (Zhang *et al*., 2006). This study showed that the liver enzymes AP, ALT, AST and GGT which were elevated due to the damage of the structural integrity of the hepatic cells by TAA intoxication were significantly low in the PA- treated animals (Table **4.17**). Together with the histopathology results, we hypothesize that Panduratin A may be able to preserve the normal architecture of the liver from the damaging effects of TAA.

In the present research, assessment of the oxidative damage markers revealed that the damage level to hepatocytes due to oxidative stress was elevated in the untreated cirrhosis rats as presented by the increased level of 8-OH-dG, nitrotyrosine and MDA (Figure **4.29**). However, PA-treatment decreased significantly the level of these markers to approach normal values and encouragingly close to that of Silymarin-treated animals. These positive results may be explained by free-radical scavenging power of the chalcone nature of PA (Lai *et al*., 2012). Moreover, the release of ROS causes parenchymal cell necrosis (Sadasivan, *et al*., 2006) and the up-regulation of pro-inflammatory and fibrogenic mediators activating HSCs (Bruck *et al*., 2007). In this study, α-smooth muscle actin was detected in cirrhosis control group by using immunohistochemistry stain compared to other groups (Figure **4.35**). This indicates the increased activity of HSCs in the cirrhotic livers of cirrhosis group rats and the inhibitory effect of Panduratin A to their activity.

TAA metabolism may trigger myofibroblasts that discharge fibrinogen and growth factors (Bassiouny *et al*., 2011) such as the profibrogenic cytokine TGF-β1 that can up-regulate the deposition of extracellular matrix (ECM) (Gressner *et al*., 2002). Upon activation, HSCs acquire a highly proliferative catalog and generate fibrillar collagen within the injured liver (Elsharkawy *et al*., 2005). The present study showed more deposition of Collagen-I as detected histologically by Masson's Trichrome stain in the cirrhosis control group rats (Figure **4.34**) compared to PA-treated rats. It is noteworthy to suggest that PA-treatment interrupted this vicious cycle by its quenching activity as an antioxidant (Sohn *et al*., 2005).

Hepatocellular anti-oxidant enzymes SOD, CAT and GPx were reported to be reduced in TAA-induced hepatotoxicity (Wang *et al*., 1999). In this experiment, oral administration of PA to the cirrhotic rats considerably reduced the TAA-suppressive effect, diminished the damage in liver cells and inhibited free radicals by enhancing antioxidants phagoradicals. The action of these enzymes at higher levels very close to normal values (Figure **4.31**) suggests the antioxidative activity of PA as reported by previous studies (Sohn *et al*., 2005). Figure **5.2** shows the hepatoprotective effect of *B. rotunda* extract in comparison to that of its active compound PA.

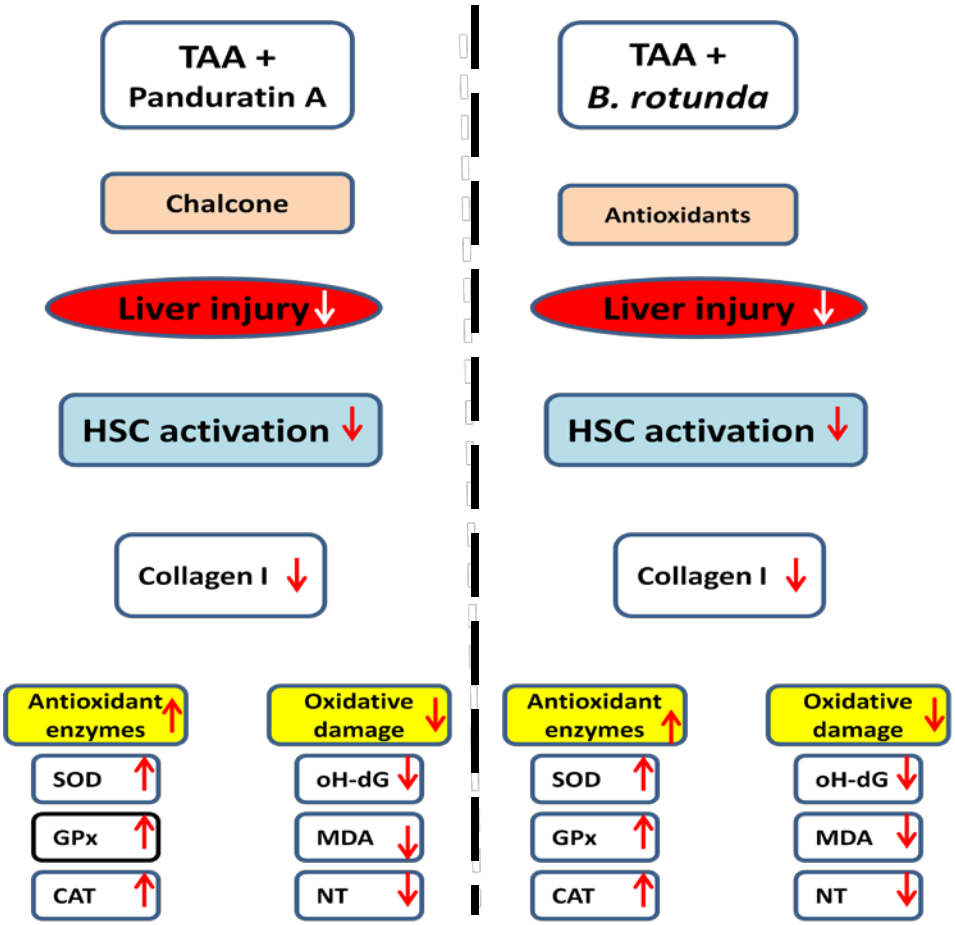

Figure 5.2: A diagram showing the hepatoprotective effect of *B. rotunda* extract compared to its active compound Panduratin A.

5.2. Conclusions

- Due to their phenolic constituents as Quercetin, Kaemferol and Panduratin A in *Boesenbergia rotunda* and curcumin and curcuminoids in *Curcuma longa*, both plants extracts exhibit high antioxidant properties.
- *Boesenbergia rotunda* and *Curcuma longa* extracts are not toxic even at higher doses.

- *Boesenbergia rotunda* and *Curcuma longa* extracts showed significant hepatoprotective activities against TAA-induced liver damage in rats. Therefore they can be recommended as a remedy in liver diseases similar to silymarin.
- *Boesenbergia rotunda* and *Curcuma longa* protected the liver from further damage by shifting necrosis into apoptosis and suppressing inflammatory mediators.
- The significant suppressive activity of *Boesenbergia rotunda* and *Curcuma longa* to the formation of Collagen I in the liver tissues reveals therapeutic effect of both plant extracts on HSC activation.
- Panduratin A and Germacrone exhibited protective activity against TAA-induced liver damage *in vitro* adding new compounds to liver disease therapy.
- Panduratin A showed hepatoprotective activity against TAA-induced liver *in vivo* damage suggesting a promising remedy in treating liver disease that may challenge silymarin in its hepatoprotective activity.
- The suppressive effect of Panduratin A to the formation of α-SMA in the liver tissues of rats reveals direct inhibitory effect of Panduratin A on the activation of HSCs following the new therapeutic strategy in treating liver cirrhosis by inhibiting HSCs activation.

5.3. Future Work

Based on the results of the present study which indicate the efficacy of *Boesenbergia rotunda* and *Curcuma longa* in protecting the liver from progressive damage via their antioxidant and anti-inflammatory activities, more studies need to be conducted on the

HSCs which are the main target for treating liver cirrhosis. The following studies are suggested:

- **Evaluating the efficacy of *B. rotunda* and *C. longa* extracts on the treatment of liver-induced toxicity.**
- **Evaluate the effect of Panduratin A on the intrinsic apoptotic mitochondrial pathway in HSCs.**

REFERENCES

Abraham, D., Ponticos, M., & Nagase, H. (2005). Connective tissue remodeling: cross-talk between endothelins and matrix metalloproteinases. *Current Vascular Pharmacology, 3*(4), 369-379.

Agur, A. M., & Dalley, A. F. (2008). *Grant's atlas of anatomy*: Lippincott Williams & Wilkins, *P.150*.

Ahmad, A., Pillai, K. K., Najmi, A. K., Ahmad, S. J., Pal, S. N., & Balani, D. K. (2002). Evaluation of hepatoprotective potential of jigrine post-treatment against thioacetamide induced hepatic damage. *Journal of Ethnopharmacology, 79*(1), 35-41.

Akshatha, K. S. (2011). *Phytochemical investigation and screening of hepatoprotective activity of aporosa lindleyana (wt.) bail. roots.* National College. *P.7*

Al-Attar, A. M. (2012). Attenuating Effect of Ginkgo biloba Leaves Extract on Liver Fibrosis Induced by Thioacetamide in Mice. *BioMed Research International, 2012*, 1-9.

Al Bayaty, F., Abdulla, M., Abu Hassan, M., & Masud, M. (2010). Wound healing potential by hyaluronate gel in streptozotocin-induced diabetic rats. *Scientific Research and Essays, 5*(18), 2756-2760.

Ali, S. S., Kasoju, N., Luthra, A., Singh, A., Sharanabasava, H., Sahu, A., & Bora, U. (2008). Indian medicinal herbs as sources of antioxidants. *Food Research International, 41*(1), 1-15.

Alshawsh, M. A., Abdulla, M. A., Ismail, S., & Amin, Z. A. (2011). Hepatoprotective Effects of Orthosiphon stamineus Extract on Thioacetamide-Induced Liver Cirrhosis in Rats. *Evidence-Based Complementary and Alternative Medicine*, 1-6.

Amali, A. A., Rekha, R. D., Lin, C. J. F., Wang, W. L., Gong, H. Y., Her, G. M., & Wu, J. L. (2006). Thioacetamide induced liver damage in zebrafish embryo as a disease model for steatohepatitis. *Journal of Biomedical Science, 13*(2), 225-232.

An, J. H., Seong, J., Oh, H., Kim, W., Han, K. H., & Paik, Y. H. (2006). [Protein expression profiles in a rat cirrhotic model induced by thioacetamide]. *The Korean Journal of Hepatology, 12*(1), 93-102.

Antoine, M., Wirz, W., Tag, C. G., Gressner, A. M., Marvituna, M., Wycislo, M., Kiefer, P. (2007). Expression and function of fibroblast growth factor (FGF) 9 in hepatic stellate cells and its role in toxic liver injury. *Biochemical and Biophysical Research Communications, 361*(2), 335-341.

Asghar, Z., & Masood, Z. (2008). Evaluation of antioxidant properties of silymarin and its potential to inhibit peroxyl radicals in vitro. *Pakistan Journal of Pharmaceutical Sciences, 21*(3), 249-254.

Avunduk, C. (2008). *Manual of Gastroenterology: Diagnosis and Therapy*: Lippincott Williams & Wilkins, 516 pages.

Aydın, A. F., Küskü-Kiraz, Z., Doğru-Abbasoğlu, S., Güllüoğlu, M., Uysal, M., & Koçak-Toker, N. (2010). Effect of carnosine against thioacetamide-induced liver cirrhosis in rat. *Peptides, 31*(1), 67-71.

Bacon, B. R. (2006). *Comprehensive clinical hepatology*: Mosby Incorporated, 177-190.

Barrero, A. F., Herrador, M. M., del Moral, J. F. Q., Arteaga, P., Meine, N., Pérez-Morales, M. C., & Catalán, J. V. (2011). Efficient synthesis of the anticancer β-elemene and other bioactive elemanes from sustainable germacrone. *Organic and Biomolecular Chemistry, 9*(4), 1118-1125.

Basak, S., Sarma, G. C., & Rangan, L. (2010). Ethnomedical uses of Zingiberaceous plants of Northeast India. *Journal of Ethnopharmacology, 132*(1), 286-296.

Bassiouny, A. R., Zaky, A. Z., Abdulmalek, S. A., Kandeel, K. M., Ismail, A., & Moftah, M. (2011). Modulation of AP-endonuclease1 levels associated with hepatic cirrhosis in rat model treated with human umbilical cord blood mononuclear stem cells. *International Journal of Clinical and Experimental Pathology, 4*(7), 692-707.

Bataller, R., & Brenner, D. A. (2005). Liver fibrosis. *Journal of Clinical Invest, 115*(2), 209-218.

Beale, G., Chattopadhyay, D., Gray, J., Stewart, S., Hudson, M., Day, C., Reeves, H. (2008). AFP, PIVKAII, GP3, SCCA-1 and follisatin as surveillance biomarkers for hepatocellular cancer in non-alcoholic and alcoholic fatty liver disease. *BMC Cancer, 8*(1), 200.

Beckman, K. B., & Ames, B. N. (1997). Oxidative decay of DNA. *Journal of Biological Chemistry, 272*(32), 19633-19636.

Benzie, I. F., & Strain, J. (1996). The ferric reducing ability of plasma (FRAP) as a measure of "antioxidant power": the FRAP assay. *Analytical Biochemistry, 239*(1), 70-76.

Block, B. (2011). Guide to abdominal scaning. *Abdominal Ultrasound: Step by Step*: TIS. P.93

Bove, K., Neumann, P., Gertzberg, N., & Johnson, A. (2001). Role of ecNOS-derived NO in mediating TNF-induced endothelial barrier dysfunction. *American Journal of Physiology-Lung Cellular and Molecular Physiology, 280*(5), L914-L922.

Bruck, R., Ashkenazi, M., Weiss, S., Goldiner, I., Shapiro, H., Aeed, H., Pines, M. (2007). Prevention of liver cirrhosis in rats by curcumin. *Liver International, 27*(3), 373-383.

Brunati, A. M., Pagano, M. A., Bindoli, A., & Rigobello, M. P. (2010). Thiol redox systems and protein kinases in hepatic stellate cell regulatory processes. *Free Radical Research, 44*(4), 363-378.

Budak, N. H., Kumbul Doguc, D., Savas, C. M., Seydim, A. C., Kok Tas, T., Ciris, M. I., & Guzel-Seydim, Z. B. (2011). Effects of Apple Cider Vinegars Produced with Different Techniques on Blood Lipids in High-Cholesterol-Fed Rats. *Journal of Agricultural and Food Chemistry, 59*(12), 6638-6644.

Cárdenas, A., & Chopra, S. (2002). Chylous ascites. *The American Journal of Gastroenterology, 97*(8), 1896-1900.

Cheah, S.-C., Appleton, D. R., Lee, S.-T., Lam, M.-L., Hadi, A. H. A., & Mustafa, M. R. (2011). Panduratin A inhibits the growth of A549 cells through induction of apoptosis and inhibition of NF-KappaB translocation. *Molecules, 16*(3), 2583-2598.

Chen, L. H., Hsu, C. Y., & Weng, C. F. (2006). Involvement of P53 and Bax/Bad triggering apoptosis in thioacetamide-induced hepatic epithelial cells. *World Journal of Gastroenterology, 12*(32), 5175-5181.

Chen, X. (2010). Protective effects of quercetin on liver injury induced by ethanol. *Pharmacognosy Magazine, 6*(22), 135-141.

Cheng, Y., Ping, J., & Xu, L. (2007). Effects of curcumin on peroxisome proliferator-activated receptor gamma expression and nuclear translocation/redistribution in culture-activated rat hepatic stellate cells. *Chinese Medical Journal-Beijing-English Edition, 120*(9), 794-801.

Chilakapati, J., Korrapati, M. C., Hill, R. A., Warbritton, A., Latendresse, J. R., & Mehendale, H. M. (2007). Toxicokinetics and toxicity of thioacetamide sulfoxide: a metabolite of thioacetamide. *Toxicology, 230*(2-3), 105-116.

Chilakapati, J., Shankar, K., Korrapati, M. C., Hill, R. A., & Mehendale, H. M. (2005). Saturation toxicokinetics of thioacetamide: role in initiation of liver injury. *Drug Metabolism and Disposition, 33*(12), 1877-1885.

Ching, A. Y. L., Tang, S. W., Sukari, M. A., Lian, G. E. C., Rahmani, M., & Khalid, K. (2007). Characterization of flavonoid derivatives from *Boesenbergia rotunda* (L.). *The Malaysian Journal of Analytical Sciences, 11*(1), 154-159.

Choi, J., & Ou, J.-H. J. (2006). Mechanisms of liver injury. III. Oxidative stress in the pathogenesis of hepatitis C virus. *American Journal of Physiology-Gastrointestinal and Liver Physiology, 290*(5), G847-G851.

Choudhury, J. D., Kumar, S., Mayank, V., Mehta, J., & Bardalai, D. (2012). A review on apoptosis and its different pathway. *International Journal of Biological and Pharmaceutical Research, 3*(7), 848-861.

Chouhan, S., Yadav, A., Kushwah, P., Kaul, R. K., & Flora, S. J. (2011). Silymarin and quercetin abrogates fluoride induced oxidative stress and toxic effects in rats. *Molecular & Cellular Toxicology, 7*(1), 25-32.

Chow, J. H., & Chow, C. (2006). *The Encyclopedia of Hepatitis and Other Liver Diseases*: Infobase Publishing, 201-202.

Cinghită, D., Radovan, C., & Dascălu, D. (2008). Anodic Voltammetry of Thioacetamide and its Amperometric Determination in Aqueous Media. *Sensors, 8*(8), 4560-4581.

Cook, N., & Samman, S. (1996). Flavonoids—chemistry, metabolism, cardioprotective effects, and dietary sources. *The Journal of Nutritional Biochemistry, 7*(2), 66-76.

Cragg, G. M., & Newman, D. J. (2005). Plants as a source of anti-cancer agents. *Journal of Ethnopharmacology, 100*(1), 72-79.

Crosignani, A., Battezzati, P. M., Setchell, K. D., Camisasca, M., Bertolini, E., Roda, A., . . . Podda, M. (2005). Effects of ursodeoxycholic acid on serum liver enzymes and bile acid metabolism in chronic active hepatitis: A dose-response study. *Hepatology, 13*(2), 339-344.

Cunniff, P. (1995). *Official methods of analysis of AOAC International*: AOAC international Arlington. 16th ed. *Arlington*, Va:42-1-42-2.

Cunningham, C. C., & Van Horn, C. G. (2003). Energy availability and alcohol-related liver pathology. *Alcohol Research and Health, 27*, 291-299.

Damiani, E., Belaid, C., Carloni, P., & Greci, L. (2003). Comparison of antioxidant activity between aromatic indolinonic nitroxides and natural and synthetic antioxidants. *Free Radical Research, 37*(7), 731-741.

Dancygier, H. (2010). Microscopic anatomy. *Clinical Hepatology, 1,* 15-51.

Dandekar, D. V., & Gaikar, V. (2003). Hydrotropic extraction of curcuminoids from turmeric. *Separation Science and Technology, 38*(5), 1185-1215.

Debjit Bhowmik, C., Kumar, K. S., Chandira, M., & Jayakar, B. (2009). Turmeric: A Herbal and Traditional Medicine. *Archives of Applied Science Research, 1*(2), 86-108.

Del Rio, D., Stewart, A. J., & Pellegrini, N. (2005). A review of recent studies on malondialdehyde as toxic molecule and biological marker of oxidative stress. *Nutrition, Metabolism and Cardiovascular Diseases, 15*(4), 316-328.

Dimitrios, B. (2006). Sources of natural phenolic antioxidants. *Trends in Food Science & Technology, 17*(9), 505-512.

Djordjević, V. B. (2004). Free radicals in cell biology. *International Review of Cytology, 237*, 57-89.

Dourakis, S., & Sevastianos, V. (2007). Pathogenesis, diagnosis and therapy of Infections complicating patients with chronic liver disease. *Annals of Gastroenterology, 16*(4).

Edgtton, K. L., Gow, R. M., Kelly, D. J., Carmeliet, P., & Kitching, A. R. (2004). Plasmin is not protective in experimental renal interstitial fibrosis1. *Kidney International, 66*(1), 68-76.

Elsharkawy, A., Oakley, F., & Mann, D. (2005). The role and regulation of hepatic stellate cell apoptosis in reversal of liver fibrosis. *Apoptosis, 10*(5), 927-939.

Emi, M., Kim, R., Tanabe, K., Uchida, Y., & Toge, T. (2005). Targeted therapy against Bcl-2-related proteins in breast cancer cells. *Breast Cancer Research, 7*(6), R940-R952.

Fan, S., & Weng, C.-F. (2005). Co-administration of cyclosporine an alleviates thioacetamide-induced liver injury. *World Journal of Gastroenterology, 11*(10), 1411-1419.

Fatemi, F., Allameh, A., Khalafi, H., & Ashrafihelan, J. (2010). Hepatoprotective effects of γ-irradiated caraway essential oils in experimental sepsis. *Applied Radiation and Isotopes, 68*(2), 280-285.

Fernández, J., Navasa, M., Planas, R., Montoliu, S., Monfort, D., Soriano, G., . . . Vargas, V. (2007). Primary prophylaxis of spontaneous bacterial peritonitis delays hepatorenal syndrome and improves survival in cirrhosis. *Gastroenterology, 133*(3), 818-824.

Fischer, A., & Mullin, G. (2012). Inflammation and Nutraceutical Modulation. *Bioactive Food as Dietary Interventions for Arthritis and Related Inflammatory Diseases: Bioactive Food in Chronic Disease States*, 337.

Fraschini, F., Demartini, G., & Esposti, D. (2002). Pharmacology of silymarin. *Clinical Drug Investigation, 22*(1), 51-65.

Friedman, A. D. (2002). Runx1, c-Myb, and C/EBPα couple differentiation to proliferation or growth arrest during hematopoiesis. *Journal of Cellular Biochemistry, 86*(4), 624-629.

Friedman, S. L., Rockey, D. C., & Bissell, D. M. (2006). Hepatic fibrosis 2006: report of the third AASLD single topic conference. *Hepatology, 45*(1), 242-249.

Fu, Y., Zheng, S., Lin, J., Ryerse, J., & Chen, A. (2008). Curcumin protects the rat liver from CCl4-caused injury and fibrogenesis by attenuating oxidative stress and suppressing inflammation. *Molecular Pharmacology, 73*(2), 399-409.

Gaedeke, J., Noble, N. A., & Border, W. A. (2004). Curcumin blocks multiple sites of the TGF-β signaling cascade in renal cells. *Kidney International, 66*(1), 112-120.

Giannini, E. G., Testa, R., & Savarino, V. (2005). Liver enzyme alteration: a guide for clinicians. *Canadian Medical Association Journal, 172*(3), 367-379.

Girish, C., Koner, B. C., Jayanthi, S., Ramachandra Rao, K., Rajesh, B., & Pradhan, S. C. (2009). Hepatoprotective activity of picroliv, curcumin and ellagic acid compared to silymarin on paracetamol induced liver toxicity in mice. *Fundamental and Clinical Pharmacology, 23*(6), 735-745.

Girish, C., & Pradhan, S. C. (2008). Drug development for liver diseases: focus on picroliv, ellagic acid and curcumin. *Fundamental & Clinical Pharmacology, 22*(6), 623-632.

Gorinstein, S., Martin-Belloso, O., Katrich, E., Lojek, A., Číž, M., Gligelmo-Miguel, N., Trakhtenberg, S. (2003). Comparison of the contents of the main biochemical compounds and the antioxidant activity of some Spanish olive oils as determined by four different radical scavenging tests. *The Journal of Nutritional Biochemistry, 14*(3), 154-159.

Gressner, A., & Weiskirchen, R. (2007). Modern pathogenetic concepts of liver fibrosis suggest stellate cells and TGF-β as major players and therapeutic targets. *Journal of Cellular and Molecular Medicine, 10*(1), 76-99.

Gressner, A. M., Weiskirchen, R., Breitkopf, K., & Dooley, S. (2002). Roles of TGF-beta in hepatic fibrosis. *Front Biosci, 7*(1), d793-807.

Gressner, O. A., Weiskirchen, R., & Gressner, A. M. (2007). Evolving concepts of liver fibrogenesis provide new diagnostic and therapeutic options. *Comparative Hepatology, 6*(1), 7.

Guangwei, X., Rongzhu, L., Wenrong, X., Suhua, W., Xiaowu, Z., Shizhong, W., Bishnoi, M. (2010). Curcumin pretreatment protects against acute acrylonitrile-induced oxidative damage in rats. *Toxicology, 267*(1-3), 140-146.

Gurib-Fakim, A. (2006). Medicinal plants: traditions of yesterday and drugs of tomorrow. *Molecular Aspects of Medicine, 27*(1), 1-93.

Gurtsevitch, V. (2008). Human oncogenic viruses: hepatitis B and hepatitis C viruses and their role in hepatocarcinogenesis. *Biochemistry (Moscow), 73*(5), 504-513.

Gutiérrez-Ruiz, M., Bucio, L., Souza, V., Gomez, J., Campos, C., & Cárabez, A. (1994). Expression of some hepatocyte-like functional properties of WRL-68 cells in culture. *In Vitro Cellular and Developmental Biology-Animal, 30*(6), 366-371.

Hamed, G. M., Bahgat, N. M., Abdel Mottaleb, F., & Emara, M. M. (2011). Effect of Flavonoid Quercetin Supplement on the Progress of Liver Cirrhosis in Rats. *Life Science Journal, 8*(2), 641-651.

Heidelbaugh, J. J., & Bruderly, M. (2006). Cirrhosis and chronic liver failure: part I. Diagnosis and evaluation. *American Family Physician, 74*(5), 756-762.

Heindryckx, F., Colle, I., & Van Vlierberghe, H. (2009). Experimental mouse models for hepatocellular carcinoma research. *International Journal of Experimental Pathology, 90*(4), 367-386.

Higuchi, A., Sugiyama, K., Yoon, B. O., Sakurai, M., Hara, M., Sumita, M., . . . Shirai, T. (2003). Serum protein adsorption and platelet adhesion on pluronic adsorbed polysulfone membranes. *Biomaterials, 24*(19), 3235-3245.

http://www.indonesian-culinary.com, 2010.

http://www.ramuantaufiq.com, 2011.

Iredale, J. P. (2007). Models of liver fibrosis: exploring the dynamic nature of inflammation and repair in a solid organ. *Journal of Clinical Investigation, 117*(3), 539.

Itokawa, H., Shi, Q., Akiyama, T., Morris-Natschke, S. L., & Lee, K.-H. (2008). Recent advances in the investigation of curcuminoids. *Chinese Medicine, 3*,11-23.

Jankun, J., Aleem, A. M., Malgorzewicz, S., Szkudlarek, M., Zavodszky, M. I., DeWitt, D. L., Skrzypczak-Jankun, E. (2006). Synthetic curcuminoids modulate the arachidonic acid metabolism of human platelet 12-lipoxygenase and reduce sprout formation of human endothelial cells. *Molecular Cancer Therapeutics, 5*(5), 1371-1382.

Jantan, I. (2004). Medicinal plant research in Malaysia: scientific interests and advances. *Jurnal Sains Kesihatan Malaysia, 2*(2), 27-46.

Jayaprakasha, G., Jagan Mohan Rao, L., & Sakariah, K. (2005). Chemistry and biological activities of *C. longa*. *Trends in Food Science and Technology, 16*(12), 533-548.

Jing, L. J., Mohamed, M., Rahmat, A., & Bakar, M. A. (2010). Phytochemicals, antioxidant properties and anticancer investigations of the different parts of several gingers species (Boesenbergia rotunda, Boesenbergia pulchella var attenuata and Boesenbergia armeniaca). *Journal of Medicinal Plant Research, 4*(1), 27-32.

Kang, M. H., & Reynolds, C. P. (2009). Bcl-2 inhibitors: targeting mitochondrial apoptotic pathways in cancer therapy. *Clinical Cancer Research, 15*(4), 1126-1132.

Karamanakos, P. N., Trafalis, D. T., Geromichalos, G., Pappas, P., Harkitis, P., Konstandi, M., & Marselos, M. (2009). Inhibition of rat hepatic CYP2E1 by quinacrine: molecular modeling investigation and effects on 4-(methyl nitrosamino)-1-(3-pyridyl)-1-butanone (NNK)-induced mutagenicity. *Archives of Toxicology, 83*(6), 571-580.

Kim, K. H., Bae, J. H., Cha, S. W., Han, S. S., Park, K. H., & Jeong, T. C. (2000). Role of metabolic activation by cytochrome P450 in thioacetamide-induced suppression of antibody response in male BALB/c mice. *Toxicology Letters, 114*(1-3), 225-235.

Kisseleva, T., & Brenner, D. A. (2007). Role of hepatic stellate cells in fibrogenesis and the reversal of fibrosis. *Journal of Gastroenterology and Hepatology, 22*(s1), S73-S78.

Koek, H., Soedamah-Muthu, S., Kardaun, J. W., Gevers, E., de Bruin, A., Reitsma, J., Grobbee, D. (2007). Short-and long-term mortality after acute myocardial infarction: comparison of patients with and without diabetes mellitus. *European Journal of Epidemiology, 22*(12), 883-888.

Kroemer, G., & Martin, S. J. (2005). Caspase-independent cell death. *Nature Medicine, 11*(7), 725-730.

Kumar, G. S., Nayaka, H., Dharmesh, S. M., & Salimath, P. (2006). Free and bound phenolic antioxidants in amla *Emblica officinalis* and turmeric *Curcuma longa*. *Journal of Food Composition and Analysis, 19*(5), 446-452.

Kumar, M., & Sarin, S. (2007). Is cirrhosis of the liver reversible? *Indian Journal of Pediatrics, 74*(4), 393-399.

Kurien, B. T., Everds, N. E., & Scofield, R. H. (2004). Experimental animal urine collection: a review. *Laboratory Animals, 38*(4), 333-361.

Kuwana, T., Bouchier-Hayes, L., Chipuk, J. E., Bonzon, C., Sullivan, B. A., Green, D. R., & Newmeyer, D. D. (2005). BH3 domains of BH3-only proteins differentially regulate Bax-mediated mitochondrial membrane permeabilization both directly and indirectly. *Molecular Cell, 17*(4), 525-536.

Lai, S. L., Cheah, S. C., Wong, P. F., Noor, S. M., & Mustafa, M. R. (2012). *In Vitro* and *in Vivo* Anti-Angiogenic activities of panduratin A. *PLoS One, 7*(5), e38103.

Lee, E. S., Lee, H. E., Shin, J. Y., Yoon, S., & Moon, J. O. (2003). The flavonoid quercetin inhibits dimethylnitrosamine-induced liver damage in rats. *Journal of Pharmacy and Pharmacology, 55*(8), 1169-1174.

Lemberg, A., & Fernández, M. A. (2009). Hepatic encephalopathy, ammonia, glutamate, glutamine and oxidative stress. *Annal Hepatology, 8*(2), 95-102.

Levey, A. S., Coresh, J., Balk, E., Kausz, A. T., Levin, A., Steffes, M. W.,Eknoyan, G. (2003). National Kidney Foundation practice guidelines for chronic kidney disease: evaluation, classification, and stratification. *Annals of Internal Medicine, 139*(2), 137-147.

Li, J.-T., Liao, Z.-X., Ping, J., Xu, D., & Wang, H. (2008). Molecular mechanism of hepatic stellate cell activation and antifibrotic therapeutic strategies. *Journal of Gastroenterology, 43*(6), 419-428.

Lin, S.-Z., Chang, Y.-J., Liu, J.-W., Chang, L.-F., Sun, L.-Y., Li, Y.-S.,Chen, T.-M. (2010). Transplantation of human Wharton's Jelly-derived stem cells alleviates chemically induced liver fibrosis in rats. *Cell Transplantation, 19*(11), 1451-1463.

Liu, Y., Peterson, D. A., Kimura, H., & Schubert, D. (1997). Mechanism of cellular 3-(4, 5-dimethylthiazol-2-yl)-2, 5-diphenyltetrazolium bromide (MTT) reduction. *Journal of Neurochemistry, 69*(2), 581-593.

Liu, Y., Wang, W., Fang, B., Ma, F., Zheng, Q., Deng, P., He, G. (2012). Anti-tumor effect of germacrone on human hepatoma cell lines through inducing G2/M cell cycle arrest and promoting apoptosis. *European Journal of Pharmacology, 698*(1-3), 95-102.

Lowry, O. H., Rosebrough, N. J., Farr, A. L., & Randall, R. J. (1951). Protein measurement with the Folin phenol reagent. *Journal of Biological Chemistry, 193*(1), 265-275.

Madani, H., Talebolhosseini, M., Asgary, S., & Naderi, G. (2008). Hepatoprotective activity of Silybum marianum and Cichorium intybus against thioacetamide in rat. *Pakistan Journal of Nutrition, 7*(1), 172-176.

Mahmood, A., Mariod, A. A., Abdelwahab, S. I., Ismail, S., & Al-Bayaty, F. (2010). Potential activity of ethanolic extract of *Boesenbergia rotunda* (L.) rhizomes extract

in accelerating wound healing in rats. *Journal of Medicinal Plants Research, 4*(15), 1570-1576.

Malhi, H., Gores, G. J., & Lemasters, J. J. (2006). Apoptosis and necrosis in the liver: a tale of two deaths? *Hepatology, 43*(S1), S31-S44.

Mandato, C., Lucariello, S., Licenziati, M. R., Franzese, A., Spagnuolo, M. I., Ficarella, R., Meli, R. (2005). Metabolic, hormonal, oxidative, and inflammatory factors in pediatric obesity-related liver disease. *The Journal of Pediatrics, 147*(1), 62-66.

Mandrekar, P., & Szabo, G. (2009). Signalling pathways in alcohol-induced liver inflammation. *Journal of Hepatology, 50*(6), 1258-1266.

Marcolin, E., San-Miguel, B., Vallejo, D., Tieppo, J., Marroni, N., González-Gallego, J., & Tuñón, M. J. (2012). Quercetin Treatment Ameliorates Inflammation and Fibrosis in Mice with Nonalcoholic Steatohepatitis. *The Journal of Nutrition, 142*(10), 1821-1828.

Marieb, E. N., & Hoehn, K. (2007). *Human anatomy & physiology*: Pearson Education. 144 pp.

Masalkar, P. D., & Abhang, S. A. (2005). Oxidative stress and antioxidant status in patients with alcoholic liver disease. *Clinica Chimica Acta, 355*(1), 61-65.

Mau, J.-L., Lai, E. Y., Wang, N.-P., Chen, C.-C., Chang, C.-H., & Chyau, C.-C. (2003). Composition and antioxidant activity of the essential oil from *Curcuma zedoaria*. *Food Chemistry, 82*(4), 583-591.

Mehendale, H. M. (2005). Tissue repair: an important determinant of final outcome of toxicant-induced injury. *Toxicologic Pathology, 33*(1), 41-51.

Melhem, A., Stern, M., Shibolet, O., Israeli, E., Ackerman, Z., Pappo, O., Zabrecky, G. (2005). Treatment of chronic hepatitis C virus infection via antioxidants: results of a phase I clinical trial. *Journal of Clinical Gastroenterology, 39*(8), 737-742.

Moayedi, B., Gharagozloo, M., Esmaeil, N., Maracy, M. R., Hoorfar, H., & Jalaeikar, M. (2013). A randomized double-blind, placebo-controlled study of therapeutic effects of silymarin in β-thalassemia major patients receiving desferrioxamine. *European Journal of Haematology, 90*(3), 202-209.

Moungjaroen, J., Nimmannit, U., Callery, P. S., Wang, L., Azad, N., Lipipun, V., Rojanasakul, Y. (2006). Reactive oxygen species mediate caspase activation and apoptosis induced by lipoic acid in human lung epithelial cancer cells through Bcl-2 down-regulation. *Journal of Pharmacology and Experimental Therapeutics, 319*(3), 1062-1069.

Mukai, M., Bischoff, K., & Ramaiah, S. K. (2012). Liver toxicity. *Veterinary Toxicology: Basic and Clinical Principles*, 246 pp.

Murayama, H., Ikemoto, M., Fukuda, Y., Tsunekawa, S., & Nagata, A. (2007). Advantage of serum type-I arginase and ornithine carbamoyltransferase in the evaluation of acute and chronic liver damage induced by thioacetamide in rats. *Clinica Chimica Acta, 375*(1), 63-68.

Muriel, P. (2009). Role of free radicals in liver diseases. *Hepatology International, 3*(4), 526-536.

Muriel, P., & Rivera-Espinoza, Y. (2008). Beneficial drugs for liver diseases. *Journal of Applied Toxicology, 28*(2), 93-103.

Nakatani, K., Kaneda, K., Seki, S., & Nakajima, Y. (2004). Pit cells as liver-associated natural killer cells: morphology and function. *Medical Electron Microscopy, 37*(1), 29-36.

Nemeth, E., Baird, A. W., & O'Farrelly, C. (2009). *Microanatomy of the liver immune system.* Paper presented at the Seminars in Immunopathology, *31*:333–343.

Nishiyama, T., Mae, T., Kishida, H., Tsukagawa, M., Mimaki, Y., Kuroda, M., Nakagawa, K. (2005). Curcuminoids and sesquiterpenoids in turmeric (*Curcuma longa* L.) suppress an increase in blood glucose level in type 2 diabetic KK-Ay mice. *Journal of Agricultural and Food Chemistry, 53*(4), 959-963.

Okazaki, I., Ninomiya, Y., Kyuichi, T., & Friedman, S. I. (2003). *Extracellular Matrix and the Liver: Approach to Gene Therapy*: Academic Press.

Okuyama, H., Shimahara, Y., Nakamura, H., Araya, S., Kawada, N., Yamaoka, Y., & Yodoi, J. (2004). Thioredoxin prevents thioacetamide-induced acute hepatitis. *Comparative Hepatology, 3*(Suppl 1), S6.

Orlikova, B., Tasdemir, D., Golais, F., Dicato, M., & Diederich, M. (2011). Dietary chalcones with chemopreventive and chemotherapeutic potential. *Genes & Nutrition, 6*(2), 125-147.

Oz, H. S., McClain, C. J., Nagasawa, H. T., Ray, M. B., de Villiers, W. J., & Chen, T. S. (2005). Diverse antioxidants protect against acetaminophen hepatotoxicity. *Journal of Biochemical and Molecular Toxicology, 18*(6), 361-368.

Panasiuk, A., Zak, J., Panasiuk, B., & Prokopowicz, D. (2007). Increase in expression of monocytic tissue factor (CD142) with monocytes and blood platelet activation in liver cirrhosis. *Blood Coagulation & Fibrinolysis, 18*(8), 739-744.

Park, S. Y., Shin, H. W., Lee, K. B., Lee, M.-J., & Jang, J.-J. (2010). Differential expression of matrix metalloproteinases and tissue inhibitors of metalloproteinases in thioacetamide-induced chronic liver injury. *Journal of Korean Medical Science, 25*(4), 570-576.

Parsons, C. J., Bradford, B. U., Pan, C. Q., Cheung, E., Schauer, M., Knorr, A., Brocks, B. (2004). Antifibrotic effects of a tissue inhibitor of metalloproteinase-1 antibody on established liver fibrosis in rats. *Hepatology, 40*(5), 1106-1115.

Pinelo, M., Rubilar, M., Jerez, M., Sineiro, J., & Núñez, M. J. (2005). Effect of solvent, temperature, and solvent-to-solid ratio on the total phenolic content and antiradical activity of extracts from different components of grape pomace. *Journal of Agricultural and Food Chemistry, 53*(6), 2111-2117.

Pinzani, M., Rosselli, M., & Zuckermann, M. (2011). Liver cirrhosis. *Best Practice & Research Clinical Gastroenterology, 25*(2), 281-290.

Plonné, D., Schulze, H. P., Kahlert, U., Meltke, K., Seidolt, H., Bennett, A. J., Dargel, R. (2001). Postnatal development of hepatocellular apolipoprotein B assembly and secretion in the rat. *Journal of Lipid Research, 42*(11), 1865.

Pradhan, S., & Girish, C. (2006). Hepatoprotective herbal drug, silymarin from experimental pharmacology to clinical medicine. *Indian Journal of Medical Research, 124*(5), 491.

Preedy, V. R., & Watson, R. (2007). *The encyclopedia of vitamin E*: CABI, 773-782.

Ptitsyn, A. A., Zvonic, S., Conrad, S. A., Scott, L. K., Mynatt, R. L., & Gimble, J. M. (2006). Circadian clocks are resounding in peripheral tissues. *PLoS Computational Biology, 2*(3), e16.

Purohit, V., & Brenner, D. A. (2006). Mechanisms of alcohol-induced hepatic fibrosis: A summary of the Ron Thurman Symposium. *Hepatology, 43*(4), 872-878.

Ramasamy, K., & Agarwal, R. (2008). Multitargeted therapy of cancer by silymarin. *Cancer Letters, 269*(2), 352-362.

Rana, S. V. S. (2008). Metals and apoptosis: recent developments. *Journal of Trace Elements in Medicine and Biology, 22*(4), 262-284.

Rees, K., Sinha, K., & Spector, W. (2005). The pathogenesis of liver injury in carbon tetrachloride and thioacetamide poisoning. *The Journal of Pathology and Bacteriology, 81*(1), 107-118.

Reeves, H. L., & Friedman, S. L. (2002). Activation of hepatic stellate cells-a key issue in liver fibrosis. *Frontiers in Bioscience, 7*(4), 808-826.

Rockey, D. C. (2005). Antifibrotic therapy in chronic liver disease. *Clinical Gastroenterology and Hepatology*, *3*(2), 95-107.

Roguin, A. (2006). Rene Theophile Hyacinthe Laënnec (1781–1826): The Man Behind the Stethoscope. *Clinical Medicine and Research, 4*(3), 230-235.

Roy, C. K., Kamath, J. V., & Asad, M. (2006). Hepatoprotective activity of Psidium guajava Linn. leaf extract. *Indian Journal of Experimental Biology, 44*(4), 305-311.

Rukayadi, Y., Lee, K.-H., & Hwang, J.-K. (2009). Activity of panduratin A isolated from Kaempferia pandurata Roxb. against multi-species oral biofilms in vitro. *Journal of Oral Science, 51*(1), 87-95.

Sadasivan, S., Latha, P. G., Sasikumar, J. M., Rajashekaran, S., Shyamal, S., & Shine, V. J. (2006). Hepatoprotective studies on Hedyotis corymbosa (L.) Lam. *Journal of Ethnopharmacology, 106*(2), 245-249.

Sakr, S. A., & Shalaby, S. Y. (2012). Metiram-induced histological and histochemical alterations in Liver and kidney of pregnant mice. *Life Science Journal, 9*(1), 71-76.

Saleem, T. M., Chetty, C. M., Ramkanth, S., Rajan, V., Kumar, K. M., & Gauthaman, K. (2010). Hepatoprotective herbs—a review. *International Journal of Research in Pharmaceutical Sciences, 1*, 1-5.

Sarkar, M. K., & Sil, P. C. (2007). Hepatocytes are protected by herb Phyllanthus niruri protein isolate against thioacetamide toxicity. *Pathophysiology, 14*(2), 113-120.

Sato, R., Maesawa, C., Fujisawa, K., Wada, K., Oikawa, K., Takikawa, Y.,Masuda, T. (2004). Prevention of critical telomere shortening by oestradiol in human normal hepatic cultured cells and carbon tetrachloride induced rat liver fibrosis. *Gut, 53*(7), 1001-1009.

Schuppan, D., & Afdhal, N. H. (2008). Liver cirrhosis. *The Lancet, 371*(9615), 838-851.

Shapiro, H., Ashkenazi, M., Weizman, N., Shahmurov, M., Aeed, H., & Bruck, R. (2005). Curcumin ameliorates acute thioacetamide-induced hepatotoxicity. *Journal of Gastroenterology and Hepatology*, *21*(2), 358-366.

Shehzad, A., Wahid, F., & Lee, Y. S. (2010). Curcumin in cancer chemoprevention: molecular targets, pharmacokinetics, bioavailability, and clinical trials. *Archiv der Pharmazie, 343*(9), 489-499.

Shen, Z., Chen, G., Wang, Q., Yu, Y., Zhou, C., & Wang, Y. (2012). Sonochemistry synthesis and enhanced photocatalytic H2-production activity of nanocrystals embedded in CdS/ZnS/In2S3 microspheres. *Nanoscale*, *4*(6), 2010-2017.

Sherlock, S., & Dooley, J. (2002). *Diseases of the liver and biliary system*: Wiley Online Library.

Shi, G.-F., & Li, Q. (2005). Effects of oxymatrine on experimental hepatic fibrosis and its mechanism in vivo. *World J Gastroenterol, 11*(2), 268-271.

Sindhu, R. K., Koo, J.-R., Sindhu, K. K., Ehdaie, A., Farmand, F., & Roberts, C. K. (2006). Differential regulation of hepatic cytochrome P450 monooxygenases in streptozotocin-induced diabetic rats. *Free radical research, 40*(9), 921-928.

Singh, A. P. (2004). Kutkins-A Review of Chemistry and Pharmacology. *Ethnobotanical Leaflets, 2004*(1), 9.

Singh, G., Singh, O. P., & Maurya, S. (2002). Chemical and biocidal investigations on essential oils of some Indian Curcuma species. *Progress in Crystal Growth and Characterization of Materials, 45*(1), 75-81.

Škerget, M., Kotnik, P., Hadolin, M., Hraš, A. R., Simonič, M., & Knez, Ž. (2005). Phenols, proanthocyanidins, flavones and flavonols in some plant materials and their antioxidant activities. *Food Chemistry, 89*(2), 191-198.

Sohn, J. H., Han, K.-L., Lee, S.-H., & Hwang, J.-K. (2005). Protective effects of panduratin A against oxidative damage of tert-butylhydroperoxide in human HepG2 cells. *Biological and Pharmaceutical Bulletin, 28*(6), 1083-1086.

Solter, P. F. (2005). Clinical pathology approaches to hepatic injury. *Toxicologic Pathology, 33*(1), 9-16.

Spelman, K., Burns, J., Nichols, D., Winters, N., Ottersberg, S., & Tenborg, M. (2006). Modulation of cytokine expression by traditional medicines: a review of herbal immunomodulators. *Alternative Medicine Review, 11*(2), 128-150.

Spierings, D., McStay, G., Saleh, M., Bender, C., Chipuk, J., Maurer, U., & Green, D. R. (2005). Connected to death: the (unexpurgated) mitochondrial pathway of apoptosis. *Science Signalling, 310*(5745), 66.

Standring, S. (2008). Gray's anatomy. 1576 pp.

Stickel, F., & Schuppan, D. (2007). Herbal medicine in the treatment of liver diseases. *Digestive and Liver Disease, 39*(4), 293-304.

Sun, W. Y., Wei, W., Gui, S. Y., Wu, L., & Wang, H. (2008). Protective Effect of Extract from Paeonia lactiflora and Astragalus membranaceus against Liver Injury Induced by Bacillus Calmette-Guérin and Lipopolysaccharide in Mice. *Basic and Clinical Pharmacology and Toxicology, 103*(2), 143-149.

Te Sligte, K., Bourass, I., Sels, J., Driessen, A., Stockbrűgger, R., & Koek, G. (2004). Non-alcoholic steatohepatitis: review of a growing medical problem. *European Journal of Internal Medicine, 15*(1), 10-21.

Tiribelli, C., & Rigato, I. (2006). Liver cirrhosis and pregnancy. *Annal Hepatology, 5*(3), 201.

Tortora, G., & Derrickson, B. (2009). Principles of Anatomy and Physiology, Volume 2–Maintenance and Continuity of the Human Body, 12th International Student Edition, 1174: John Wiley & Sons, Inc.

Tsukada, S., Parsons, C. J., & Rippe, R. A. (2006). Mechanisms of liver fibrosis. *Clinica Chimica Acta, 364*(1), 33-60.

Turkmen, N., Sari, F., & Velioglu, Y. S. (2006). Effects of extraction solvents on concentration and antioxidant activity of black and black mate tea polyphenols determined by ferrous tartrate and Folin–Ciocalteu methods. *Food chemistry, 99*(4), 835-841.

Valavanidis, A., Vlachogianni, T., & Fiotakis, C. (2009). 8-hydroxy-2′-deoxyguanosine (8-OHdG): a critical biomarker of oxidative stress and carcinogenesis. *Journal of Environmental Science and Health Part C, 27*(2), 120-139.

Wallach, J. (2006). *Interpretation of diagnostic tests*: Lippincott Williams & Wilkins, P. 144

Wang, H., Peng, R., Kong, R., & Li, Y. (1999). Serum glutathione S-transferase activity as an early marker of thioacetimide-induced acute hepatotoxicity in mice]. *Wei sheng yan jiu= Journal of Hygiene Research, 28*(3), 179.

Wang, L., Wang, B.-E., Wang, J., Xiao, P.-G., & Tan, X.-H. (2008). Herbal compound 861 regulates mRNA expression of collagen synthesis-and degradation-related genes in human hepatic stellate cells. *World Journal of Gastroenterology: WJG, 14*(11), 1790.

Wang, L., Wang, J., Wang, B.-E., Xiao, P.-G., Qiao, Y.-J., & Tan, X.-H. (2004). Effects of herbal compound 861 on human hepatic stellate cell proliferation and activation. *World Journal of Gastroenterology, 10*(19), 2831-2835.

Wang, M. E., Chen, Y. C., Chen, I. S., Hsieh, S. C., Chen, S. S., & Chiu, C. H. (2012). Curcumin protects against thioacetamide-induced hepatic fibrosis by attenuating the inflammatory response and inducing apoptosis of damaged hepatocytes. *The Journal of Nutritional Biochemistry, 23*(10), 1352-1366.

Wang, Y., Zhang, J.-S., Huang, G.-C., Cheng, Q., & Zhao, Z.-H. (2005). Effects of adrenomedullin gene overexpression on biological behavior of hepatic stellate cells. *World Journal of Gastroenterology, 11*(23), 3549.

Wong, W.-L., Abdulla, M. A., Chua, K.-H., Kuppusamy, U. R., Tan, Y.-S., & Sabaratnam, V. (2012). Hepatoprotective Effects of *Panus giganteus* (Berk.) Corner against Thioacetamide-(TAA-) Induced Liver Injury in Rats. *Evidence-Based Complementary and Alternative Medicine, 2012*, 10 pp.

Wu, S.-L., Yu, L., Pan, C.-E., Jiao, X.-Y., Lv, Y., Fu, J., & Meng, K.-w. (2006). Apoptosis of lymphocytes in allograft in a rat liver transplantation model induced by resveratrol. *Pharmacological Research, 54*(1), 19-23.

Yadav, N. P., Pal, A., Shanker, K., Bawankule, D. U., Gupta, A. K., Darokar, M. P., & S. Khanuja, S. P. (2008). Synergistic effect of silymarin and standardized extract of Phyllanthus amarus against CCl4-induced hepatotoxicity in Rattus norvegicus. *Phytomedicine, 15*(12), 1053.

Yob, N., Jofrry, S. M., Affandi, M., Teh, L., Salleh, M., & Zakaria, Z. (2011). Zingiber zerumbet (L.) Smith: a review of its ethnomedicinal, chemical, and pharmacological uses. *Evidence-Based Complementary and Alternative Medicine, 2011*, 12 pp.

Yoshikawa, M., Nishida, N., Ninomiya, K., Ohgushi, T., Kubo, M., Morikawa, T., & Matsuda, H. (2006). Inhibitory effects of coumarin and acetylene constituents from the roots of *Angelica furcijuga* on d-galactosamine/lipopolysaccharide-induced liver injury in mice and on nitric oxide production in lipopolysaccharide-activated mouse peritoneal macrophages. *Bioorganic & Medicinal Chemistry, 14*(2), 456-463.

You, J., Cui, F.-d., Li, Q.-p., Yong-sheng, W., Han, X., & Yu, Y.-w. (2005). A HPLC method for the analysis of germacrone in rabbit plasma and its application to a pharmacokinetic study of germacrone after administration of zedoary turmeric oil. *Journal of Chromatography B, 823*(2), 172-176.

Yun, J.-M., Kweon, M.-H., Kwon, H., Hwang, J.-K., & Mukhtar, H. (2006). Induction of apoptosis and cell cycle arrest by a chalcone panduratin A isolated from Kaempferia pandurata in androgen-independent human prostate cancer cells PC3 and DU145. *Carcinogenesis, 27*(7), 1454-1464.

Zeisberg, M., Yang, C., Martino, M., Duncan, M. B., Rieder, F., Tanjore, H., & Kalluri, R. (2007). Fibroblasts derive from hepatocytes in liver fibrosis via epithelial to mesenchymal transition. *Journal of Biological Chemistry, 282*(32), 23337-23347.

Zhang, J.-J., Wang, Y.-L., Feng, X.-B., Song, X.-D., & Liu, W.-B. (2011). Rosmarinic acid inhibits proliferation and induces apoptosis of hepatic stellate cells. *Biological and Pharmaceutical Bulletin, 34*(3), 343-348.

Zhang, S., Ji, G., & Liu, J. (2006). Reversal of chemical-induced liver fibrosis in Wistar rats by puerarin. *The Journal of Nutritional Biochemistry, 17*(7), 485-491.

Zimmermann, T., Franke, H., Peuker, M., & Dargel, R. (1992). Quantitative studies on fatty acid metabolism in isolated parenchymal cells from normal and cirrhotic livers in rats. *Journal of Hepatology, 15*(1), 10-16.

Zimmermann, T., Müller, A., Machnik, G., Franke, H., Schubert, H., & Dargel, R. (1987). Biochemical and morphological studies on production and regression of experimental liver cirrhosis induced by thioacetamide in Uje: WIST rats. *Zeitschrift Fur Versuchstierkunde, 30*(5-6), 165-180.

Publications and Publications

Publications

1- Salama, S. M., Abdulla, M. A., AlRashdi, A. S., Ismael, S., Alkiyumi, S. S., & Golbabapour, S. (2013). Hepatoprotective effect of ethanolic extract of *Curcuma longa on thioacetamide induced liver cirrhosis in rats. BMC Complementary and Alternative Medicine, 13(1), 56.* (Q1)

2- Salama, S. M., Bilgen, M., Al Rashdi, A. S., & Abdulla, M. A. (2012). Efficacy of *Boesenbergia rotunda Treatment against Thioacetamide-Induced Liver Cirrhosis in a Rat Model. Evidence-Based Complementary and Alternative Medicine, 2012, 12 pages.* (Q1)

Conferences

1- 3rd International conference on Natural Products for Health and Beauty, March 2011-Bangkok-Thailand.

2- 22nd International Invention, Innovation& Technology Exhibition, ITEX 2011-May 2011, Kuala Lumpur-Malaysia.

APPENDIX I

FORMS

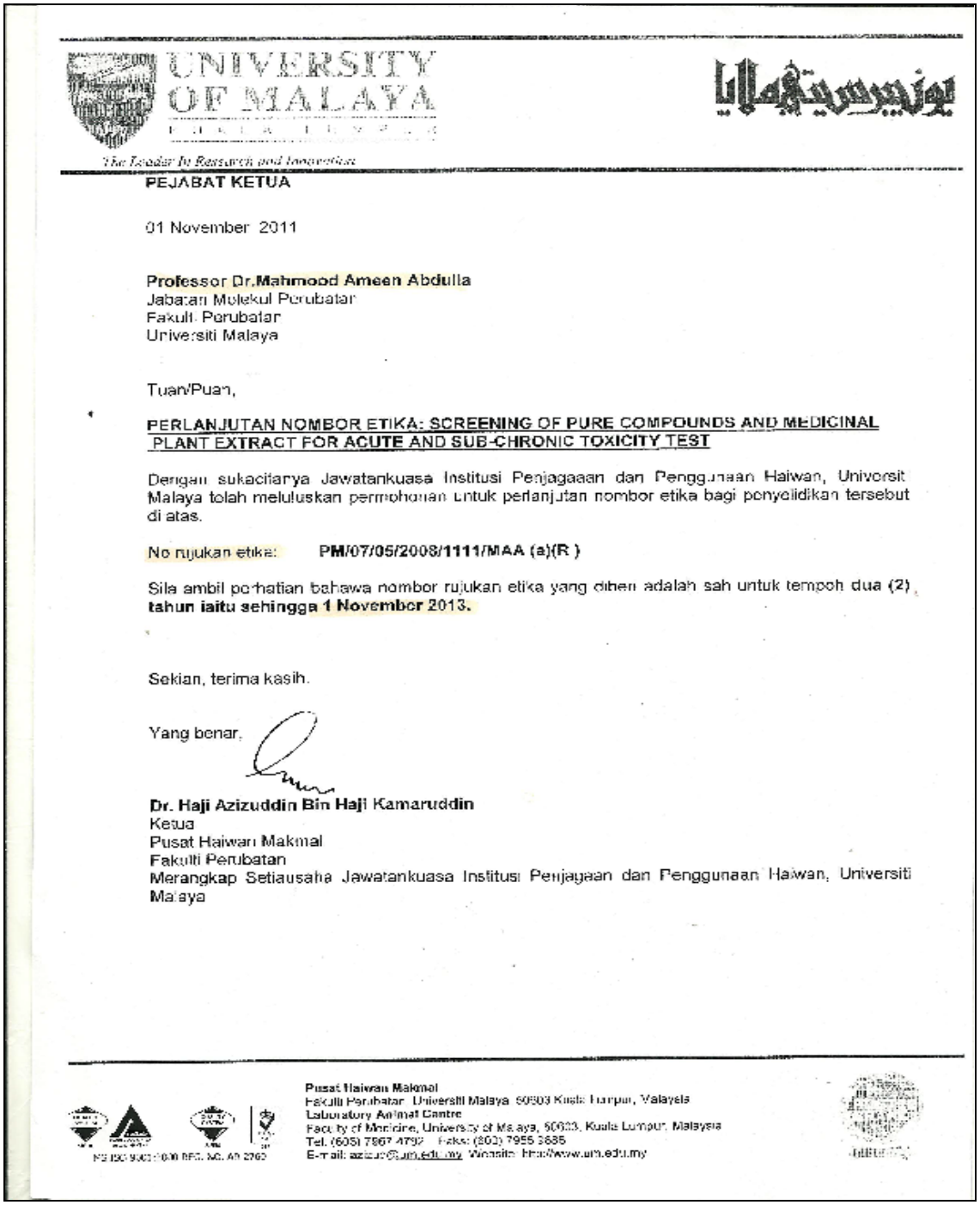

UNIVERSITY OF MALAYA

The Leader in Research and Innovation

PEJABAT KETUA

01 November 2011

Professor Dr.Mahmood Ameen Abdulla
Jabatan Molekul Perubatan
Fakulti Perubatan
Universiti Malaya

Tuan/Puan,

PERLANJUTAN NOMBOR ETIKA: SCREENING OF PURE COMPOUNDS AND MEDICINAL PLANT EXTRACT FOR ACUTE AND SUB-CHRONIC TOXICITY TEST

Dengan sukacitanya Jawatankuasa Institusi Penjagaaan dan Penggunaan Haiwan, Universit Malaya telah meluluskan permohonan untuk perlanjutan nombor etika bagi penyelidikan tersebut di atas.

No rujukan etika: **PM/07/05/2008/1111/MAA (a)(R)**

Sila ambil perhatian bahawa nombor rujukan etika yang diberi adalah sah untuk tempoh dua (2) **tahun iaitu sehingga 1 November 2013.**

Sekian, terima kasih.

Yang benar,

Dr. Haji Azizuddin Bin Haji Kamaruddin
Ketua
Pusat Haiwan Makmal
Fakulti Perubatan
Merangkap Setiausaha Jawatankuasa Institusi Penjagaan dan Penggunaan Haiwan, Universiti Malaya

Pusat Haiwan Makmal
Fakulti Perubatan, Universiti Malaya, 50603 Kuala Lumpur, Malaysia
Laboratory Animal Centre
Faculty of Medicine, University of Malaya, 50603, Kuala Lumpur, Malaysia
Tel: (603) 7967 4792 Fax: (603) 7955 3685
E-mail: azizuc@um.edu.my Website: http://www.um.edu.my

APPENDIX II

REAGENTS AND LABORATORY PROTOCOLS

A1. DPPH free radical scavenging assay

Reagents: 2, 2-diphenyl-1-picrylehydrazyl (C18H12N5O0) solution. Ascorbic acid 0.001761 g/ml

Preparation of reagent was prepared as a standard. The DPPH solution was prepared by dissolving 0.001972 g of DPPH in 50 ml of absolute ethanol then stirred until the DPPH was completely dissolved.

B1. Total Phenolic Content (TPC)

Reagents Commercial Folin-Ciocalteu solution Sodium carbonate Gallic acid

Preparation of reagent

1- A ratio of (1:10) of Folin-Ciocalteu solution was prepared by diluting 10 ml of it with 90 ml dH2O in a dark place.

2- 5.75 g of sodium carbonate was dissolved in 50 ml of dH2O to give a final concentration of 0.115 mg/ml.

3- 0.2 mg/ml of gallic acid solution was prepared and used as the standard solution

C1. Ferric reducing power (FRAP)

Reagents Iron (II) sulfate hepatohydrate (FeSO4. 7H2O) Sodium acetate trihydrate buffer (C2H3O2N9. 3H2O) 2,4,6-tris(2-pyridyl)-s-triazine (TPTZ) 98% FeCl3. 6H2O

Preparation of reagents 0.0278 g of FeSO4.7H2O was dissolved in 100 ml dH2O. 0.0775 g of acetate buffer was dissolved in 25 ml dH2O mixed previously with 0.4 ml glacial acetic acid.

0.00781 g of TPTZ was dissolved in 2.5 ml dH2O mixed previously with 0.1 ml (1M HCL). 0.0135g FeCl3. 6H2O was dissolved in 2.5 ml dH2O. The freshly prepared: acetate buffer, TPTZ and FeCl3. 6H2O solutions were mixed and vortexed to obtain the ready to use FRAP reagent.

D1. Haematoxylin and Eosin Staining

(i) Haematoxylin preparation